UNIVERSITÀ DI PARMA

UNIVERSITA' DEGLI STUDI DI PARMA

Dottorato di Ricerca in
BIOTECNOLOGIE E BIOSCIENZE

CICLO XXXV

Unlocking the hidden potential of genetic diversity to improve durum wheat tolerant to heat stress

Coordinatore:
Chiar.mo Prof. **Marco Ventura**

Supervisore:
Chiar.mo Prof. **Nelson Marmiroli**
Dott.ssa **Michela Janni**

Tutore:
Chiar.ma Prof.ssa **Elena Maestri**

Candidato: **Nadia Palermo**

2019/2020-2021/2022

UNIVERSITÀ DI PARMA

UNIVERSITY OF PARMA

Ph.D. in Biotechnology and Biosciences

XXXV COURSE

Unlocking the hidden potential of genetic diversity to improve durum wheat tolerant to heat stress

Coordinator:
Prof. **Marco Ventura**

Supervisor:
Prof. **Nelson Marmiroli**
Dr. **Michela Janni**

Tutor:
Prof. **Elena Maestri**

Candidate: **Nadia Palermo**

2019/2020-2021/2022

Index

Abstract

According to the Intergovernmental Panel on Climate Change report, the average global temperature will increase by 0.5 to 4°C in the 21st century, leading to a reduction in crop yields.

Wheat is one of the world's oldest and most widespread food crops and an important component of the human diet; it is very sensitive to heat stress (HS), and it is considered that for every 1°C increase in average temperature during the reproductive phase, wheat production is estimated to decrease by 6%.

Moreover, the fast increases in food demand due to population growth must be considered. A strategy to overcome the ongoing climate change is to understand the morphological and physiological traits associated with tolerance to high temperatures to produce crops more tolerant to abiotic stresses.

Possible approaches to succeed in maintaining high crop yields include (i) the exploitation of natural and induced mutations; (ii) the exploitation of available genetic resources to produce new genetic material that is more tolerant to HS and related secondary stresses; (iii) improve the ability to identify available sources of resilience; and (iv) developing new selection techniques.

The involvement of *sHsp26* in the heat stress response was analyzed, by dissecting the natural mutations of *TdHsp26* in some durum genotypes belonging to a germplasm collection.

A target enrichment PCR for NGS followed by KASP analysis was used to determine the SNPs present on the gene of interest in the different genotypes analyzed; a total of 17 haplotype combinations were found.

A phenotyping analysis was performed on the target genotypes subjected to thermal stress in three different phases of wheat development: seedlings (Z10), accession (Z31) and anthesis (Z65) Biochemical, morphological, and physiological traits were recorded during the experiment and contrasting genotypes were identified and selected through the experiments. Cultivated varieties were also included in the trials.

On the basis of the results obtained SSD69 and SSD397 were finally identified as putative tolerant and susceptible to heat stress.

These results support the importance of plant phenotyping of the identification of superior genotypes under heat stress.

1. INTRODUCTION

1.1 Greenhouse Effects and Global Warming

Earth's atmosphere is a mixture of gases called greenhouse gasses (GHG), and it retains heat like the walls of a greenhouse.

Solar radiation passes through the atmosphere unimpeded, heating the earth's surface. In turn, the energy is re-emitted as infrared, much of which is absorbed by CO_2 and water vapor in the atmosphere. The latter acts as a "blanket" of the right thickness, absorbing the appropriate solar energy to maintain a global average temperature adequate for life. Without this natural greenhouse effect, the average surface temperature would fall to about -21°C, much less than the current 14°C (Anderson, Hawkins, and Jones 2016). Gasses that contribute to the greenhouse effect include: Carbon dioxide (CO_2), methane (CH_4), Nitrous oxide (NO_2) and Chlorofluorocarbons (CFCs) (Kweku et al. 2018).

Many of these come from natural processes, such as:

- evaporation, which adds water vapor to the atmosphere;
- respiration of animals or plants, which contributes carbon dioxide;
- decomposition resulting in the release of methane (‘The Greenhouse Effect and Our Planet National Geographic Society’ 2022).

The sharp increase in greenhouse gasses over the past 100 years has been caused by anthropogenic activities (Kazancoglu, Ozbiltekin-Pala, and Ozkan-Ozen 2021).

Main players in increasing greenhouse gasses are fossil fuel combustion, deforestation, logging, and agricultural activities (Wang et al. 2021).

1) Fossil fuels, such as coal, oil, and natural gas burning are the main source of energy for electricity, heating, and transportation, as well as for the manufacture of a wide range of products, from steel to plastics. This process causes the release of greenhouse gasses (particularly CO_2) at high rates.

2) Deforestation seriously contributes to the increase in greenhouse gasses. During photosynthesis, plants, and trees store carbon (C) and release oxygen (O_2) into the air. Due to deforestation and logging, carbon is released as CO_2. According to the Food and Agriculture

Organization of the United Nations (FAO, 2006), deforestation releases between 25–30% of GHGs annually (Al-Yasiri and Géczi 2021).

3) Agriculture plays a key role in greenhouse gas emission, the global food system responsible for 21-37% of annual emissions and generates around half of all anthropogenic methane emissions and around three-quarters of anthropogenic N_2O (Lynch et al. 2021).

The strong increase in greenhouse gasses due to all the above activities has resulted in the global warming effect that has been so far defined as "the increase in the surface average temperature of the earth" because of the increase in the concentration of greenhouse gasses (Al-Ghussain 2019).From 1990 to 2019, the increase in global warming is 45% (US EPA 2022).

1.1.1 Climate changes: global temperature rise

Global warming has drastic consequences on changes in the world climate, leading to an increase in the frequency and intensity of heat waves and droughts, as well as other abiotic stress conditions such as flooding, salinity, and freezing (Bigot et al. 2018).

In October 2018, the Intergovernmental Panel on Climate Change (IPCC) released a special report on global warming, highlighting that average global temperatures have increased by about 1Cº since pre-industrial times (Figure 1). Furthermore, in that report it was pointed out that average global temperatures are increasing by about 0.2°C every decade ('IPCC — Intergovernmental Panel on Climate Change' 2018). In addition, in the paper it is predicted that average global warming will likely reach 1.5°C between 2030 and 2052 considering the rate of current anthropogenic greenhouse gas (GHG) emissions (Ogunbode, Doran, and Böhm 2020).

According to climate models (Driedonks et al. 2015) and the report from the Intergovernmental Panel on Climate Change, the world mean temperature will rise by 0.5 to 4°C in the twenty-first century (Hansen et al. 2016; Zandalinas, Fritschi, and Mittler 2021).

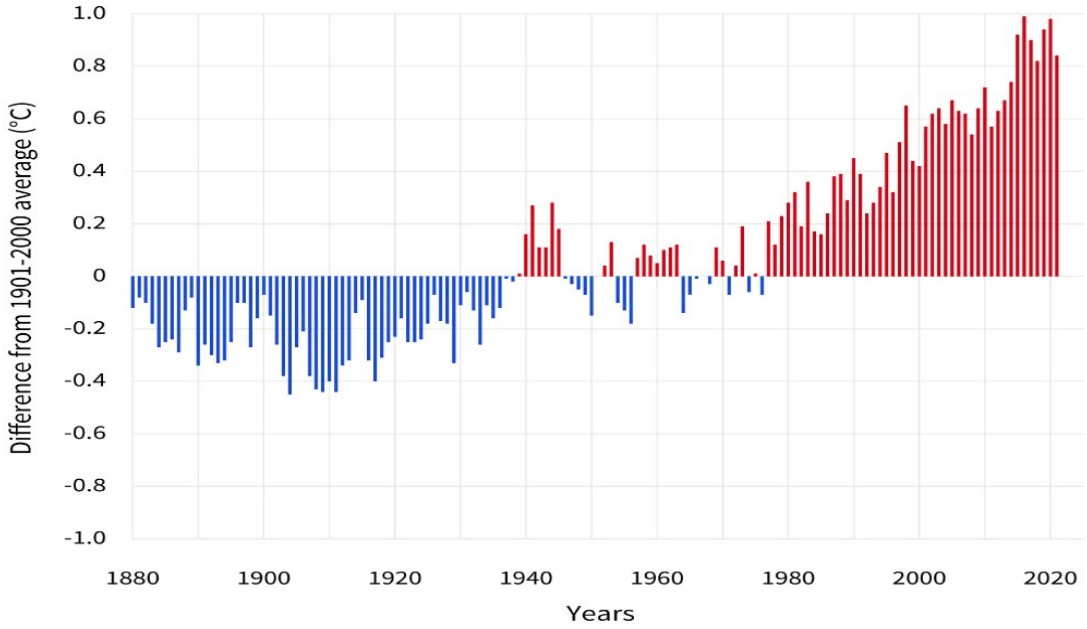

Fig 1. Yearly surface temperature compared to the 20th-century average from 1880–2021. Blue bars indicate cooler-than-average years; red bars show warmer-than-average years. NOAA Climate.gov graph, based on data from the National Centers for Environmental Information *(reproduced from https://www.climate.gov/news-features/understanding-climate/climate-change-global-temperature* accessed January 2023).

1.1.2 High temperature impact on agriculture

The Intergovernmental Panel on Climate Change (IPCC) in its Fifth Assessment Report, drew up new development scenarios called "Representative Concentration Pathways" (RCPs) that describe projected radiative forcings, i.e., the sum of climate perturbations in the atmosphere, in watts per square meter. Model calculations translate the forcings into the climate changes they evoke and reveal the greenhouse gas emissions on which they are based.

There are four such RCPs in the Fifth Interim Report: RCP2.6 (relatively low radiative forcing); RCP4.5 (medium radiative forcing); RCP6.0 (high radiative forcing); and RCP8.5 (very high radiative forcing). But specifically in the reports is shown the increase in global mean surface temperature for each RCP, corresponding to: 0.3°C-1.7°C with RCP2.6, by 1.1°C-2.6°C with RCP4.5, by 1.4°C-3.1°C with RCP6.0 and by 2.6°C-4.8°C with RCP8.5 (‘Fifth Assessment Report — IPCC’ 2014).

Crops are very sensitive to climate change, particularly to rising temperature, which has the most negative impact on crop yields and the materialization of these RCPs can have a detrimental effect on crops (Zhao et al. 2017).

Demonstrating the effect that rising temperatures can have on some crops was done by Zhao et al. (2017) through a 'multi-method' analysis. This group of researchers analyzed the impact of temperature on the yields of four globally important crops: corn, wheat, rice and soybeans (Figure 2). They estimated an average decrease in global crop yields of 5.6% due to temperature change alone under the lowest emissions scenario (RCP2.6), rising to 18.2% under the highest emissions scenario (RCP8.5).

	Yield changes (%) due to temperature changes by the end of century				
Scenario	Wheat	Rice	Maize	Soybean	Mean
RCP2.6	-6.9	-3.3	-8.6	-3.6	-5.6
	[-15.0, -1.4]	[-9.2, 0.8]	[-18.6, -1.8]	[-11.2,1.7]	[-14.4, -0.1]
RCP4.5	-11.4	-5.5	-14.2	-5.9	-9.2
	[-21.7, -3.9]	[-13.8, 1.0]	[-27.9, -4.9]	[-17.0, 3.1]	[-21.2, -0.3]
RCP6.0	-14.0	-6.8	-17.4	-7.2	-11.3
	[-25.7, -5.1]	[-16.8, 1.3]	[-33.1, -5.8]	[-20.2, 3.6]	[-25.6, 0.1]
RCP8.5	-22.4	-10.8	-27.8	-11.6	-18.2
	[-40.2, -8.5]	[-25.3, 2.4]	[-50.4, -9.7]	[-31.0, 6.0]	[-38.6, -0.7]

Fig 2. Projected changes in yield due to temperature changes by the end of the 21st century. Confidence intervals of 95% are given in square brackets (reproduced from *Zhao et al., 2017*).

While global crop yields are declining due to climate change, the human population is increasing and with it the demand for food. From 1960 to 2010, the global human population doubled and is expected to reach about 9.7 billion in 2050 and 10.9 billion in 2100 (Sekaran et al. 2021) and this will require an increase of about 70 percent in food production (Ngoune and Shelton 2020).

1.2 Wheat

Wheat is one of the world's oldest and most widespread food crops, domesticated more than 10,000 years ago in the Near East. Wheat, rice, and maize are considered the world's staple cereals. Wheat in particular is an important component of the human diet, providing nearly half of dietary calories and two-fifths of protein intake (Erenstein et al. 2022). In addition, it is a major source of starch and energy in the diet and also provides substantial amounts of several essential health-beneficial compounds, particularly protein, vitamins (especially B vitamins), dietary fiber, minerals, and phytochemicals, which are concentrated in the bran and germ of whole grains (Pandino et al. 2020).

To date, the most widely used wheat species are two: hexaploid bread wheat *(Triticum aestivum L.)* and tetraploid durum wheat *(Triticum turgidum subsp. durum* (Desf.) Husn.*)*, which are different in genome, grain composition, and quality characteristics that result in two different end uses (Ribeiro et al. 2018). Durum wheat (*T. turgidum)* accounts for about 8% of the world's total wheat production and can be used as such or processed into semolina for the production of pasta, couscous, bulgur, and bread (Mattiolo et al. 2017), while common wheat can be used for baked goods and noodles.

.

1.2.1 Wheat production

Wheat is the second most produced grain after corn, and global trade in wheat is greater than that of all other crops combined. In 2020, total global wheat production was 760 million tons. China, India and Russia are the three largest wheat producers in the world, contributing 41% of total production. The United States rank fourth in wheat production, however, the European Union, if it were counted as a single country, would have more wheat production than any other country except China (Figure 3) (‘Wheat Production by Country 2022’ 2022).

The European Union with its 28 countries (EU-28), contributes about 35% of world wheat production (‘FAOSTAT’ 2022). While soft wheat is grown in almost all European countries, durum wheat is mainly harvested in southern EU countries. The EU, in 2020, harvested 119.1 million tons of soft wheat and spelt, which compared to 2019 coincides with 12.7 million tons less, a decrease of 9.7%.

This reduction in production is due to the weather conditions, but also to the marked reduction in harvested areas (about 5.9% less), due to adverse autumn weather conditions that hampered sowing (‘Agricultural Production - Crops’ 2022) (EUROSTAT 2020).

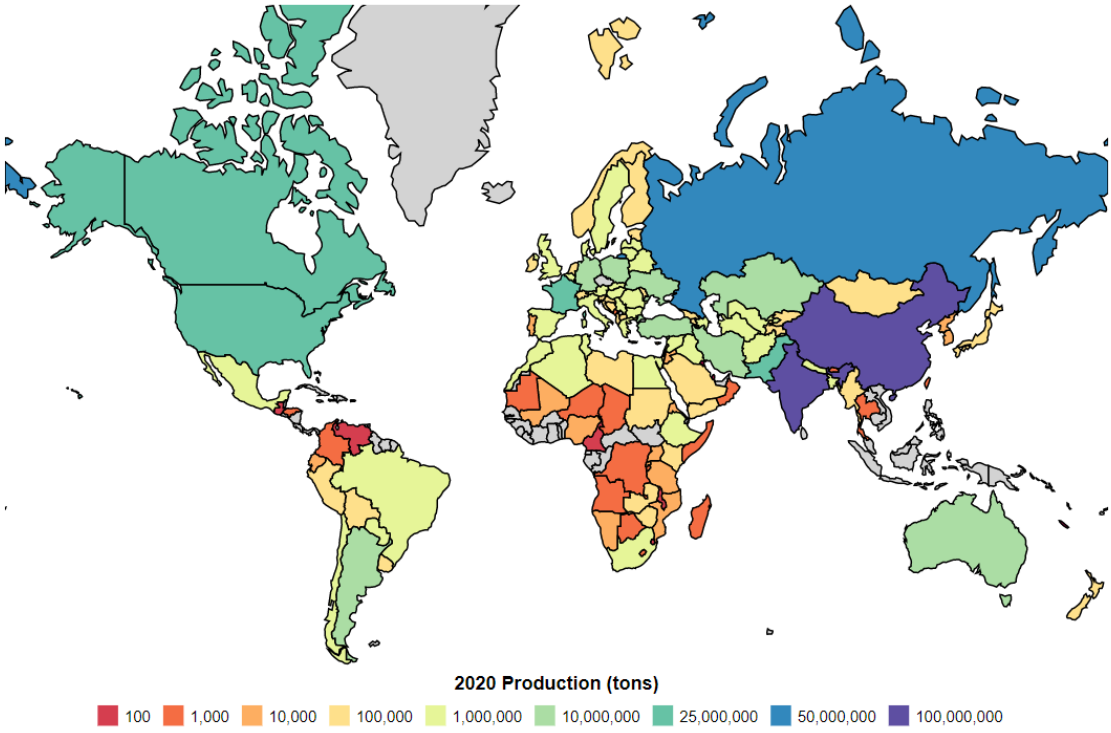

Fig 3. Wheat Production by Country 2022 (reproduced from https://worldpopulationreview.com/country-rankings/wheat-production-by-country accessed January 2023)

Italy, Greece, and Spain are the main producers of durum wheat in the EU, contributing 80% of total production (Zingale et al. 2022). Specifically, the pasta industry produces about 16.5 million tons of pasta per year worldwide, of which 21.2% and 12.1% is produced in Italy and the United States of America, respectively (UNAFPA 2022).

Italmopa, the Italian Millers' Industrial Association (Federalimentare-Confindustria) announces that the amount of domestic production of durum wheat projected for 2022 in Italy was 3.5 million tons. This figure indicates that production is expected to be more than 10% lower than in 2021. This is certainly not a comforting figure, which goes along with that for bread wheat, which is expected to end the year with 2.5 million tons produced, a negative record never reached in the last 100 years (EFA 2022).

1.2.2 Wheat life cycle

Wheat belongs to the Poaceae (Gramineae) family which includes major crop plants such as wheat (*Triticum* spp. L.), barley (*Hordeum vulgare* L.), oat (*Avena sativa* L.), rye (*Secale cereale* L.), maize (*Zea mays* L.) and rice (*Oryza sativa* L.). The Triticeae tribe, within the Pooideae subfamily, contains more than 15 genera and 300 species (Soreng et al. 2015).

The growth cycle of wheat is divided in different phases: germination, seedling establishment and leaf production, tillering and head differentiation, stem and head growth, head emergence and flowering, and grain filling and maturity. Several systems have been developed to provide numerical designations for growth and developmental stages. The Feekes, Zadoks, and Haun scales are used the most frequently. The Zadoks Decimal Code (Zadoks, Chang, and Konzak 1974) is internationally used to describe growth stages of cereals (Figure 4) and it is the most widely accepted system for describing wheat development. This system is based on two-digit code: the first digit refers to the principal stage of development beginning with germination (stage 0) and ending with kernel ripening (stage 9); the second digit, between 0 and 9 subdivides each principal growth stage code:

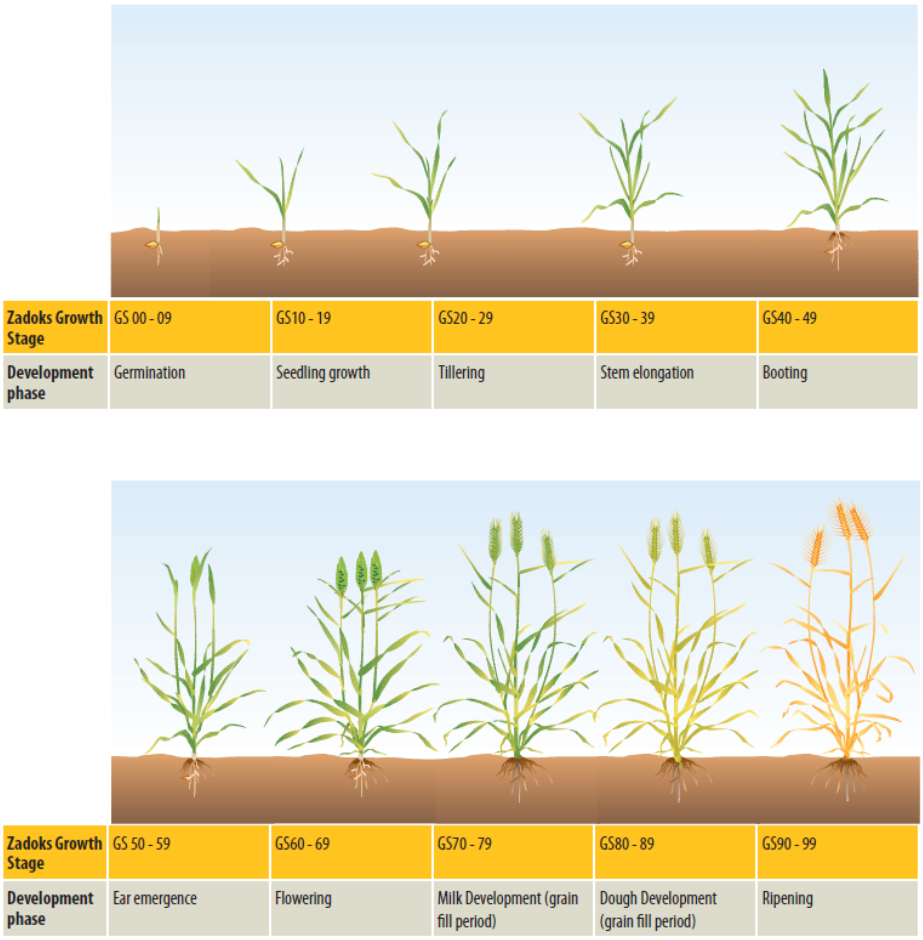

Fig 4. Zadoks cereal growth stages (image derived from the GRDC Cereal Growth Stages Guide).

Wheat can be classified into spring or winter wheat (Crofts 1989) according to the sowing season,: spring wheat is sown in the spring and matures in late summer, while winter wheat is sown before winter and thus seedlings (Zadoks code 10-19) are exposed to a prolonged cold period (vernalization) which is necessary to trigger reproductive stage in the early spring and to produce good yields. A definition by Crofts (1989) suggests that the distinction between winter and spring wheat is based on the presence or absence of genes controlling the vernalization requirement (*Vrn).*

1.2.3 Wheat allopolyploidization

Cultivated wheat can differ in ploidy levels, being diploid (2n = 2x = 14, AA), tetraploid (2n = 4x = 28, BBAA) and hexaploid (2n = 6x = 42, BBAADD, Tadesse 2019).

Durum wheat (DW), *Triticum turgidum* L. ssp. *Durum* (Desf.) Husn., genome BBAA, evolved from domesticated emmer wheat (DEW), *T. turgidum* ssp. *dicoccum* (Schrank ex Schübl.) Thell. DEW itself derived from wild emmer wheat (WEW), *T. turgidum* ssp. *dicoccoides* (Körn. ex Asch. & Graebn.) Thell., in the Fertile Crescent about 10,000 years ago. Although the earliest evidence of DW dates back to 6,500–7,500 years ago (Maccaferri et al. 2019). Instead, *Triticum aestivum L.* derived from a polyploidization event between *Triticum turgidum ssp. durum* (*AABB* genome) *and Aegilops tauschii* (*DD* genome) (Levy and Feldman 2022).

Allopolyploidy of the wheat genome is one of the key factors in wheat success as a global staple crop. The presence of two or three copies of a gene may confer greater plasticity and thus allow adaptation to changing environmental conditions (The International Wheat Genome Sequencing Consortium (IWGSC) et al. 2014).

The first step to exploit the genetic potential of wheat was the complete assembly of its genome, which took a long time to complete, as the large size of the genome (16 Gb for *T. aestivum* and 12 Gb for *T. turgidum*) and the high sequence similarity between subgenomes and the abundance of repetitive elements (about 85% of the genome) hampered early attempts at assembly (The International Wheat Genome Sequencing Consortium (IWGSC) et al. 2014).

In 2017, both tetraploid and hexaploid wheat genomes were made available (Avni et al. 2017; Zimin et al. 2017).

Next Generation Sequencing (NGS) technologies are also providing more opportunities to study gene structure and expression. Heritable variation in the genome that underlies important agronomic traits can be identified more rapidly and systematically (Jia et al. 2017).

The comprehensive sequencing of these wheat genomes with the help of NGS technology is a milestone for wheat biology and provides resources for functional wheat genomics. However, to link phenotypic traits to functional genes, wheat researchers are working on additional platforms and technical resources, such as mutant libraries, complete cDNA clones, and SNP microarrays (Jia et al. 2017).

1.3 Heat stress on plants

1.3.1 Heat damage and ROS production

Heat stress affects several physiological processes of the plant, such as: photosynthesis, respiration, transpiration, membrane thermostability, and osmotic regulation.

Among all, membrane dysfunction is the main physiological consequence of plant exposure to HS. Under high temperature conditions, the kinetic energy and movement of biomolecules across membranes increases, which causes weakening of chemical bonds, leading to disintegration of membrane lipids resulting in increased fluidity (Jaconis et al. 2021).

Photosynthesis is another process that is greatly impaired by heat, causing severe repercussions on the plant (Haworth et al. 2018). Under HS conditions, photochemical reactions in the thylakoid lamellae and carbon metabolism in the chloroplast stroma are subject to damage (Hu, Ding, and Zhu 2020). Heat stress causes thylakoid membranes to rupture, thereby inhibiting the activities of electron transporters and membrane-associated enzymes, reducing the rate of photosynthesis. Among chloroplast membrane protein complexes, PSII is the most sensitive target of heat stress. It can detach from the membrane, due to increased membrane fluidity, resulting in impairment of its integrity and affecting photosynthetic electron transfer (Mathur, Agrawal, and Jajoo 2014). Photosynthetic electron transport and ATP synthesis are severely impaired if PSII suffers severe thermal damage (Wang et al. 2018, 2).

Another component of the photosynthetic apparatus that is affected by thermal stress is the Rubisco enzyme, which, under non-stress conditions, is responsible for the fixation of about 10^{11} tons of atmospheric CO_2 (Galmés et al. 2013). It acts in the Calvin-Benson-Bassham cycle, catalyzing the carboxylation of the 5-carbon-atom sugar ribulose-1,5-bisphosphate (RuBP), (Wang et al. 2018). At moderately elevated temperatures, Rubisco activase (RCA) activity is inhibited, resulting in thermal inactivation of Rubisco activity. Under high temperatures, the stability of the Rubisco activating chaperone enzyme decreases, resulting in the inhibition of photosynthesis (Perdomo et al. 2017).

All these alterations lead to increased concentrations of reactive oxygen species (ROS). ROS are normally produced in plant cells, particularly in the chloroplast the following are formed: hydrogen peroxide (H_2O_2), superoxide, hydroxyl radicals (-OH) and $^1O_2$ during

photosynthesis (Asada 2006; Khorobrykh et al. 2020). ROS production occurs during excitation energy transfer in the antenna complex of PSII and during electron transport in the reaction center of PSII (Suzuki et al. 2012; Pospíšil 2016). In particular, $^1O_2$ is formed through excitation energy transfer, while the superoxide anion radical ($O_2^{\cdot-}$), H_2O_2 and -OH are formed through electron transport (Pospíšil and Prasad 2014). Under stress conditions, due to malfunction of PSII and the Calvin cycle ROS synthesis increase, leading to lipid peroxidation and cell membrane damage (Nelson et al. 2014).

Under non-stress conditions, a balance exists between ROS production and removal, known as redox homeostasis (Caverzan, Casassola, and Brammer 2016). When ROS production exceeds the cell ability to recover, the cell is subjected to a stress known as oxidative stress (Figure 5). The HS-induced increase in ROS production causes a change in membrane potential (depolarization), lipid peroxidation, protein oxidation, nuclear acid damage, obstruction of enzyme function, and activation of programmed cell death (Sarita Srivastava and Dubey 2011).

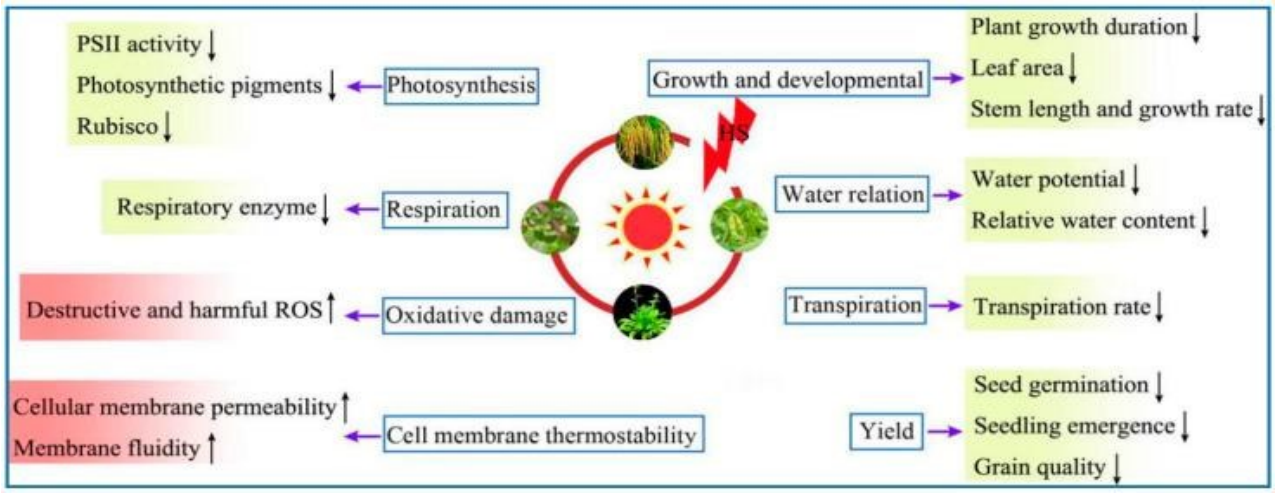

Fig 5. Effects of heat stress on plants *(*reproduced from *J. Zhao et al. 2020).*

1.3.2 Heat stress effects on wheat development

Wheat is very sensitive to heat stress (Akter and Rafiqul Islam 2017), and crop growth is significantly impaired depending on the severity and timing of the stress. High temperature affects almost all stages of wheat growth and development, including seed germination, root and leaf emergence, stem growth, flowering initiation, pollination, fertilization, seed yield and

seed quality (Buttar et al. 2020). Optimal temperatures for wheat growth and development are shown in Table 1.

The reproductive and grain-filling stages are the most sensitive to heat stress, and plants are less likely to recover if stressed at this critical stage (Barlow et al. 2015; Aiqing et al. 2018). In fact, high temperatures during the reproductive stages can cause pollen sterility, sterile ovules, decreased fertilization, and aborted flowers (Prasad and Djanaguiraman 2014) which ultimately reduce grain numbers and yield. Grain size is also reduced due to shorter duration of the filing period and early senescence (Shirdelmoghanloo et al. 2016), whereas grain quality decreases (Nuttall et al. 2015; Ullah et al. 2020) with an increase in the percentage of shriveled/broken grains (also called screens) (Ferreira et al. 2012). For each 1°C increase in mean temperature during the reproductive phase, grain production is estimated to decrease by 6% (Chen et al. 2020).

Table 1. Optimal temperature requirements of wheat at different growth stages from *(Khan et al. 2020)*

Stages	**Optimum Temperature (°C)**	**Minimum Temperature (°C)**	**Maximum Temperature (°C)**
Seed germination	20-25 ± 1.2	3.5-5.5 ± 0.44	35 ± 1.02
Root growth	17.2 ± 0.87	3.50 ± 0.73	24.0 ± 1.21
Shoot growth	18.5 ± 1.90	4.50 ± 0.76	20.1 ± 0.64
Leaf initiation	20.5 ± 1.25	1.50 ± 0.52	23.5 ± 0.95
Terminal spikelet	16.0 ± 2.30	2.50 ± 0.49	20.0 ±1.60
Anthesis	23.0 ± 1.75	10.0 ±1.12	26.0 ± 1.01
Grain filling duration	26.0 ± 1.53	13.0 ± 1.45	30.0 ± 2.13

However, even the early stages of growth can be severely affected by high temperatures. For example, growth and development begin with seed germination, which requires optimal temperature and humidity. The germination index and potential are reduced under high temperatures (Liu et al. 2019).

High temperature also heavily affects the rooting of wheat seedlings in the early vegetative stages of the crop; if the temperature is high, there is a reduction in root growth, shoots, green leaf area, and the number of effective shoots per plant (Gupta et al. 2013).

A better understanding of the morphological and physiological traits associated with HS tolerance would allow defense measures against heat stress to be defined (Janni et al. 2018; Langridge and Reynolds 2021).

1.3.3 Plant adaptation strategies to heat stress

Plants have three main adaptation strategies for heat resistance: heat tolerance (HT), heat escape (HE) and heat avoidance (HA) (Shanker, Bhanu, and Maheswari 2020); almost all of the adaptive traits that enable the plant to counteract stress are encapsulated in the term Heat Resilience (Figure 6).

1) Heat tolerance is the ability of the plant to resist and withstand continuous exposure to hot conditions with a varying degree of plant damage, the less the greater the tolerance. The term includes mobilization of heat shock proteins, activation of the antioxidant system, induction of membrane thermostability and photoprotective metabolites (Wahid et al. 2007).
2) Heat avoidance is the ability of plants to avoid the effects of heat by maintaining tissue homeostasis and enzyme activity thereby countering heat; short term avoidance includes leaf rolling or change in leaf position, change in lipidic membrane composition, and cooling as the result of transpiration and rapid water uptake (Sangeeta Srivastava et al. 2012).
3) Heat escape is the ability of the plant to escape heat-like conditions by adjusting its phenology, developmental plasticity, growth pattern so that its critical physiological stage that can be affected by heat escapes it (Shanker, Bhanu, and Maheswari 2020).

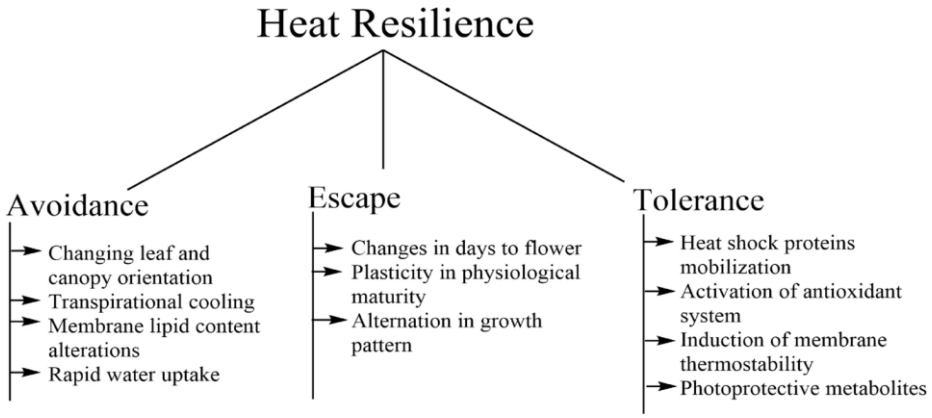

Fig 6. Heat resilience and the processes leading to heat stress in plants (from *Shanker et al., 2020*).

1.3.4 Heat resilience

To achieve "zero hunger" among the sustainable development goals and ensure food security, crops must be improved especially under changing climatic conditions (Janni et al. 2020). To do this, scientists must be able to produce crops that are resistant to abiotic stresses; this involves the use of advanced technical techniques such as high-throughput genotyping and phenotyping and genome editing (Hickey et al. 2019).

Conventional plant breeding strategies based on phenotypic selection and qualitative genetics were used in the past (Setia and Setia 2018). However, population growth resulting in increased demand for food has resulted in the search for elite cultivars that are more adaptable to ongoing changes. The mechanisms for responding to various stresses are very complex and understanding the mechanisms that regulate the various responses is crucial in order to continue with the search for cultivars that can adapt to stresses.

Advances in "omics" technologies, particularly genomics, transcriptomics, proteomics, metabolomics, and phenomics allowed to monitor factors and traits that influence crop growth and yield in response to environmental threats (Soda 2015;Setia and Setia 2018).

- **Genomics**. Next-generation sequencing techniques have accelerated advances in crop functional genomics studies (Li et al. 2018). Numerous genes have been identified in plants that control key agronomic traits, especially under abiotic stresses (Sharma et al. 2017; Wen et al. 2021). Genome-wide association study (GWAS) has been applied to link traits to their underlying genetics. Many association studies have been conducted on various crops, such as wheat under heat stress (Rong Zhou et al. 2022).

- **Transcriptomics**. In recent years, RNA-seq (RNA sequencing) with next-generation sequencing techniques has enabled more accurate characterization of the transcriptome than microarray. MicroRNAs (miRNAs), circular RNAs (circRNAs) and long ncRNAs (lncRNAs) also play key roles in the response to abiotic stresses. These ncRNAs, including miRNA, circRNA and lncRNA, are considered an emerging target for crop improvement (Rong Zhou et al. 2022). It is of considerable importance to study plant transcriptome responses at individual cell level because different cell types are known to play different biological roles in plant growth and development. Single-cell RNA-sequencing (scRNA-seq) is a high-resolution

approach to study the functional genomes and transcriptional activity of plants at the single-cell level (Rich-Griffin et al. 2020), which helps scientists explore plant heterogeneity within cell types. A significant difference in some genes has been found among *Arabidopsis thaliana* (L.) Heynh. cell types under heat stress, although the heat shock protein response dominates gene expression in different cell types (Jean-Baptiste et al. 2019).

- **Proteomics**. Proteins, like gene products, can directly play roles in crop response to heat stress. A number of proteins involved in crop heat tolerance have been identified using proteomics (Zhao et al. 2016; Lu et al. 2017; Mu et al. 2017) as for example the study conducted by Lu et al. (2017) which led to the identification of 258 thermo-protein reactive in wheat that were playing a role in regulating redox, chlorophyll synthesis, protein turnover and carbon fixation (Lu et al. 2017).

- **Metabolomics.** It provides an efficient method for characterizing heat tolerance in plants and metabolome composition and dynamics in various cultures to heat stress have been identified using metabolomics (Chebrolu et al. 2016; Paupière et al. 2017). Overall, metabolomics is required to complete knowledge of other omics and to develop models for the system as a whole (Paupière et al. 2017), which can contribute to heat tolerance lighting by the appearance that other omics cannot cover.

- **Phenomics**. Over the past decade, plant phenomics has made impressive progress, developing novel sensors and imaging techniques for a wide range of traits, organs and situations (Tardieu 2017). Phenomics also characterized the plasticity of the plant phenome when exposed to a range of environmental conditions by capturing and interpreting a multidimensional matrix of functional and architectural variables measured at different scales (organ, plant, canopy), developmental stages and environmental scenarios (Danzi et al. 2021).

The integration of genomics, transcriptomics, proteomics, metabolomics, and phenomics data not only allowed to explain various biological processes (Rong Zhou et al. 2022), but gave innovative tools to fight the growing challenges of climate change on crops (Janni et al. 2020), resulting in the development of new high-yield varieties with increased heat tolerance and adaptation to climate change. Multi-omics can facilitate technique-assisted breeding, genetic engineering, and genome editing and thus accelerate crop improvement.

Current data indicate that at least two different genetic systems can protect plants from the otherwise lethal effects of heat stress: (i) a series of Mendelian HS genes acting possibly

in a dominant or semi-dominant way; and (ii) a small number of QTLs which allow plant growth and reproduction under different stress conditions (Janni et al. 2020).

1.4 Molecular mechanisms of Heat tolerance

1.4.1. Signal transduction

The plasma membrane acts as the first sensor for thermal stress; the change in plasma membrane fluidity causes cyclic nucleotide calcium channels (CNGCs) controlled by nucleotide cyclases to open, causing Ca^{2+} to move into the cytosol from the nuclear membrane (Mittler, Finka, and Goloubinoff 2012).

Ca^{2+} ions are associated with protein calmodulin 3 (CaM3) during HS; the Ca^{2+}- CaM3 complex interacts with calcium/calmodulin-binding protein kinase 3 (CBK3) and phosphatase PP7 to transduce cytosol heat-stress response (HSR) signals from the cytosol to the nucleus by modulating phosphorylation and de-phosphorylation of HSFA1, respectively (Ohama et al. 2017). Heat Shock Factors (HSFs) are encoded by large gene families with variable expression and functions and are components of complex signaling systems that control responses not only to high temperatures, but also to a range of abiotic stresses such as cold, drought, hypoxic conditions, soil salinity, toxic minerals, strong irradiation, and pathogen threats (Andrási, Pettkó-Szandtner, and Szabados 2021).

Signal transduction also occurs with increased levels of Inositol-1,4,5-triphosphate (IP_3), through the phosphoinositide signaling pathway, which results in Ca^{2+} influx into the cytoplasm from intracellular Ca^{2+} pools such as the endoplasmic reticulum (ER) and vacuole during HS (Ohama et al. 2017).

ROS also contribute to signal transduction with the accumulation of nitric oxide (NO), which induces CaM3 activation (Rengang Zhou et al. 2009).

1.4.2 Heat Shock Factors (HSF)

As mentioned in the previous paragraph, signal transduction leads to the activation of Heat Shock Factors, HSFs.

HSFs play a crucial role in the response to high temperatures in plants. They are the activators of production of heat shock proteins, which in turn are major players in the heat stress response (Liao et al. 2022).

Generally, plant HSFs proteins share a well-conserved structure characterized by 3 main domains. The N-terminal DNA-binding domain (DBD) is characterized by a central helix-turn-helix motif that specifically binds to heat stress elements (HSEs) in target

promoters and subsequently activates transcription of stress-inducible genes (Scharf 2012). The oligomerization domain (OD) with a bipartite pattern of hydrophobic amino acid residues (HR-A/B region) is linked to the DBD by a flexible linker. The C-terminal activation domains of plant HSFs are characterized by short peptide motifs (AHA motifs), which in many cases are crucial for activator function (Meng et al. 2016).

Despite many conserved features, HSF family members show a strong diversification of expression patterns and functions within the HSF family (Chen et al. 2018).

In wheat, 56 *TaHsf* members were identified, classified into classes A, B and C (Xue et al. 2014).

When plants experience heat stress, *HsfA1s* induce the expression of HSPs by binding the HSE in the corresponding promoter DNA sequence. The HSEs are central trinucleotide sequences, 5′-nGAAn-3′ or 5′-nTTCn-3′, with alternating orientation, separated by two nucleotides (Arofatullah et al. 2018). In addition, *HsfA1s* activate TFs, triggering a transcriptional cascade composed of various TFs, including *HsfAs (HsfA1e, HsfA2, HsfA3, HsfA7a and HsfA7b), HsfBs* (*HsfB1, HsfB2a* and *HsfB2b*), DREB2A and MBF1c (Liu and Charng 2013).

The HSF interacts with the ROS system activated, not only by the signal cascade initiated by signal transduction, but also by the accumulation of hydrogen peroxide (H_2O_2) molecules (Kollist et al. 2019).

The study by Perez-Salamo et al., showed that a subset of *Hsfs* genes is up-regulated by treatments that generate ROS (Pérez-Salamó et al. 2014).

The mechanism of sensing is not well understood. Function of HSFs might be affected by the presence of H_2O_2, as the latter can stabilize HSF trimers through reversible oxidation of Cys residues and formation of Cys-Cys bonds (Miller and Mittler 2006).

In addition, several studies have shown that the HSE region of *Hsfs* does not interact only with Heat shock proteins (HSPs). Storozhenko et al. (1998) showed that *HsfB1* cloned from tomato binds the HSE of the ascorbate peroxidase 1 *(apx1)* gene by activating its transcription under HS in arabidopsis (Storozhenko et al. 1998). An *apx* with a similar HSE motif was upregulated after exposure of rice seedlings to 42°C (Sato et al. 2001).

Thus, *Hsfs* can drive the production of key regulatory elements in plant defense against heat stress: the HSPs and enzymes with scavenger activity such as: ascorbate peroxidase (APX), superoxide dismutase (SOD), catalase (CAT) (Driedonks et al. 2015).

1.4.3 Heat-Shock Proteins (HSPs), master Players for Heat Stress Tolerance

Under heat stress, plants reduce the synthesis of normal proteins and transcribe and translate heat shock proteins (Laloum, Martín, and Duque 2018).

The induction of HSPs is the mechanism triggered by plants in response to the temperature and is observed in all organisms from bacteria to humans (De Jong, Moreau, and Thiéry 2008). In the past, HSPs were thought to be produced only under thermal stress conditions, as the name implies, but it is now established that these biomolecules are produced in response to various biotic and abiotic stresses (Ul Haq et al. 2019).

Plant HSPs are classified into different classes based on their molecular weight in kilodalton (kDa), such as HSP100, HSP90, HSP70, HSP60, and small HSPs (Shaw et al. 2016).

Several studies have shown the HSPs functions (Figure 7), such as: stabilize and ensure the protein function under HS conditions; folding of denatured proteins into the correct shapes protect the protein function; they also enable the proteins movements between cell compartments and promote the transport of older proteins to disposal sites within the plant (Hassan et al. 2020); they also support protein translation and translocation, perform proteolysis and protein folding, and reactivate denatured proteins (Díaz-Villanueva, Díaz-Molina, and García-González 2015). In addition, HSPs protect PSII from oxidative stress (Neta-Sharir et al. 2005; Almoguera et al. 2012) and maintain membrane permeability (Barua, Downs, and Heckathorn 2003; Bourgine and Guihur 2021). The HSPs participate in ATP-dependent reactions for protein folding, preventing their denaturation (Iba 2002; Hasan et al. 2017).

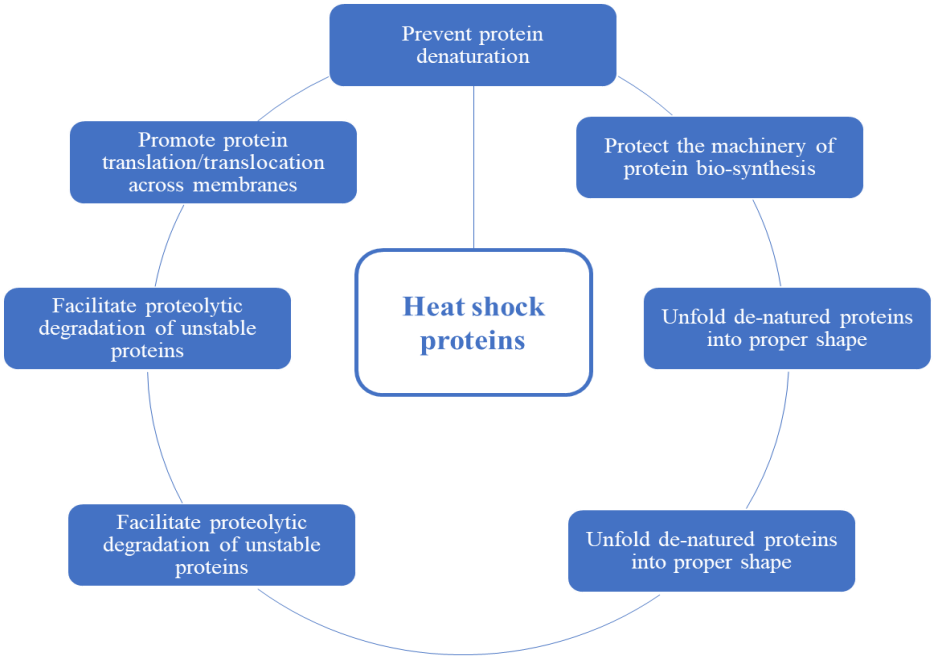

Fig 7. Defense mechanisms carried out by HSPs under conditions of stress.

The HSFAs regulate the HSP cycle (Figure 8), and under normal conditions HSFAs are inhibited by HSP90 (Prodromou 2016); under stress conditions, this repression is reversed and HSP90 is dissociated and HSFA is transformed into a functional trimeric state. This homo-trimer of HSFA binds to the HSE in the promoter region (Zou et al. 1998), activating the transcription of HSPs (Calderwood et al. 2010).

Protein HSFA1 is the master regulator of the response, and HSFA2 also plays an important role by creating a hetero-oligomeric super activator structure with HSFA1 in stress situations, which is more efficient than individual HSFs, regulating not only stress-related HSP genes but also protective enzyme genes such as *GST, GR, POX,* and *APX* (Ul Haq et al. 2019). Post-transcriptional modifications, such as alternative splicing, also regulate HSFs. Protein HSFA2 under heat stress conditions activates its transcription in a positive autoregulatory loop. Similarly, HSFAs are regulated by DREB2 under stress conditions, which in turn regulates stress-related genes in many plants (Laloum, Martín, and Duque 2018).

Similarly, miRNAs also play a key role in the stress response through down-regulation of stress-related genes (Kushawaha et al.,2021).

When the heat stress response diminishes, HSBP1 (Heat Shock Binding Protein1) and HSP70 participate in the negative regulation converting the active HSFA2 homotrimers into inactive monomers that participate in the recycling of HSFs. Regulative mechanisms of the heat stress response have been proposed also for HSP90 which participates through the interaction of HSP70 in the negative regulation of HSF in absence of stress (Saidi, Finka, and Goloubinoff 2011).

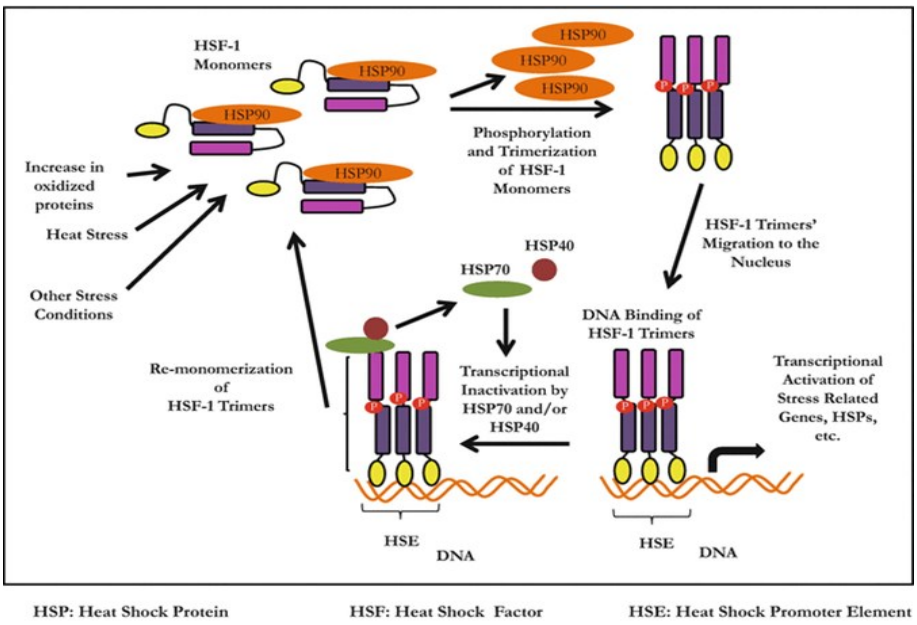

Fig 8. Mechanisms of HSPs activation, from *(Karademir and Sari-Kaplan 2016).*

1.4.3.1 HSP100s

Heat Shock Proteins with molecular weights between 100 and 104 kDa are classified into the HSP100 family. Under severe heat stress conditions, HSP100 proteins maintain the functionality of some polypeptides, allowing the resolution of nonfunctional protein aggregates and contributing to the degradation of irreversibly damaged polypeptides Gupta et al. 2010). Protein HSP100 plays an important role in solubilizing protein aggregates through interactions with the sHSP chaperone system (Bösl, Grimminger, and Walter 2006). A positive feedback loop between HSP100 and heat stress-associated protein 32-KD (HSA32) is known to prolong the effects of heat acclimation in rice seedlings (Lin et al. 2014).

Members of the *Hsp100* gene family were first described as components of the bacterial two-unit Clp protease system. The large ClpA unit represents an adenosine triphosphate (ATP)-dependent unfoldase, while the small ClpP unit is the protease. ClpA

alone has no proteolytic activity, but it can prevent aggregation of target proteins. Interestingly, many ClpA-related proteins have been characterized in bacteria and eukaryotes as stress-induced proteins and thus have been summarized as members of the HSP100 family (Park and Seo 2015).

1.4.3.2 HSP90s

The proteins in the class of HSP90s have a structure characterized by the N-terminal ATPase domain (ND), the central domain (MD) involved in substrate binding, and the C-terminal dimerization domain (CD) (Pearl and Prodromou 2006). Protein HSP90 needs to bind ATP to be activated; after binding, the "lid" segment of HSP90-ND rotates nearly 180° to enclose ATP, and the two HSP90-NDs come into contact to form a closed conformation of the dimer, creating an enzymatically active site for ATPase (Ali et al. 2006). Once ATP is hydrolyzed, the lid segment rotates and the dimer of HSP90 forms an open conformation (Kadota and Shirasu 2012).

The HSP90s and their co-chaperones are involved in abiotic stress responses; HSP90 and HSP70 negatively regulate heat stress transcription factors (HSFs) (Hahn et al. 2011).

The HSP90s also mediate disease resistance signal transduction pathways in plants and are involved in plant insect resistance signal transduction pathway (Xu et al. 2012).

1.4.3.3 HSP70s

The HSP70 family represents one of the most highly conserved classes of HSPs. In both animals and plants, HSP70s act as a chaperone for newly synthesized proteins to prevent their accumulation as aggregates and to ensure proper folding of proteins during their transfer to their final site (Hafrén et al. 2010). HSP70s localized in different cell compartments of the cell.

Proteins HSP70 are characterized by an ATPase domain in the N-terminal and a peptide-binding domain in the C-terminal of about 40 and 25 kDa in size respectively. They are separated by a hinge region susceptible to protease cleavage. A C-terminal subdomain of 5 kDa or less for many HSP70s is required for some interactions with co-chaperones (Sung, Kaplan, and Guy 2001).

HSP70 requires ATP to bind the substrate; these proteins switch from a state of low affinity for ATP to one of high affinity for ADP. The former state allows open conformation of the protein and binding to the substrate. HSP70s in order to function properly need the help of HSP40s, which act as co-chaperones (Hýsková et al. 2021).

1.4.3.4 HSP60s

HSP60 are a known class of chaperonins and are noted because they assist plastid proteins such as Rubisco (Wang et al. 2004). In addition, HSP60 are involved in the folding and aggregation of many proteins destined for organelles such as chloroplasts and mitochondria (Lubben et al. 1989). These proteins have double-ring-like structures and capture denatured substrate proteins in the central cavity.

1.4.3.5 Small HSPs

Some of the key players in the heat stress response are the small heat shock proteins (sHSPs) (Sun, Van Montagu, and Verbruggen 2002), known to be primarily involved in allowing the acquisition of heat stress tolerance and represent the first cellular defense lines against irreversible protein aggregation that occurs during various stresses (Waters 2013).

These are monomeric proteins and range in size from 12 to 42 kDa; many of them can form large oligomers with up to 40-50 subunits (Basha, O'Neill, and Vierling 2012).

All members of the sHSP superfamily are structurally characterized by the α-crystalline domain composed of about 90 amino acids within which lie two consensus regions (CRI and CRII), determining a β -sheet known to be essential for dimerization and higher order assembly (Figure 9). The N-terminal domain participates in the substrate binding and binds denatured proteins, while the C-terminal domain is involved in the homo-oligomerization and the Some of the key players in the heat stress response are the small heat shock proteins (sHSPs) (Sun, Van Montagu, and Verbruggen 2002), known to be primarily involved in allowing the acquisition of heat stress tolerance and represent the first cellular defense lines against irreversible protein aggregation that occurs during various stresses (Waters 2013).

These are monomeric proteins and range in size from 12 to 42 kDa; many of them can form large oligomers with up to 40-50 subunits (Basha, O'Neill, and Vierling 2012).

All members of the sHSP superfamily are structurally characterized by the α-crystalline domain composed of about 90 amino acids within which lie two consensus regions (CRI and CRII), determining a β -sheet known to be essential for dimerization and higher

order assembly (Figure 9). The N-terminal domain participates in the substrate binding and binds denatured proteins, while the C-terminal domain is involved in the homo-oligomerization and the

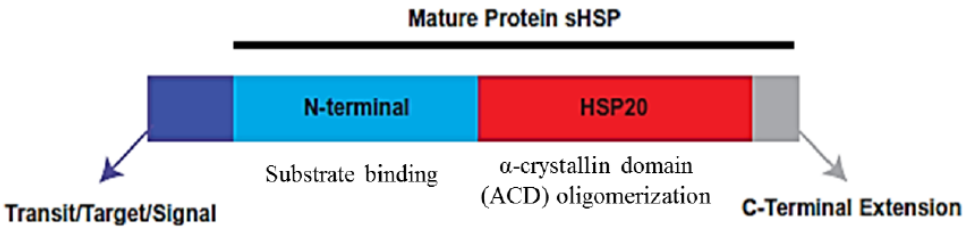

*Fig 9. s*HSPs protein structure. The sHSP monomer contains a variable N-terminal domain (light blue), a conserved α-crystalline domain (ACD) involved in oligomerization, and a variable C-terminal extension (grey). The sHSPs that localize to the organelles (chloroplast, mitochondrion, ER, peroxisome) have a transit, targeting or signal sequences (dark blue) that are needed for the entry into the organelles and are not part of the mature sHSP (reproduced from *Comastri 2016).*

The sHSPs are commonly induced by heat stress, some are induced exclusively either at a specific developmental stage(s) (Waters 2013) or in response to other abiotic stress agents (Rampino et al. 2012).

Plant sHSPs are all encoded by nuclear genes and are divided into six classes. Three classes (classes CI, CII, and CIII) of sHSPs are localized in the cytosol or in the nucleus and the other three in the plastids (P) the endoplasmic reticulum (ER) and the mitochondria (M) (Sun, Van Montagu, and Verbruggen 2002).

Specifically, eleven subfamilies of sHSPs have been identified in Angiosperms, of which six are deposited in the cytoplasm/nucleus; the other five localize in the endoplasmic reticulum, peroxisome, chloroplast or mitochondria (Waters 2013). Members of different subfamilies do not share a high degree of sequence similarity, although the overall secondary structure of the whole HSP protein family is relatively well conserved (Liu et al. 2021).

The involvement of the chloroplast small HSP in thermotolerance and thermomemory in Arabidopsis has been recently described (Sedaghatmehr, Mueller-Roeber, and Balazadeh 2016). The *A. thaliana* genome encodes 19 sHSPs (Cao 2022), compared to 23 in rice and 36 in poplar. At least 37 putative sHSPs encoding genes have been isolated in wheat (Comastri et al. 2018).

1.4.3.6 sHSP26

The *sHsp26* gene family in durum wheat was isolated and characterized by Comastri et al.2018, exploiting a TILLING approach. Four putative *TaHsp26* genes, namely *TaHsp26-A1, -A2, -A3*, and *-B1* were retrieved in the durum wheat genome (Comastri et al. 2018). The three A genome loci are localized on the short arm of chromosome 4A, while the single B genome locus is mapped on 4BL. The gene's topography is shown in Figure 10 (Comastri et al. 2018).

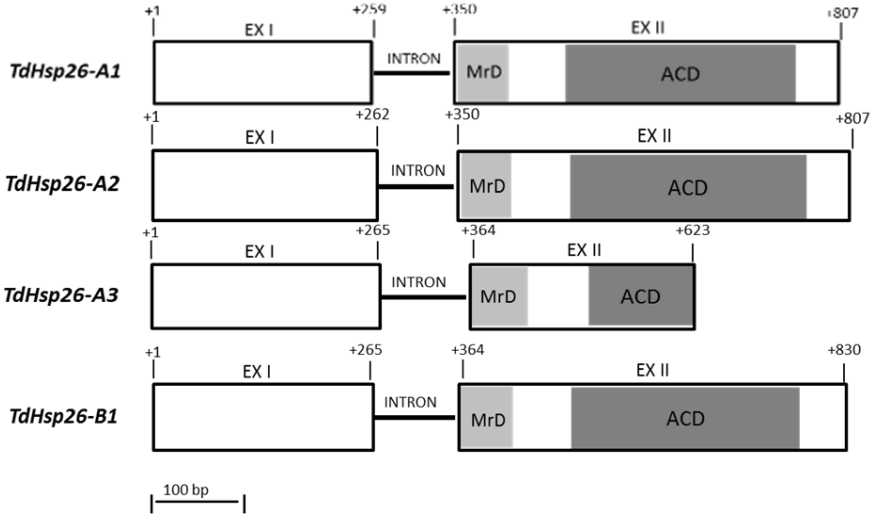

Fig 10. TdHsp26 gene structures. The conserved N-terminal MrD (Methionine-rich Domain) amphipathic a-helix is highlighted in light gray and the ACD in dark gray. The exon/intron junctions are indicated from (*Comastri et al. 2018*) .

In silico analyses placed these proteins in the chloroplast, thanks to the presence of a chloroplast Transit Peptide (cTP).

TdHsp26 genes were differently regulated upon direct heat stress and especially after acclimation. *TdHsp26-A1* showed the highest upregulation following direct heat stress and *TdHsp26-B1* the highest one when the heat stress was imposed after acclimation. This prompted us to focus on *TdHsp26-A1* and *-B1* genes in this research thesis.

1.5 Heat resilience

1.5.1 Genetic diversity and breeding to cope climate changes and heat stress

Climate change is strongly affecting crop yields and the increasing world's population, the development of improved crops more tolerant to the ongoing changes is needed to ensure food security and safety (Kholová et al. 2021).

Thus, understanding the mechanisms of heat tolerance, based on genetics and physiology, is critical to achieving this goal. The knowledge gained will be used to develop heat-tolerant cultivars suitable for sustainable growth under heat stress conditions (Shanmugavel et al. 2021).

Possible approaches to maintain high crop yields are (i) exploiting natural and induced mutations; (ii) harnessing available genetic resources to produce new genetic material more tolerant to HS and related secondary stresses; (iii) improving the ability to screen and identify available sources of resilience; and (iv) developing new breeding techniques (Janni et al. 2020).

Much of the genomic information is provided by sequencing, highlighting the presence of millions of Single nucleotide polymorphisms (SNPs), but resequencing of diverse germplasm (including wild species) also contributes. The SNPs are the most common form of DNA sequence variation between alleles, in several plant species. The discovery and application of SNPs increased our knowledge about genetic diversity and provided a better understanding on crop improvement (Morgil et al. 2020).

Modern breeding selection methods have been based on improvement of elite lines which have a narrow genetic base; this limits the genetic pool which breeders can exploit for the production of new varieties ready to face the predicted climate changes or adaptation to new cultivation areas (Pignone et al. 2015).

Germplasm resources could help mitigate the effects of climate change on agricultural production (Branlard et al. 2020).

Here, we explored the natural genetic diversity within the *sHsp26* gene family in a collection of durum wheat genotypes, mainly landraces, to identify novel sources of genetic diversity for breeding. The durum wheat germplasm collection was developed by Pignone et al, in 2015 in CNR to and consists of 452 genotypes originated in about 40 different world countries. (Pignone et al. 2015). From this collection, 33 genotypes were chosen for their

potential abiotic stress tolerance traits (Danzi et al. 2019; 2022) and qualities (Janni et al. 2018).

Previous works have reported the success in exploiting natural diversity to discover novel useful traits and QTL for abiotic stress tolerance mainly drought.

Allele mining approach was used to find SNPs in the *sHsp26* gene. Allele mining is useful for identifying nucleotide variation in a genomic region (candidate gene) associated with phenotypic variation for a trait. In this way, the frequency, type and extent of the occurrence of new haplotypes and the resulting phenotypic variations can be assessed (Kumar et al. 2010).

1.5.2 TILLING and EcoTILLING

To meet the demand for increased production of food crops it is necessary to introduce new selection strategies that accelerate the development of plants that are adapted to the changing environment. The use of induced mutations, combined with modern genomics tools, is an effective strategy to identify and manipulate genes for crop improvement. The high-throughput TILLING (Targeting Induced Local Lesions IN Genomes) methodology identifies mutations in mutagenized populations, while EcoTILLING identifies SNPs within a natural population and associates these variations with traits of breeding interest. The main advantage of these techniques as a "reverse genetics" strategy is that they can be applied to any species, regardless of genome size and ploidy level (Barkley and Wang 2008).

Germplasm collections can be useful resources for researchers for TILLING and EcoTILLING experiments, providing so much genetic information and/or to acquire the material needed for a study. On the other hand, TILLING could be applied in association/collaboration with germplasm repositories to develop mutant lines that have advantageous characteristics for breeders (Wang et al. 2017).

Previous work reported the efficacy of TILLING and ECOTILLING in producing and selecting novel material for the upcoming needs of wheat breeding (Sestili et al. 2010; Chen et al. 2012; Comastri et al. 2018; Irshad et al. 2020).

1.5.3 Phenotyping

Plants respond to abiotic stressors in a dynamic and complicated manner, both reversibly and irreversibly. Plant abiotic reactions have been studied physiologically,

biochemically, cellularly, and molecularly, revealing intricate cellular responses to abiotic stressors. However, phenotyping remains a cornerstone of plant breeding. Despite advances in genetics and the application of molecular technologies in crop research (Reynolds et al. 2020), crop breeding still relies heavily on the expression of grain yield and a handful of agronomically important traits for making selections and defining commercial products.

The phenotype is the functional body of a plant, formed during plant growth and development. It depends on the dynamic interaction between the genetic background and the physical world in which the plant develops. These interactions determine plant performance and productivity measured as accumulated biomass and commercial yield and resource use efficiency (Watt et al. 2020).

The term "phenotyping" refers to the application of methodologies and protocols to measure a specific trait related to plant structure or function, with traits ranging from the cell level to the whole plant level (Carvalho et al. 2021). In recent decades, phenotyping has developed as an essential tool for characterizing an enormous amount of plant processes, functions, and structures, mostly by non-destructive image-based optical analysis of plant traits. Therefore, plant phenotyping has started to become a tool applicable to plant scientists to understand plant-environment interaction and to plant breeders to select desirable genotypes for their specific field of interest, such as tolerance to abiotic stresses (Watt et al. 2020).

Technological improvement in the last decades in plant phenotyping has allowed the introduction of new non-invasive tools, ensuring a rapid and faithful structural parameters' extraction (Zhang et al. 2016). In this context, crop phenotyping platforms are considered a valid solution (Chawade et al. 2016). Phenotyping platform-based approaches enable high-throughput, automated and simultaneous multiple-plant screening, resulting in saving processing time and improved accuracy in the analysis of plant traits (Acharjee et al. 2018).

Automated platforms have been designed mainly for plant phenotyping in growth chambers or greenhouses and combine robotics, remote sensors and data analysis systems.

The drawbacks of most time-consuming phenotyping methods in terms of throughput and standardization have been overcome, in recent years, using image-based data collection (Araus, Buchaillot, and Kefauver 2022). Remote sensing technologies (Figure 11), with the respective controllers and data loggers that complement the imaging systems, are usually assembled into what are termed as phenotyping platforms (Araus et al. 2018). The use of

these platforms allows for a more efficient and accurate phenotyping with stable error across all genotypes, whether as single plants or in micro-plots. However, currently many of these platforms are costly and/or not applicable on a wide scale. Therefore, there is a strongly expressed need by the crop breeding community to develop both state-of-the-art and cost-effective, easy to use, and nonstationary (High Throughput Phenotyping Platforms (HTFP).

Within the hand-held category of platforms, smartphones are becoming an alternative since they may carry out different imagers (e.g., RGB and thermal), data management activities and geo-referencing functions (Araus et al. 2018; Sanchez-Bragado et al. 2020).

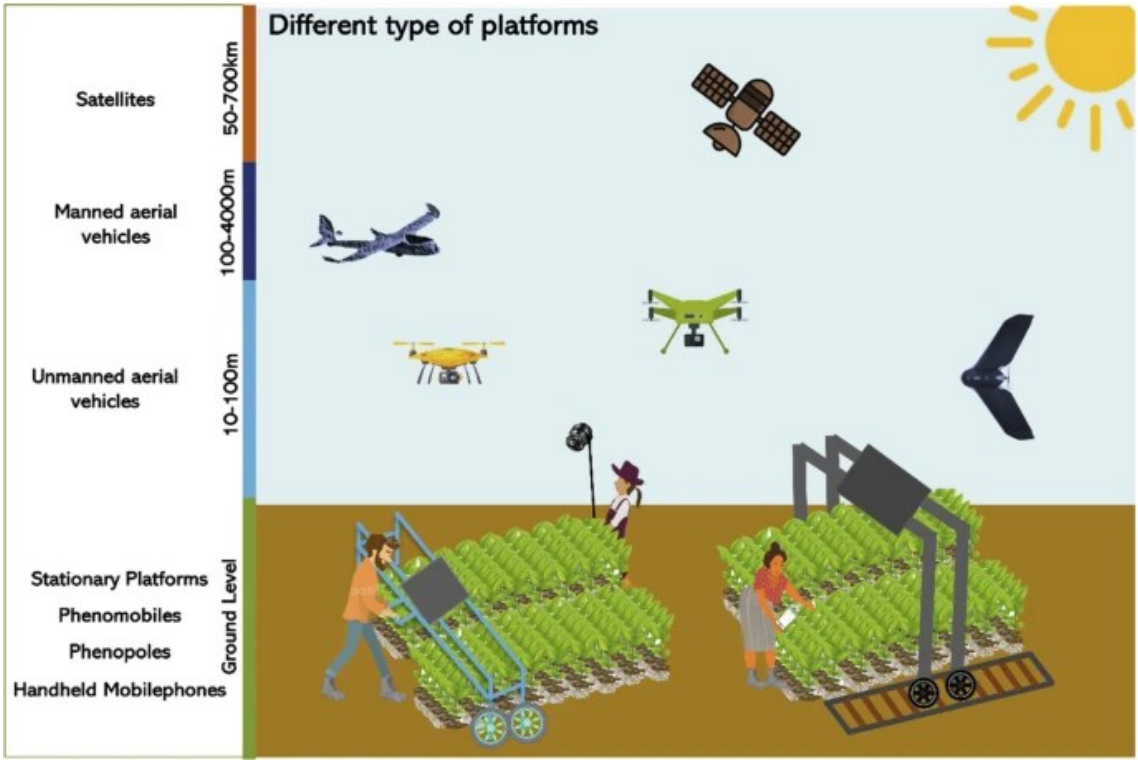

Fig 11. Different Categories of Ground and Aerial Phenotyping Platforms. Ground level: these include from Handheld sensors (in this case just a person holding a mobile), to Phenopoles, Phenomobiles, Stationary Platforms. From 10 to 100 m: Unmanned Aerial Vehicles, as drones of different sizes and compactness, fixed-wind drone. From 100 to 4000 m Manned Aerial Vehicles as airplanes or helicopters. In the near future different categories of satellites (Nanosatellite, Microsatellite and Satellites) from 50 to 700 km. (reproduced from *Araus, Buchaillot, and Kefauver 2022).*

Identifying the key traits for phenotyping may result in convergent approaches and in particular the genetic advance in wheat for a wide range of environmental conditions, has been associated with a higher stomatal conductance (Roche 2015) and higher final biomass.

To this end remote sensing techniques such as infrared thermometry or thermography may be deployed as proxies for higher transpiration (Impollonia et al. 2022). Greater biomass is also considered as a key target trait for selection under heat stress, since harvest index is reaching theoretical maximum, an increase in biomass becomes a target. The most canonical way to assess biomass is by using LiDAR (Light Detection and Ranging) mounted in an aerial platform or in a "phenomobile" (Madec et al. 2017). However still today the most common way to assess green biomass is through vegetation indices, either multispectral or RGB-derived, given the common perception these approaches being more affordable and easier to use than the LiDAR (Patrignani and Ochsner 2015, Figure 11).

Recently, a different class of sensor, referred to as a "bioristor," has been shown to be able to detect, in vivo and in real time, the changes in the composition of the plant sap in a growing tomato (*Solanum lycopersicum* L.) plant (Coppedè et al. 2017; Janni et al. 2019) , without interfering with plant functions. Bioristor is an organic electrochemical based transistor (OECT) realized on textile thread (Coppedè et al. 2017) and enables measuring the changes in ion concentration in the plant sap.

The pioneering application of bioristor in dicotyledonous plant species, such as tomato, successfully allowed detection of changes occurring in the plant sap composition following the day/night circadian cycle (Coppedè et al. 2017), as well as early detection of plant stress conditions under drought (Janni et al. 2019; Finco et al. 2022) and saline stress in monocots (Janni et al. 2021). The correlations among bioristor sensor response, changes in relative humidity, and vapor pressure deficit have been recently demonstrated, proposing the bioristor as a novel sensor to improve water use efficiency (Vurro et al. 2019).

2. AIM OF THE PROJECT

Climate change and the rise in temperature severely hamper crop growth and development. Several physiological drawbacks affect crop yields, also causing a modification in cultivated areas. At the same time, food production must double by 2050 to meet the demand of the world's growing population and innovative strategies are needed to help combat hunger, which already affects more than 1 billion people in the world. Wheat is one of the major cereal crops worldwide, providing 20% of the total dietary calories and proteins worldwide. FAO has projected a 43% increase in global demand for cereals, including wheat, by 2050, mainly from developing countries. To address these needs, the availability of new genetic materials exploitable in breeding programs is mandatory to achieve these goals.

The exploitation of the hidden in the genetic diversity contained in germplasm collections can be a key strategy to achieve this goal. Small *Hsps* represent a good target to improve heat resilience due to their strong involvement in the heat stress response in plants and in particular in wheat.

Here, an innovative approach, based on cost-effective targeted resequencing coupled with low-cost phenotyping techniques was applied to a set of durum wheat landraces to assess and exploit a possible genetic variation within the *sHsp26* gene family as a source of new improved heat resilience.

Plants have been subjected to heat stress at different developmental stages and we associated the different haplotypes of *TdHsp26* with the different responses to thermal stress, increasing the knowledge on the role of *TdHsp26* in the response to thermal stress.

3. MATERIAL AND METHODS

3.1 EcoTILLING and detection of natural variation in *TdHsp26-A1* and *TdHsp26-B1* in durum wheat genotypes

3.1.1 Plant material

This study was conducted on 33 durum wheat genotypes as a core set of a single seed descent (SSD) durum wheat collection, developed by IBBR-CNR in Bari (Pignone et al. 2015) and selected on the basis of a phenotyping selection (Danzi et al. 2019; 2022). In addition, 5 commercial varieties (Svevo, Saragolla, Cappelli, Colosseo and Kronos) were included as references in the experiments. A list of the genotypes and their geographic origin is provided in Table 2.

Table 2. List of genotypes and country of origin used for the allele mining approach.

SSD Entry	Origin
35	Algeria
44	Tunisia
64	Morocco
69	Morocco
92	USA-ND North Dakota
99	Ethiopia
109	Iraq
112	Iraq
116	Iraq
122	USA-ND North Dakota
135	Turkey
171	Peru
178	France
195	Saudi Arabia
244	Ethiopia
253	Cyprus
269	Iran
278	Bulgaria
322	Turkey
325	Syria
335	Iraq
343	Iran
397	Crete
409	Grece
415	Crete
416	Grece
441	Crete
451	Iraq
459	USA
487	Grece
494	Grece
499	
511	Libya
Colosseo	Italy
Kronos	USA
Cappelli	Italy
Saragolla	Italy
Svevo	Italy

Plants were grown in a growth chamber till seedlings stage (Zadoks 10) at 16°C with a photoperiod of 18/6 day/night. DNA was extracted as described in the next section (3.1.2).

3.1.2 DNA extraction and gene targeting

Genomic DNA was extracted with the GenElute™ Plant Genomic DNA Miniprep Kit (Sigma-Aldrich) from leaves tissues of durum wheat genotypes and analyzed through allele

mining approach that combines targeted enrichment PCR with next generation sequencing as described in (Buffagni 2019). Genomic region corresponding to *TdHsp26-A1 (LT220905)* and *TdHsp26-B1 (LT220911)* (1171 bp and 2575 bp respectively) were amplified by PCR to identify SNPs in the selected genotypes listed in Table 2 (Comastri et al. 2018). All the DNA of the SSD genotypes was kindly provided by IBBR-CNR (Bari, Italy).

TdHsp26-A1 and *TdHsp26-B1* (total 3.74 kb Mb) were targeted by PCR with 3 homeologous-specific primer pairs (PPs), 1 for *TdHsp26-A1* (PP1 F:5'-TGTTGGGCCTCCTGATCG-3'; R: 5'-AGCCTCAGATGCAGGGTAC) and 2 for *TdHsp26-B1* (PP2 F:5'-CAATTGGTTCGCACAAACAC-3'; R:5'-CCCTCCAGGCACGGATG-3' and PP3 F:5'-GACACTCTCTCGTTTCAATTCTC-3'; R:5'-GTTATCAGCTTCTTCCGGG-3'). PCR was performed in 25 µL final volume, using TaqDNA Polymerase (New England BioLabs, Hitchin, UK), 10–20 ng template DNA, 0.2 µmol/L of each forward and reverse primers, 0.2 mmol/L of each dNTPs, 1X Standard Taq Buffer (New England BioLabs).

PCR amplification with PP-2 was performed with touch-down PCR as follows: 1) initial denaturation at 95°C for 2 min 2) 10 cycles at 94 C for 25 s, annealing at 66°C for 30 s with a drop -0.5°C/cycle, elongation at 72°C for 1 min 30 s, 3) 35 cycles of 94°C for 25 s, annealing at 61°C for 45 s, elongation at 72°C for 1 min 30 s, 4) 1 cycle at 72°C for 10 min.

PCR amplifications with PP1-1 and PP-3 were performed as follows: 1) initial denaturation at 95°C for 2 min 2) 35 cycles at 95°C for 30 s, annealing at 60°C for 60 s, elongation at 72°C for 2 min, 3) 1 cycle at 72°C for 10 min. PCR products were checked on TAE agarose gel to ensure specific amplification of the targeted region.

PCR products were sequenced with BigDye™ Terminator v3.1 Cycle Sequencing Kit (Thermofisher Scientific, Waltham, MA) according to the manufacturer instructions.

As described in (Buffagni et al. 2018) 3 PCR reaction for all 38 genotypes were performed in 96 wells and then pooled in 4 tubes as follows:

- pool1 (SSD35, SSD92, SSD122, SSD171, SSD253, SSD269, SSD416, SSD487. SSD 494 and cv. Kronos),
- pool2 (SSD44, SSD109, SSD178, SSD322, SSD343, SSD397, SSD415, SSD511, cv. Colosseo),

- pool 3 (SSD69, SSD99, SSD116, SSD244, SSD335, SSD409, SSD441, SSD451, cv. Cappelli and cv. Saragolla),
- pool 4 (SSD64, SSD112, SSD135, SSD195, SSD278, SSD325, SSD459, SSD499, Svevo).

Each pool of PCR products was sequenced with the Illumina NovaSeq6000 (Novogene, Beijing, China).

3.1.3 Bioinformatics analysis of the NGS data

The paired-end (PE) reads raw data from the NGS were checked for QC using FastQC (http://www.bioinformatics.babraham.ac.uk/projects/fastqc/). The two fastq files of the PE of each sample were aligned to Kronos reference genome v.1.1 (https://opendata.earlham.ac.uk/opendata/data/Triticum_turgidum/EI/) using BWA (version 0.7.17) with parameters as default to generate the SAM files. Samtools (version 1.7) was used to convert the SAM to sorted BAM files for each sample. The BAM files were directly visualized with the Integrative Genomic Viewer IGV v. 2.4 (Broad Institute) for the SNP identification and selection. SNPs with a frequency ≥5% were selected for further investigation.

3.1.4 KASP Assay

Kompetitive Allelic Specific PCR (KASP) was used to identify SNPs within of the genes under study by defining the haplotype of each genotype. A primer master mix was constituted by two allele specific forward primers and one common reverse primer. The primers were designed through software PrimerWeb (http://primer3.ut.ee/) (Untergasser et al. 2012).Oligonucleotides were produced from Sigma-Aldrich (Gillingham, UK) and they present standard FAM or HEX compatible tails (FAM tail: 5' GAAGGTGACCAAGTTCATGCT 3'; HEX tail: 5' GAAGGTCGGAGTCAACGGATT 3'). In table 3 there is the complete list of primers. The KASP assay mix was prepared as recommended by LGC Genomics: 46 µL dH2O, 30 µL of 100 µmol/L common primer and 12 µL of each 100 µmol/L allele-specific primer. The reactions were set up in 10 µL of final volume, with 10-20 ng of DNA to test. Kronos sequence is the reference of this work, and it was considered as wild type control in the Kasp analysis. The PCR protocol comprised a 94°C/15 min denaturation, followed by 10 touchdown cycles of 94°C/20 s, 61°C [reducing by 0.6°C per cycle]/60 s, and 30 cycles of 94°C/20 s, 55°C/60 s.

Table.3. List of primer used in KASP assay

SNP ID	Position in gene	Ref base	Mut base	Primer reference/FAM gaaggtcggagtcaacggatt	Primer variant allele/VIC gaaggtgaccaagttcatgct	Primer common
TdHsp26A1_SPN1	Promoter	G	T	GCGGTGGGGATTTCATGc	AGCGGTGGGGATTTCATGa	**CAAACCTGAAGAACACCCGg**
TdHsp26A1_SPN2	Promoter	G	C	CCGCGCCCTTTTATAGAGc	CCGCGCCCTTTTATAGAGg	**CAAACCTGAAGAACACCCGg**
TdHsp26A1_SPN5	Exon 1	G	C	GCAGGGCAATGCAGTCg	GCAGGGCAATGCAGTCc	**TCTGCTTCTCCTACACCTGc**
TdHsp26A1_SPN8	Exon 2	G	A	CAGAGCCAGTCGCATGc	GCAGAGCCAGTCGCATGt	**GTGGAGGaCGACGCGCTg**
TdHsp26B1_SPN2	Promoter	G	T	TGTGTGAAAATCGTGTTTGCc	TGTGTGAAAATCGTGTTTGCa	**TGTCGCTTGTTACTTGATGTTc**
TdHsp26B1_SPN3	Promoter	A	T	CCCACTGCCACGGCAAGAt	CCACTGCCACGGCAAGAa	**TCAGGACAGGCAAACACGAt**
TdHsp26B1_SPN4	Promoter	G	A	TCTATCGCCGCTTTTCTTAATTTTc	TCTATCGCCGCTTTTCTTAATTTTt	**TGTGATGGTCAGGCTAATCg**
TdHsp26B1_SPN5	Promoter	G	A	TGCAAGTCCAAGTCCTCTATTTc	GCAGGGCAATGCAGTCc	**GGTGGACACTGGGGACAc**
TdHsp26B1_SPN6	Promoter	A	G	CACGGCATGCGAGGTGa	CACGGCATGCGAGGTGg	**CTCGTGATGTGACCTTTTCCc**
TdHsp26B1_SPN7	Promoter	C	T	TTTTCTCACGTTGCACCGc	TTTTCTCACGTTGCACCGt	**CTCGTGATGTGACCTTTTCCc**
TdHsp26B1_SPN18	Promoter	C	G	GGAAAGATGTTGAAGCTTCGg	GGAAAGATGTTGAAGCTTCGc	**AGACCTGAAGAACACCCGa**
TdHsp26B1_SPN19	Promoter	G	C	CTTCAACATCTTTCCCCGTCg	CTTCAACATCTTTCCCCGTCc	**CGGACTGCAGCTAAGTGGTt**
TdHsp26B1_SPN25	Promoter	A	C	GGTGGGAGATGGCGAGTt	GGTGGGAGATGGCGAGTg	**AGACCTGAAGAACACCCGa**
TdHsp26B1_SPN26	5'UTR	A	G	GGTTCTTATCTTGCTCGCTTGt	GGTTCTTATCTTGCTCGCTTGc	**TAAATGGGCGCGGCAAAc**
TdHsp26B1_SPN59	Exon 2	A	G	GAACAGCCGGTCCATCGt	GAACAGCCGGTCCATCGc	**AGTGTGAGAGAAGCAGAGCc**

3.1.5 Promoter functional motifs in Silico analysis

The promoters have been analyzed with the PlantCARE database (http://bioinformatics.psb.ugent.be/webtools/plantcare/html/) and NewPlace (https://www.dna.affrc.go.jp/PLACE/?action=newplace). The effect of the mutations present on the exons was analysed by SIFT software (SIFT predicts whether an amino acid substitution affects protein function).

3.2 Heat stress experiments

3.2.1 Plant growth and heat stress conditions of short-term HS

Seedlings experiment

Thirty-eight SSD genotypes were tested under heat stress conditions; 40 seeds for each line were sterilized with 10% (v/v) sodium hypochlorite for 2 minutes in agitation, briefly washed in distilled sterile water, and placed on a filter paper in 9 cm petri dishes for 7 days at 4°C. Once germinated, the plates, containing 8 seeds for each genotype with a total of 5 plates per line, were transferred to the growth chamber with light/dark 18/6h at 16°C. After 1 week the temperature was raised to 20°C. Ten-days-old seedlings (two leaves stage, Zadocks Z10) were subjected to heat stress at 38°C for 4 h (4hPS) and recovered for 1 h at 23°C (1hPR). Control plants were kept at 23°C during the experiment (Figure 12). One week post stress (1WPS), control (C1W) and stressed (S1W) plants were also sampled.

Tillering experiment

Based on the results of the seedling experiment, seeds of SSD69, SSD178, SSD244, SSD397, SSD415, Svevo and Kronos, were sterilized and placed on wet Whatman filter paper in Petri dishes for 7 days at 4°C. Once germinated, the seeds were transferred in pots containing 700g of soil mixture composed by 1/3 peat: perlite sterilized and mixed commercial soil. A total of 16 plants for each SSD were placed in 1,5 L pots, 4 plants each pot. Plants were grown in a growth chamber in controlled conditions, photoperiod light/dark 18/6 h with 18/15°C temperature. At the tillering stage (Zadoks Z31) the heat stress was imposed. The day before the stress the temperature was increased until 23°C. Temperature was set to 38°C for 4 h and recovered for 1h at 23°C. Control plants were kept at 23°C during the entire length of the experiment (Fig.12).

Leaves of control plants and stressed plants were sampled at the following timepoints: i) before the heat stress (T0), ii) 4 hours post stress (4hPS) and iii) 1 hour post recovery (1hPR). One week post stress leaves were sampled in both control and stressed plants C1W and S1W.

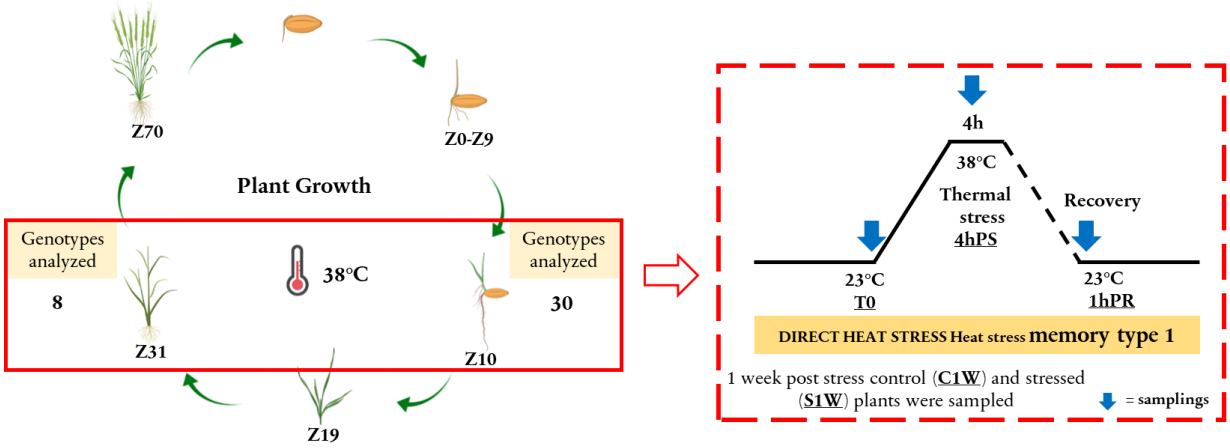

Fig 12. Sample scheme of short-term stress treatment applied. 30 genotypes were analyzed in seedlings, based on the results obtained 8 were chosen for the experiment in tillering.

Both seedlings as tillering experiments were conducted in a growth chamber and as indicated in Fig.12 the heat stress was imposed for a short time thus indicated so far as *short-term stress.*

Anthesis experiment

Based on the short-term HS in seedling and tillering experiment, two genotypes with contrasting phenotypes under heat stress were further selected and tested for the anthesis experiment: SSD69 and SSD397. Svevo and Kronos were subjected to long heat stress. Svevo is recognized in the literature to be tolerant to heat stress and is the control of our analysis, while Kronos in all previous experiments has an ambiguous phenotype.

At anthesis the stress was prolonged for the entire length of the experiments as grown in a greenhouse under natural environmental conditions thus indicated as *prolonged stress* (Figure 13).

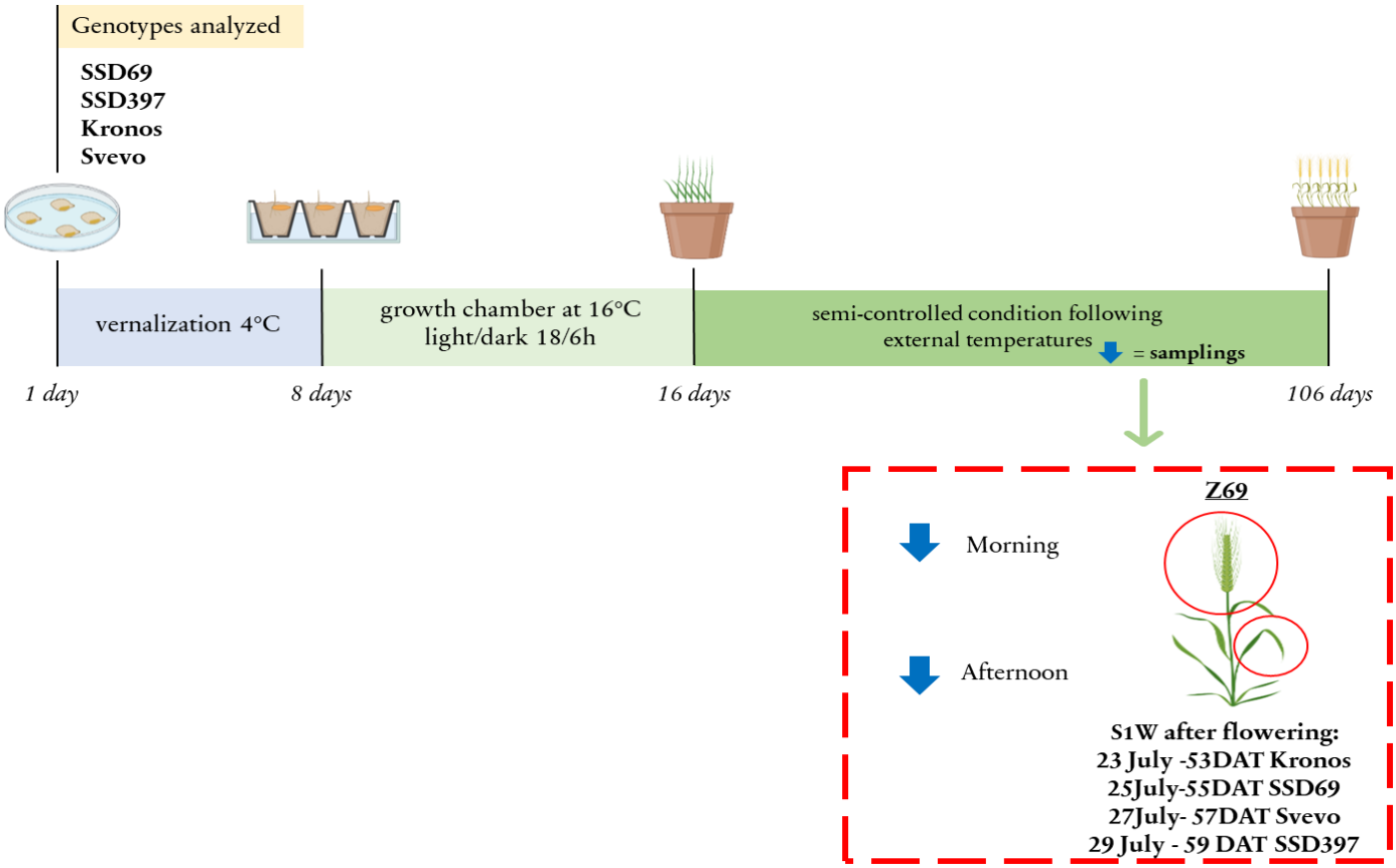

Fig 13. Experiment of heat stress in anthesis. After potting from day 16 until maturity, the plants experienced the indicated outdoor temperatures. One week after flowering Zadoks 69 leaves and spikes were sampled.

Seeds of SSD69, SSD397, Kronos and Svevo were surface sterilized with 10% (v/v) sodium hypochlorite and placed in a Petri dishes for 7 days and growth at 4°C, Once germinated, the seeds were transferred to seedbeds containing perlite soil in a 3:1 ratio and were placed in a growth chamber at 16°C with light/dark 18/6h day/night in controlled conditions in a greenhouse. After 8 days, the seedlings were transferred to 40-cm round pots containing 23.2 L of perlite potting soil in a 3:1 ratio. Each pot contained 6 plants, for a total of 4 pots for each genotype and 24 plants. The pots were kept under semi-controlled conditions in the greenhouse until sprouting, following the natural photoperiod and outdoor temperatures. Plants were regularly irrigated to avoid the occurrence of drought stress. The experiment began in June 2022 and ended in August 2022. To record the precise temperature and humidity of the environment, easylogUSB was kept in the greenhouse for the duration of the experiment.

The maximum and minimum temperatures of the environment during the experiment are shown in Fig.14.

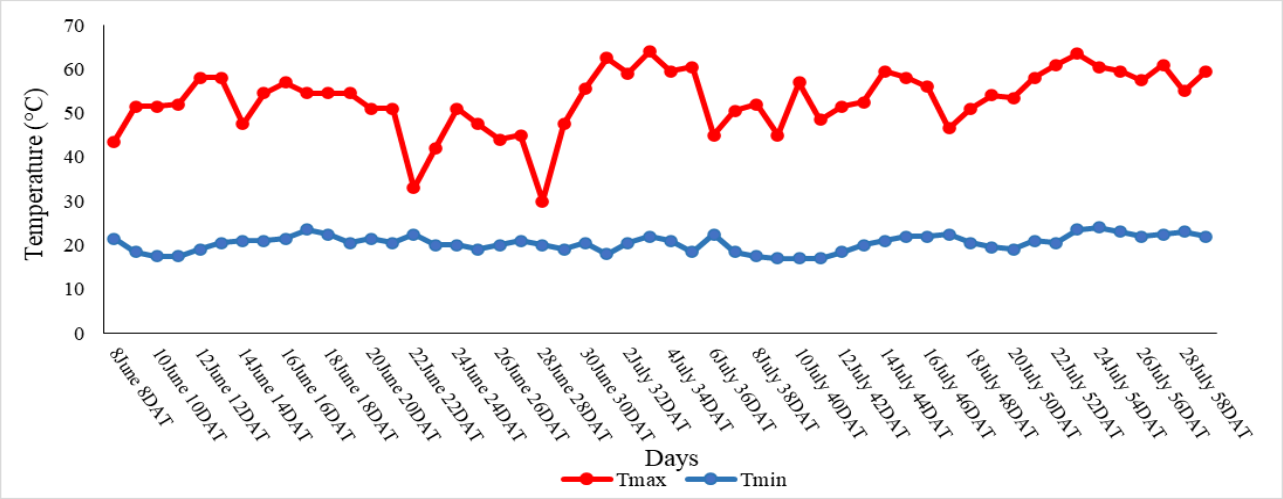

Fig 14. Environmental temperature over the experiment. Minimum and maximum temperature are indicated.

3.3 Phenotypic analysis

The list of the phenotypic analyses is reported in the following scheme (Fig. 15).

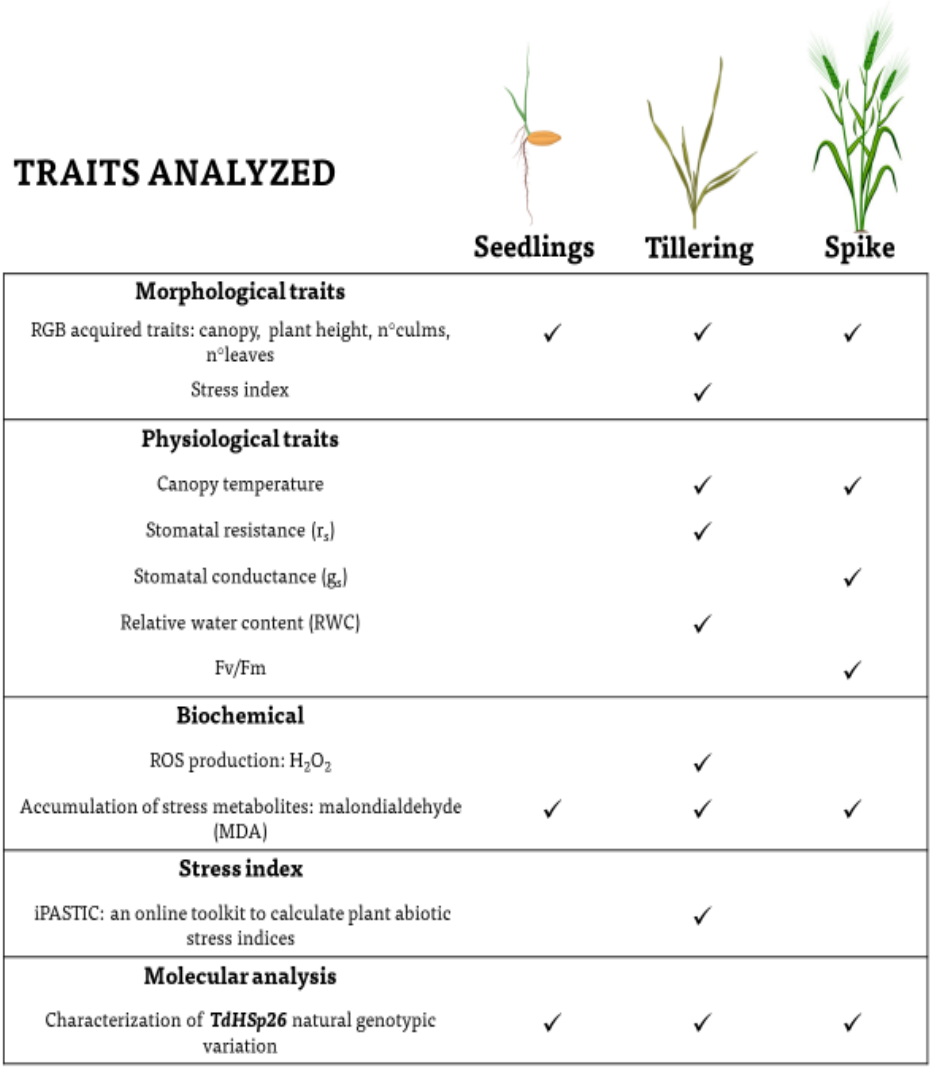

Fig 15. Phenotypic traits considered during the experimental phases in all developmental stages.

3.3.1 Morphological analysis

In *seedlings* experiment the length of C1W and S1W seedlings of the various genotypes was measured using ImageJ Software (available at http://rsb.info.nih.gov/ij/ accessed on 20 September 2021; developed by Wayne Rasband, National Institutes of Health, Bethesda, MD, USA) (Figure 16). Three replications for each condition were considered.

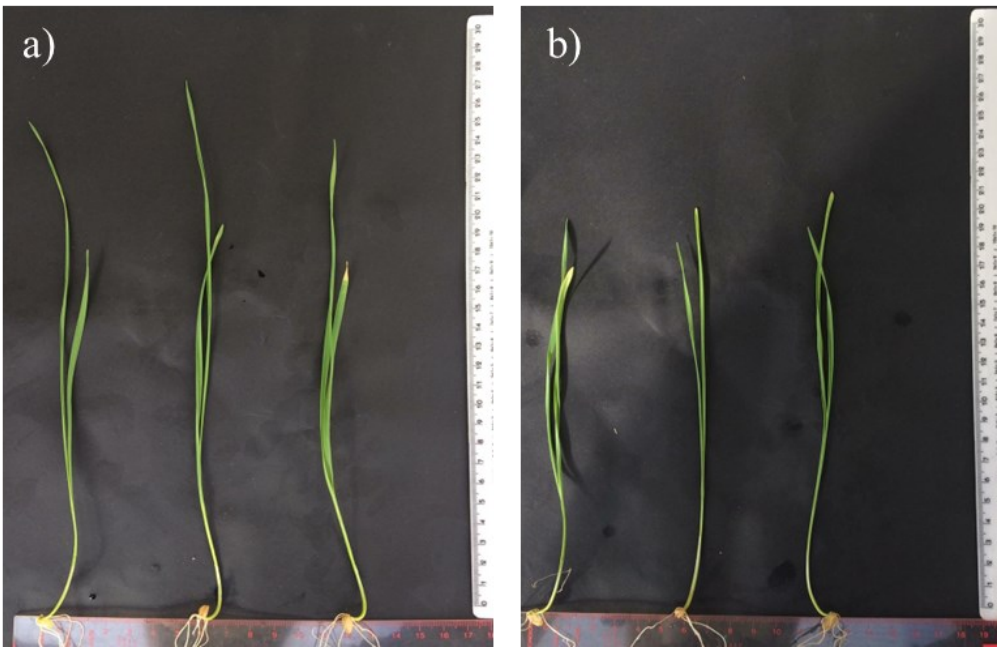

Fig 16. Images of the seedlings one week after stressing a) control b) stressed. The images were analyzed using ImageJ software.

In the tillering experiment, the plant height, number of culms, number of leaves one week post stress.

Leaf area and canopy of 3 plants for both control and stress plants were recorded before the stress, 48hPS and 1WPS. The leaf area has been calculated manually using the following formula Leaf area = Length x width x 0.75 (Kuzmanović et al. 2014; Ahmad et al. 2015); while canopy (%) was measured using CANOPEO app (Patrignani et al. 2015).

In the anthesis experiment, considering the prolonged stress, morphological traits were scored in tillering (Zadoks 31), stem elongation (Zadoks 54) and spiking (Zadoks 72) precisely at 30 DAT, 42 DAT and at 50 DAT. The number of leaves was detected only after 30 and 42 DAT, this is because at the end of elongation the arrangement of leaves changes with the death of some and the formation of new ones, which implies a loss of linearity that occurs in earlier stages instead. Plant Height, tiller number and leaves number were measured in 12 different plants, 3 plants for each pot for each line.

3.3.2 Biochemical analysis

In seedlings and tillering, samples were collected at times: T0, 4hPS, 1hPR, C1W and S1W and 8 replicates were sampled for seedlings and four in tillering for each genotype: the pools were immediately frozen with liquid nitrogen.

In anthesis sampling was performed one week after flowering (1WAF), in the morning at lower temperatures and in the afternoon at higher temperatures. Pools of 6 spikes and six leaves were made considering two leaves and two spikes from 3 plants of the same line were sampled and immediately placed in liquid nitrogen.

Malondialdehyde (MDA) content

The effect of heat stress on membrane lipid peroxidation was verified by quantifying the MDA content. To determine the concentration of malondialdehyde (MDA) the Thiobarbituric Acid (TBA) test was used following the protocol reported in Senthilkumar et al (2021)(Senthilkumar, Amaresan, and Sankaranarayanan 2021). 50 mg of leaves grounded in liquid nitrogen, 1mL 0.1% (w/v) trichloroacetic acid (TCA) has been added to precipitate the proteins. The homogenized samples were centrifuged at 14,000 *g* for 15 min. Subsequently, 250 µL of the supernatant was added to 1000 µL of 20% (w/v) TCA containing 0.67% (w/v) TBA. The mixture was boiled at 95°C for 30 min in a water bath and quickly cooled in an ice bath for 10 min to stop the reaction. The mixture has been centrifuged at 10,000 rpm for 5 min and the supernatant was collected. The absorbance was read at 532 and 600 nm and calculate the concentration of MDA-TBA concentration based on the Ɛ value using a Varian Cary 50 spectrophotometer. Where, Ɛ is the coefficient absorbance (1.55 mM^{-1} cm^{-1}). The amount of malondialdehyde is expressed as nmol mg−1 FW.

$$\frac{(MDAstressed - MDAcontrol)}{MDAcontrol} \times 100$$

Determination of Hydrogen peroxide H_2O_2

The Hydrogen peroxide (H_2O_2) concentrations were determined, in tillering experiment, following Velikova et al. (2008) (Velikova, Fares, and Loreto 2008), with some modifications. Leaf tissues (50 mg) were homogenized in an ice bath with 1mL 0.1% (w/v) trichloroacetic acid (TCA) The homogenate was centrifuged at 12,000 *g* for 15 min at 4°C. Then 250 µL of the supernatant was added to 250 µL 10 mmol/L potassium phosphate buffer

(pH 7.0) and 500 µL 1mol/L KI and the supernatant held for 20 min at room temperature, after which the absorbance was read at 390 nm using a Varian Cary 50 spectrophotometer. H_2O_2 content was determined using the extinction coefficient 0.28 µM−1cm−1 (Dong et al. 2014). The amount was expressed as nmol mg−1 FW.

3.3.3 Physiological measurements

Photosynthesis: Photosystem II (PSII) efficiency: Fv/Fm

To evaluate the effect of high temperatures on photosystem II, Fv/Fm was measured using FluorPen FP110, in the anthesis experiment. One measurement per plant was made for a total of 9 measurements. The reading was taken after 15 min of darkness. The analyses were done at day 42 DAT (near flowering) and one week after flowering (1WAF), which was recorded for each genotype. For each day, measurements were taken at two different times of the day in the morning from 8 to 10:30 am and in the afternoon from 2 to 4:30 pm to assess the effects of high temperatures on the various parameters analyzed.

Transpiration: Stomatal Resistance (r_S) and stomatal conductance (g_s)

Stomatal resistance expressed (sec cm^{-1}) and stomatal conductance (mmol m^{-2} s^{-1}) were measured in the tillering and the anthesis experiment respectively by using AP4 porometer (Delta-T Devices).

In tillering stomatal resistance was acquired at the following time points: T0 (before stress), 4hPS (4 hours post stress), 48hPS (48 hours post stress) and finally after one week post stress in C1W and S1W. Three flag leaves from three plants per plot were measured for stomatal resistance, six readings per leaf.

In anthesis g_s was measured. The measurements were done at day 42 DAT and 1WAF at two different times of the day, in the morning from 8 to 10:30 am and in the afternoon from 2:00 pm to 4:30 pm to assess the effects of high temperatures on the conductance.

Canopy temperature: Infrared Leaf Temperature (IR) and Canopy Depression Temperature (CTD)

Thermal imaging was applied using an infrared thermal camera FLIR E75 to detect the canopy temperature during the stress. The camera resolution is 320 x 240 pixels, thermal

sensitivity lower than 0.03° C, emissivity used was 0.99. three pictures. 3 photos per plant were acquired for each analysis.

In tillering the measurements were taken at the following time points T0 (before stress), 4hPS (4 hours post stress) C1W and S1W. Three pictures of each plant were acquired.

In anthesis the measurements were done at day 42 DAT (near flowering), and one week after flowering at two different times of the day, in the morning from 8 to 10:30 am and in the afternoon from 2 to 4:30 pm to assess the effects of high temperatures on the conductance. Two vessels per genotype were considered, for a total of 12 photos per genotype.

The thermal images were analyzed using R software (R Core Team, 2022) and the Therm-image package (https://cran.r-project.org/web/packages/Thermimage/index.html).

To segment vegetation from the background, pure vegetation pixels were classified by applying a k-means clustering algorithm on thermal images. The average canopy temperature for each plant was extracted from pure vegetation pixels. An example of a thermal image clustering during the experiment is shown in Figure 17.

Once leaf temperature was known, we calculated canopy thermal depression (CTD), defined as the difference between plant canopy temperature and ambient temperature, has been recognized as key trait to evaluate/compare the response of genotypes to low water use, high temperatures and other environmental stresses.

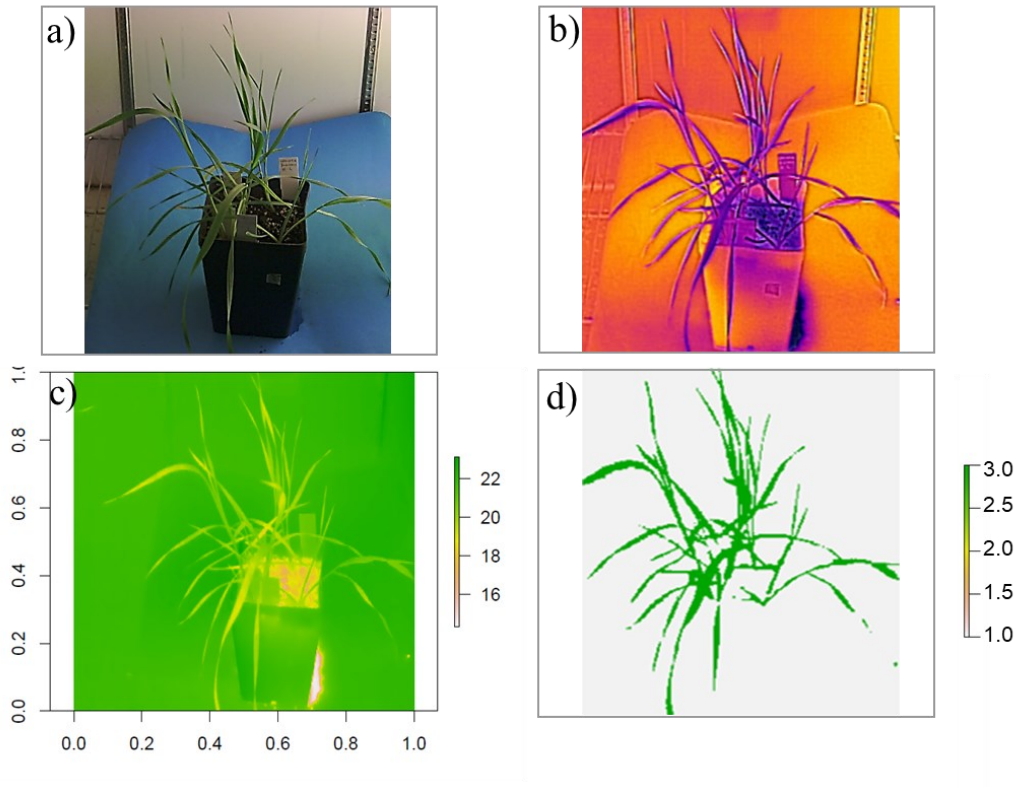

Fig 17. a) RGB image, b) thermal image acquired with the thermal camera FLIR 075, c) thermal image with graduated scale, d) image clustered by the k-means algorithm for plant segmentation.

Relative Water Content (RWC)

The RWC content was measured in leaves following the protocol reported in Celik, (Çelik, Ayan, and Atak 2017). Three leaves were randomly collected to determine relative water contents within each group. After measuring the fresh weights (FW), leaves were placed into the distilled water for 12h in order to obtain turgid weight. (DW) Following the turgid weight (TW) measurement, leaves were heated in a dry heat incubator for 24h (80°C) to obtain dry weights. Relative water contents (RWC) were calculated according to the formula as reported by Smart (Smart and Bingham 1974):

$$RWC = \frac{(FW - DW)}{(TW - DW)} * 100$$

3.3.4 Yield traits

In the *tillering* experiment, the first spike of control and stressed plants of each genotype was analyzed for the:

- number of seeds per spike.
- Kernel Yields Per Spike (KYPS), consists of weighing the seeds obtained from each ear, the weight is expressed in grams.

  In *anthesis* were measured:
- Spike Length (SL), of all spikes from the main culm, was measured from the base of the rachis to the tip of the terminal spikelet, excluding the awns;
- Grain Yield per plant, consists of weighing the seeds obtained from each plant, the weight is expressed in grams;
- number of seeds per plant;
- number of spikelets of all spikes arising from the main culm.

3.3.5 Stress indices

To calculate common stress tolerance and susceptibility indices for various crop traits, the iPASTIC (*The Plant Abiotic Stress Index Calculator)* software (Pour-Aboughadareh et al. 2019) was used. The indices acquired through iPASTIC are the following: tolerance index (TOL), relative stress index (RSI), mean productivity (MP), harmonic mean (HM), yield stability index (YSI), geometric mean productivity (GMP), stress susceptibility index (SSI), stress tolerance index (STI) and yield index (YI). The program estimates an Average Sum Ranks (ASR) for all indices to select potentially superior genotypes; the lower is the ASR value, more tolerant is the genotype. The grain yield per plant, expressed as the number of seeds per plant, was used to run iPASTIC was the yield of stressed and not stressed plants for each genotype.

3.4 *TdHsp26-A1 and TdHsp26-B1* gene expression

3.4.1 Sample collection

For the short-term stress in seedlings and tillering, leaf material for gene expression analysis was collected at times T0, 4hPS and 1hPR.

For long-term stress, sampling, again of leaf material, was done one week after flowering. The flowering time of each genotype was monitored, and sampling in target days. Seven days post the anthers emission, two samplings were done, one early in the morning and the second in the afternoon with the highest temperatures.

3.4.2 RNA extraction and cDNA retrotranscription

For all experiments, RNA was extracted with RNeasy Plant Mini Kit (Qiagen, Hilden, Germany) from all samples, and visualized on agarose gel (1,2% agarose w/v, 1X TAE buffer, GelRed™ as Nucleic Acid gel stain) to assess its integrity.

For each condition, 1 µg of total RNA samples extracted from 100 mg of frozen tissue were retro-transcribed into cDNA with QuantiTect Reverse Transcription Kit (Qiagen) according to the manufacturer instructions.

3.4.3 Quantitative Real Time PCR (qtPCR)

Real Time (RT) qPCR analysis was performed using CFX96 Touch Real-Time PCR Detection System (Biorad). PCR reactions were set up in 10µL containing 1µL of 1:10 dilution of cDNA, 0.25 nmol/L of gene-copy specific forward and reverse primers (Table 4) A1-PT31F/A1-PT31R, B1-PT10F/B1-PT10R (Comastri et al. 2018). *TdACT* gene (AB181991) was used as housekeeping.

Table 4. List of primers used for the Real time qPCR

Target	Primer Forward	Primer Reverse	Forward 5' – 3'	Reverse 5' – 3'	Amplicon size (bp)
TdHsp26-A1	A1–PT31F	A1–PT31R	CCAGGCCCAGAACGCT	CCTCCTTcTCGTCCTCCATa	338
TdHsp26-B1	B1-PT10F	B1-PT10R	CGATGCGGCAGATGCTT	TGACGAGCGCGTCGC	211
TdACT	ACT-Fw	ACT-Rev	CTTGTATGCCAGCGGTCGAA	TGAGGAAGCGTGTATCCCTCG	96-173

For the samples collected in *seedlings* and *anthesis*, we calculated expression level changes by ΔΔCT. Starting from we ΔCT as $CT_{target\ gene}$ - $\Delta CTi_{internal\ standard}$; ΔΔCT was calculated as $CT_{treatment}$ - $CT_{control}$. For seedlings the $CT_{control}$ is the sampling at T0, while for the anthesis experiment the $CT_{control}$ is the sampling done in the morning S1W after flowering. Gene expression was considered relevant when fold-change was greater than 2 (FC ≥ 2).

In the samples collected in the *tillering* experiment we applied semiquantitative RT-PCR for *Hsp26* gene expression. The amplicons were loaded on a 1.2% agarose gel. The

bands were analyzed by ImageJ software and normalized for the band of the housekeeping genes.

3.5. Data analysis

For the experiment in seedlings: Student t-Test was applied to analyze the difference of plant height and for the analysis of data inherent to gene expression.

For data analysis on MDA content, ANOVA test with p-value <0.05 was used using Past 4.03 software, the next post hoc used was Tukey's test.

In the tillering experiment: Leaf Area, number culms, Plant height, stomatal resistance, CTD and gene expression analysis were analyzed by Student t-Test.

Infrared Leaf Temperature, average sum of ranks, H_2O_2 and MDA were analyzed by ANOVA test with p-value <0.05 using Past 4.03 software, the next post hoc used was Tukey's test.

Principal component analysis (PCA) was performed using the R statistical software version 4.2.1.

In Anthesis experiment: morphological data and gene expression data were analyzed by ANOVA test with p-value<0.05 using Past 4.03 software the next post hoc used was Tukey's test. CTD, IR, MDA were analyzed with Student t-Test.

Correlation analysis was done by was performed using the R statistical software version 4.2.1.

4. RESULTS AND DISCUSSION

4.1 Materials and Approaches used to discover novel natural variability to increase heat stress resilience

In 2018 Comastri and coworkers isolated and characterized four members of the chloroplast-localized small heat shock proteins (sHSP) encoded by the *sHsp26* gene family. A TILLING approach *in vivo* and *in silico* was used to identify novel alleles within this family. The choice of the target genes used in this work was based on the known protective role played by sHSPs such as HSP26 over photosynthesis and the synthesis and compartmentalization of key metabolites in plants challenged by high temperature stress (Maestri et al. 2002; Chauhan et al. 2012; Khurana, Chauhan, and Khurana 2013). The *TdHsp26* family in durum wheat was composed of four functional genes, three mapping to the 4A chromosome and one to the 4B genome homoeologue. *TdHsp26* genes were differently regulated upon direct heat stress and especially after acclimation. *TdHsp26-A1* showed the highest upregulation following direct heat stress and *TdHsp26-B1* the highest one when the heat stress was imposed after acclimation (Comastri et al., 2018).

The *in vitro* transcriptomic analysis was extended to other tissues and to stress conditions by querying the *in silico* ExpVIP database. For instance, *TdHsp26* genes were strongly up-regulated by high temperature but even more by a combination of high temperature and drought, suggesting a role of sHSPs in both stress responses(Al-Whaibi 2011; Rampino et al. 2012; Khurana, Chauhan, and Khurana 2013).

Based on these results and considering the strong involvement of *TdHsp26-A1* and *TdHsp26-B1* genes in regulating the heat stress response, in this thesis, we exploited the natural variation represented in the durum wheat germplasm collection, targeting *TdHsp26-A1* and *-B1* genes by using an EcoTILLING approach to discover novel sources of variability to increase the heat tolerance in durum wheat.

4.2 EcoTILLING *approach* to discover the natural variance in *TdHsp26-A1* and *TdHsp26-B1* in durum wheat genotypes

4.2.1 SNPs identification in TdHSp26 genes

To identify the natural allele variants in the *TdsHsp26* genes in durum wheat, a targeted-resequencing strategy was used as proposed in (Buffagni 2018) to perform allele mining in a set of durum wheat landraces and 4 reference varieties, selected based on their behavior under heat stress.

Targeted-resequencing is a PCR-based approach that allows the sequencing of a panel of genes of interest by NGS prior to the identification of the full-length target sequences. The approach generates multiple overlapping PCR-products spanning the whole target sequences of both *TdHsp26-A1* and *-B1* genes.

The approach includes the pool of target genotypes DNAs to increase the throughput of the target sequence analyses and application of KASP markers for the SNPs detections to facilitate the identification of SNPs and reduced costs. Based on this method, a list of SNPs was identified (Supplementary table 1), but only SNPs with a frequency > 5% were selected considering that a 99% of homozygosity was expected for the 33 SSD genotypes and the 5 selected cultivars in all the loci (Figure 18). A 9-10% SNP frequency is expected for a single genotype variant. By applying this method 15 SNPs were identified. Three out of the 15 SNPs fall within the Coding Sequence (CDS), suggesting a high conservation of the genes during the durum wheat domestication. Two SNPs were in the promoter region of *-A1* gene and 9 in the promoter of *-B1* gene and 1 SNP was found in the 5'-UTR. In addition, missense mutations were found, one on the TdHSP26-B1 protein (amino acid variant M97V) and two on the TdHSP26-A1 protein (amino acid variant E73Q and G196D). The presence of the highest rate of variability in the regulatory elements allows to hypothesize a role of these mutations in the adaptation to challenging agro-climate conditions.

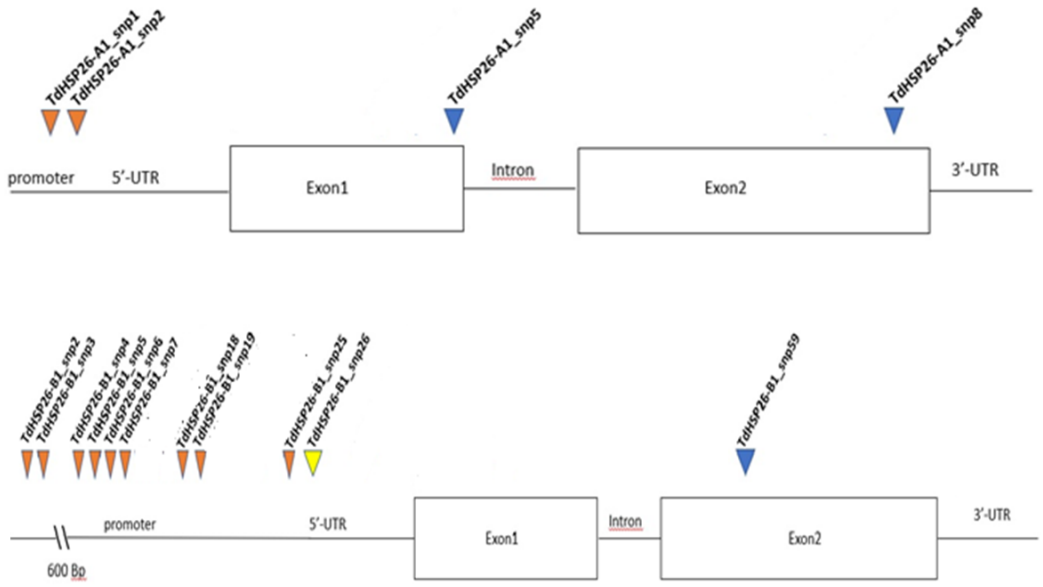

Fig 18. Schematic representation SNPs with a frequency > 5% in *TdHsp26-A1* and *TdHsp26-B1.*

4.2.2 SNPs localization and heat stress experiment

KASP assays markers were used to confirm the SNP detected and to assign the retrieved SNPs to a specific genotype (Tab.2). Only the SNPs with a frequency >5% were considered. The SNP frequency within single genotypes varied from 5% to 16%, depending on the SNP, probably due to an imperfect relative balance of the PCR-products during pooling of samples.

Fourteen different haplotypes were identified, 5 for *TdHsp26-A1* and 9 for *TdHsp26-B1* genes. The B6 SNP located in the-*B* promoter is present in all the genotypes with exception for SSD322 and SSD415. In *TdHsp26-A1* the most variable haplotype presents 3 SNPs and was identified in SSD195. The SSD244 showed the bigger number of mutations at promoter *TdHsp26-B1* level. Considering the functional redundancy typical of wheat homoeologues, it is interesting to observe the haplotypes combination retrieved for both -*A1* and -*B1* genes in each SSD/variety.

A total of 17 different haplotype combinations were identified in both *TdHsp26s* (Tables 5-7).

Table 5. List of the haplotypes identified in *TdHsp26-A1*

SSD	***SNPs in TdHsp26-A1***
64,69,92,112,116,122,135, 171,322, 325, 415,459, 499	A5 Exon1, A8 Exon2
195	A1 Promoter, A5 Exon1, A8 Exon2
253,409, 441	A5 Exon1
451	A8 Exon2
494	A2 Promoter, A5 Exon1

Table 6. List of the haplotypes identified in *TdHsp26-B1*

SSD	***SNPs in TdHsp26-B1***
35,64,99,116,122,135,171,195, 269,278,325,416,441,451,459, 487,494, 499, Colosseo, Cappelli, Svevo	B6 Promoter,
69	B6 Promoter, B19 Promoter
92	B3 Promoter, B6 Promoter
112	B6 Promoter, B59 Exon2
178	B6 Promoter, B7 Promoter
244	B6 Promoter, B18 Promoter, B25 Promoter
253	B6 Promoter, B26 5'UTR
397	B4 Promoter, B5 Promoter, B6 Promoter
409	B5 Promoter, B6 Promoter

Table 7. Haplotype combinations identified in *TdHsp26-A1 and -B1* genes through KASP analysis.

HAPLOTYPE COMBINATION	SSD	SNPs	GEOGRAPHIC ORIGIN
1	44,109,343,511	no SNPs reported	Tunisia, Iraq, Iran, Lybia
2	35,99,269,278,416,487, Cappelli, Colosseo, Saragolla, Svevo**	B6 Promoter	Algeria, Ethiopia, Bulgaria, Greece, Greece, Italy, Italy, Italy, Italy
3	64,116,122,135,171,325,459,499	B6 Promoter, A5 Exon1, A8 Exon2	Morocco, Iraq, USA-ND North Dakota, Turkey, Peru, Syria, USA
4	69**	B4 Promoter, B6 Promoter, B19 Promoter, A5 Exon1, A8 Exon2	Morocco
5	92	B3 Promoter, B6 Promoter, A5 Exon1, A8 Exon2	USA-ND North Dakota
6	112	B6 Promoter, A5 Exon1, A8 Exon2, B59 Exon2	Iraq
7	178*	B6 Promoter, B7 Promoter	France
8	195	A1 Promoter, A5 Exon1, A8 Exon2, B6 Promoter	Saudi Arabia
9	244*	B6 Promoter, B18 Promoter, B25 Promoter	Ethiopia
10	253	A5 Exon1, B2 Promoter, B6 Promoter	Cyprus
11	322,415*	A5 Exon1, A8 Exon2	Turkey, Crete
12	335	B6 Promoter, B26 5'UTR	Iraq
13	397**	B4 Promoter, B5 Promoter, B6 Promoter	Crete
14	409	B5 Promoter, B6 Promoter A5 Exon1	Greece
15	441	A5 Exon1, B6 Promoter	Crete
16	451	A8 Exon2, B6 Promoter	Iraq
17	494	A2 Promoter, B6 Promoter, A5 Exon1,	Greece

All genotypes were subjected to heat stress in the seedling stage. (*) haplotypes selected also for the tillering heat stress experiment, (**) haplotypes selected for anthesis heat stress experiment.

4.2.3 Effects of SNPs on TdHsp26 promoter

Through Place and PlantCARE, the effect of mutations on the regulatory elements (*cis*-acting element) of *TdHsp26* promoter sequences was evaluated. The SNPs that resulted in changes in the promoter regulatory elements are SNP2, SNP4, SNP6 and SNP25 present in the promoter of the *TdHsp26-B1*. SNP 4 and 6 cause the loss of two *cis*-acting elements that are annotated as being involved in plant responses to environmental factors, respectively, GT1CONSENSUS for light and salicylic acid (Villain, Mache, and Zhou 1996) and GTGANTG10 involved in primary metabolism and playing an important role in the regulation of pollen-specific gene expression (Rogers et al. 2001). In contrast, SNP2 and SNP25 lead to the formation of two cis-acting elements, respectively: RYREPEATBNNAPA involved in seed-specific expression (Ezcurra et al. 2000) and DPBFCOREDCDC3 annotated as bZIP class transcription factors in carrot (Ramkumar et al. 2015) (Table 8). The SNPs identified in the promoter region of *TdHsp26-A1* did not result in changes in the regulatory regions of the promoter from the reference sequence.

Table 8. SNPs identified in the promoter region and their effects on the regulatory elements and function. The SSD genotypes carrying the mutation in the promoter region are listed.

PROMOTER ANALYSIS						
SNP IN *TdHsp26-B1*	**Reference sequence**	**Mutant sequence**	**Effects on Promoter**	**Role**	**Reference**	**SSD**
SNP2	CAGGCA	CATGCA	Formation of RYREPEATBNN	Required for seed specific expression	*Ezcurra et al., 2000*	253
SNP4	GAAAAT	AAAAAT	Loss of GT1CONSENSUS	Consensus GT-1 binding site in many light-regulated genes	*Villain et al., 1996*	397,69
SNP6	GTGA	GTGG	Loss of GTGANTG10	Primary metabolism: tissue (late pollen)	*Rogers et al., 2021*	All genotypes except for 322, 415
SNP25	CAAACTCG	CACACTCG	formation of DPBFCORED	plant male reproductive tissue specific.	*Ramkumar et al., 2015*	244

The effect of mutations on the protein function was also verified *in silico* through SIFT software (Ng and Henikoff 2003).

It returns a number ranging from 0 to 1 and is linked to the possible damage of the protein function. Amino acid substitution is harmful when the score is < 0.05 and tolerated if the score is > 0.05. Within the SNPs retrieved, none of those caused deleterious mutations to the protein function, but different values were assigned to the SNPs.

Of great interest are SNP5 found in exon I and SNP8 in exon II, both located in *TdHsp26-A1*, other SNP of interest is in exon II of the *TdHsp26-B1*gene, all SNPs cause missense mutation (Table 9). Of high interest the SNP8 causing G196D substitution in the α-crystallin domain, which is characterized by two highly conserved regions, (Bondino, Valle, and ten Have 2012), thus the presence of a SNP in this region suggests a possible deleterious effect on the protein function.

SNP59 had the lowest tolerance value 0.10 followed by SNP5 which was assigned a value of 0.23, while SNP8 despite being in the α-crystallin domain is the one the software assigned value 1, thus tolerable.

Table 9. List of SNPs in exons analyzed with SIFT

EXONS ANALYSIS				
Gene	**Mutation type**	**Effect**	**Score Sift**	**SSD**
TdHsp26-A1	SNP5 MISSENSE	E73Q	0,23	*64,69,92,112,116,122,135,171, 195, 253, 322, 325, 409, 415,441, 459,494,499*
TdHsp26-A1	SNP8 MISSENSE	G196D	1	*64,69,92,112,116, 122, 135, 171, 195,322, 325, 415, 451, 459, 499*
TdHsp26-B1	SNP59 MISSENSE	M97V	0,10	*112*

Some of the analyzed genotypes possess many of the listed mutations: SSD69 shows SNPs 5,8 of *TdHsp26-A1* gene, the SNPs 4,6 of *TdHsp26-B1*; SSD253 has SNPs 2,5 in *TdHsp26-A1* and SNP6 in *TdHsp26-B1*; SSD112 has SNP5,8 in *TdHsp26-A1* and SNP6, 59 in *TdHsp26-B1*.

The hypothesis of a possible correlation between haplotype combination in the *TdsHSp26* genes and the different phenotypes in response to heat stress, was formulated.

4.3 Does the genetic variation identified in *TdHsp26* sequence impact on the heat stress response?

4.3.1 Heat stress response in seedling stage

Morphological traits

Plant height after one week post stress was performed. Three different trends were observed SSD44, SSD64, SSD69, SSD109, SSD116, SSD171, SSD253, SSD278, SSD441, SSD451, SSD487, SSD511 and Kronos showed shorter plants respect the control, indicating a stronger effect of the heat stress; SSD35, SSD92, SSD99, SSD112, SSD122, SSD244, SSD269, SSD397, SSD409, SSD459, SSD494 and Svevo show no difference between stressed and control; SSD178, SSD195, SSD335, SSD415 and SSD322 showed higher stressed plants than controls (Figure 19).

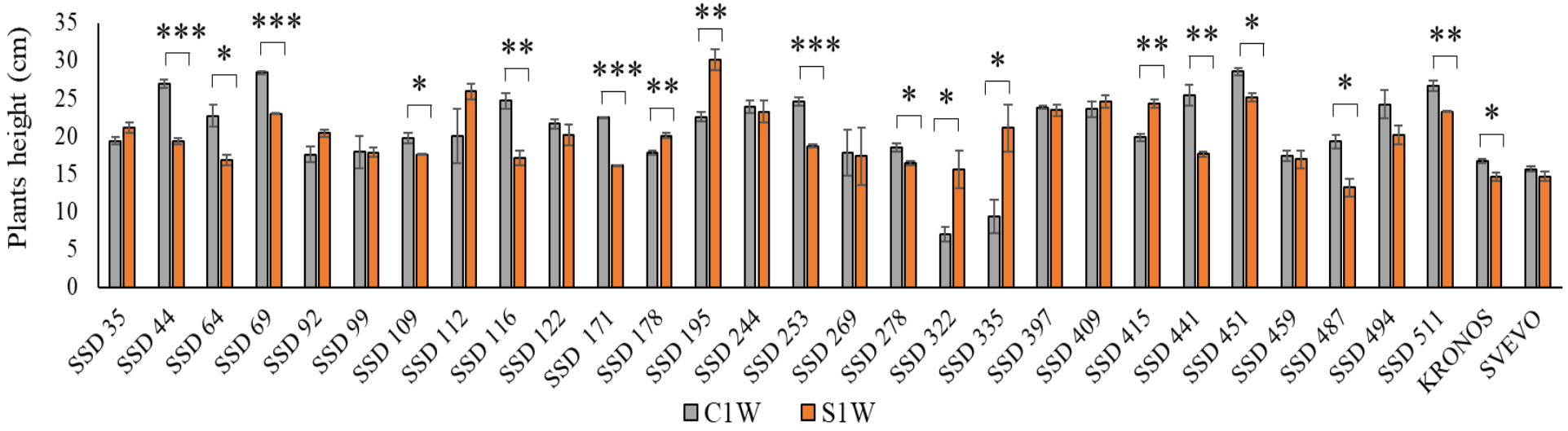

Fig 19. Plant height (cm). Student's t-test was applied for each control and stressed sample *P<0.05; **P <0.01; ***P <0.001

MDA content

The Malondialdehyde (MDA) content was assessed in the selected lines being one of the main breakdown products of polyunsaturated fatty acids in cell membranes and as a good proxy of oxidative stress in plants subjected to heat stress conditions (Figure 20). Seedlings of all genotypes were analyzed for the MDA content. The MDA trend showed an unusual behavior in wheat plants exposed to heat stress that normally increased during and under the stress. Here, in several genotypes: SSD35, SSD441, SSD451 and Kronos showed a gradual reduction in MDA from T0 to 1hPR while all other genotypes showed a strong and rapid decrease after 4h of heat stress and a significant increase already after one hour post recovery. Conversely, significant increase, consistent with the literature, in the MDA was observed in SSD 64 and SSD397 which respectively have an increase of 133,4% and 169,75%. SSD69 showed a limited and not significant increase in MDA content at 1hPR of 11,59%, in comparison with T0.

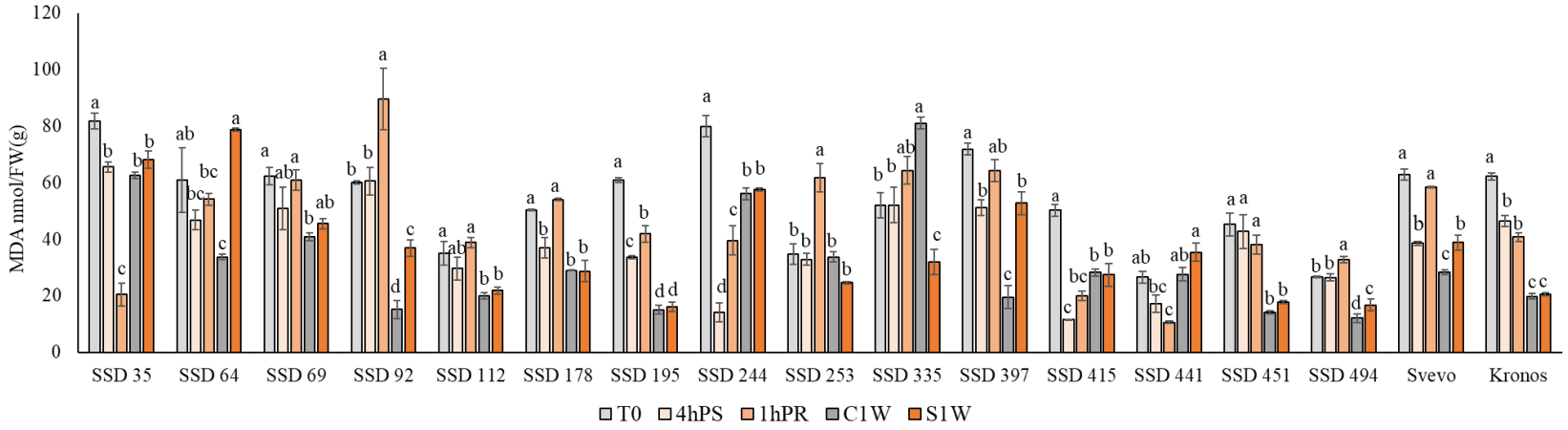

Fig 20. Plot of MDA content (nmol/FW(g)) in seedlings after heat stress exposure. SE is included. The different alphabetical letters in superscript indicate the significant differences with the ANOVA test, *p-value* < 0.05.

To better evaluate the behavior of the MDA trend, the MDA ratio was calculated (Table 10).

SSD92, SSD 112, SSD178, SSD253, SSD325, SSD335, SSD494 showed a significant variation in MDA content with a consistent accumulation of MDA at 1hPR (Table 10). SSD35 showed a strong variation in MDA during the phases of heat stress with almost a full recovery after one

week. Kronos showed a progressive decrease in MDA reaching the maximum at S1W, while SSD69 and Svevo, interestingly, showed no significant variation in MDA immediately after the stress and after the recovery (1hPR and S1W), supporting their tolerance to heat stress and a possible role link with the MDA variation (Table 10).

Table 10. MDA ratio calculated as control/stress.

SSD	%T0/4HPS	%T0/1HPR	%C1W/S1W
35	-19.86%	-75.02%	9%
64	-23.22%	-14.54%	133.4%
69	-18.43%	-2.30%	11.59%
92	1.02%	49.28%	144.03%
112	-15.47%	10.66%	9.15%
178	-26.80%	7.47%	-0.31%
195	-44.73%	-31.14%	7.93%
244	-82.33%	-50.53%	2.67%
253	-5.22%	78.36%	-27.38%
335	0.23%	23.78%	-60.53%
397	-28.85%	-10.43%	169.75%
415	-76.86%	-60.27%	1.56%
441	-35.31%	-59.95%.	28.28%
451	-5.59%	-15.88%	26.26%
494	-1.12%	22.85%	38.02%
SVEVO	-38.52%	-6.95%	36.72%
KRONOS	-25.24%	-34.47%	25.30%

TdHsp26-A1 and -B1 gene expression during heat stress in seedlings stage

Based on the results of plant height and MDA content together with the haplotype and SNPs position in the gene, SSD397 and SSD69 were chosen for *TdHsp26-A1 and -B1* gene expression analysis.

Both *TdHsp26-A1* and *TdHsp26-B1* genes were significantly upregulated in SSD69 following heat stress with a range from 10.62 fold at 4hPR to 6.62 fold at 1hPR for *TdHsp26-A1* and from 9.32 fold at 4hPR to 5.61 at 1hPR for *TdHsp26-B1* (Figure 21). SSD397 showed a remarkable lower gene expression of both genes. *TdHsp26-A1* gene expression drops from 4hPR to 1hPR from 2.84 to 1.2 fold change. *TdHsp26B1* was from 2.62 to -0.28 folds from 4hPS to 1hPR. Both lines show a higher expression of the *TdHsp26-A1* gene than the *TdHsp26-B1* gene, in accordance with what was previously reported (Comastri et al. 2018).

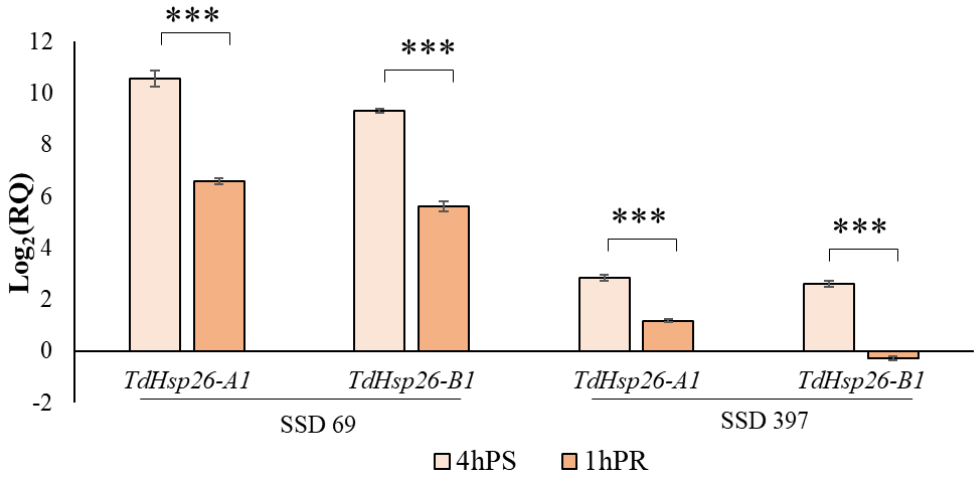

Fig 21. Expression analysis of *TdHsp26-A1* and *TdHsp26-B*1 in SSD69 and SSD397 genotypes. The induction levels are measured as the fold change (RQ) of the treated samples in respect to the controls and reported as log2(RQ) in the chart. Bars indicate the standard error. Student's t-test was applied between 4hPS and 1hPR of each group. ***p <0.001.

Summarizing, in this first experiment, the effect of short (4h) heat stress (38°C) on plants morphologically (plant height) and biochemically (MDA content) was verified, and from the data obtained, two genotypes with contrasting phenotypes for gene expression analysis of *TdHsp26-A1 and -B1* were selected.

4.3.2 The heat stress response in tillering stage

Based on the results obtained in seedlings stage and the position of SNPs in the gene of interest 7 genotypes, corresponding to 5 haplotypes were chosen for applying the heat stress in tillering stage (Table 7). Two contrasting cultivars, Svevo and Kronos, were also included as reference varieties.

4.3.2.1 Morphological traits

To perform the morphological analysis, the leaves area was measured at 48hPS and after 1 week post stress since 4hPS it was not possible to detect any morphological difference, while the number of culms and plant height were measured 1 week post stress (Figure 22). Significant differences are observed in leaf area between stressed and controls at S1W in SSD415 and between C48h/S48 and C1W/S1W in Kronos, with a reduction in area in stressed compared with controls (Figure 22a).

At S1W stressed SSD244 and SSD397 showed a significant reduction (P< 0,05 and P< 0,01) in plant height (Figure 22c). At S1W Kronos showed a reduced number of culms, while all other genotypes do not show any significant variation in the number of culms between stressed and control plants (Figure 22b).

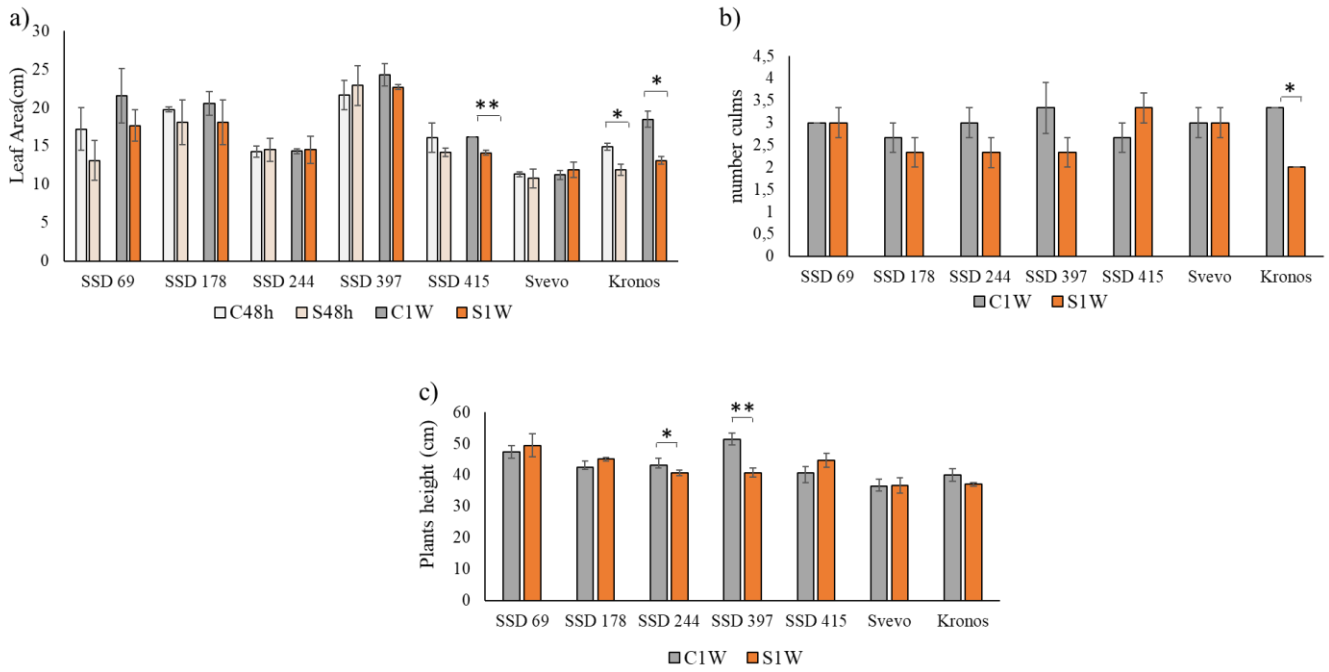

Fig 22. Morphological traits analyzed in the tillering experiment a) Leaf Area, b) number culms, c) Plant height. Student's t-test was applied. Error bars are reported and represent the standard error. *P <0.05, **P <0.01, ***P <0.001.

4.3.2.2 Physiological traits

Plant transpiration

The stomatal resistance (r_s, sec x cm^{-1}), is an efficient trait to estimate the gas exchange such as CO_2 absorption thoroughly to the leaves and water loss with transpiration depending on stomata pore.

Under heat stress the stomatal resistance is reduced under heat stress. At 4hPS under heat stress all genotypes showed a reduction in stomatal resistance indicative of increased conductance (Figure 23a), at 48hPS all genotypes show resistance equal to that of the control plants, except for SSD397, which still showed a reduction in stomatal resistance (Figure 23b).

At S1W both genotype 397 and Svevo have lower resistance in the stressed plants than in the control (Figure 23c)

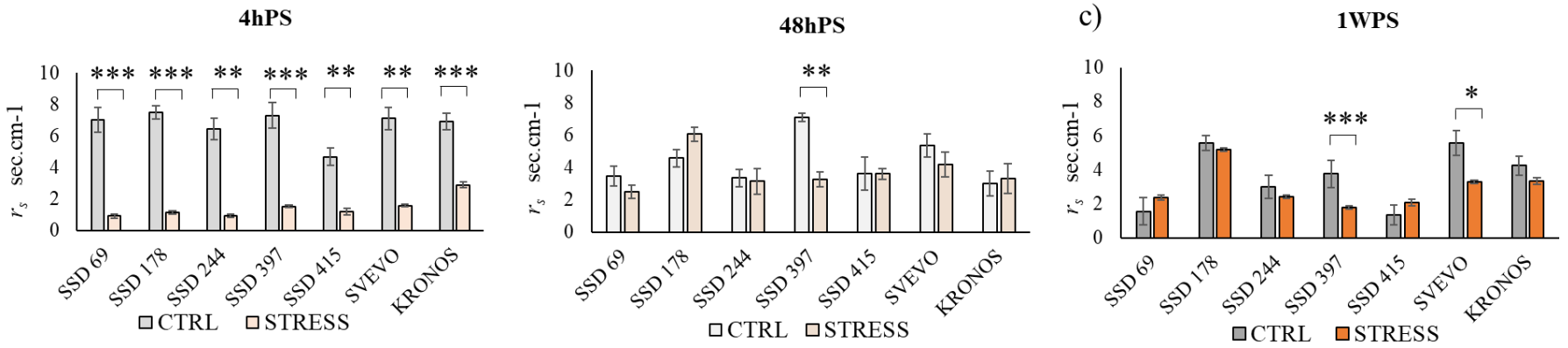

Fig 23. Plot of the stomatal resistance (r_s). a) controlled and stressed plants after 4hPS, b) controlled and stressed plants after 48hPS and c) controlled and stressed plants one week post stress. Both control and stressed conditions were considered. Student's t-test was applied. Error bars are reported and represent the standard error. *P <0.05, **P <0.01, ***P <0.001.

Plant Canopy temperature

Canopy temperature was analyzed as a good proxy of heat stress tolerance. After 4 h at 38°C, all genotypes showed, as expected, an increase in canopy temperature. However, SSD 397 showed a greater increase in canopy temperature in comparison to all other genotypes analysed, supporting its increased susceptibility to heat stress (Figure 24).

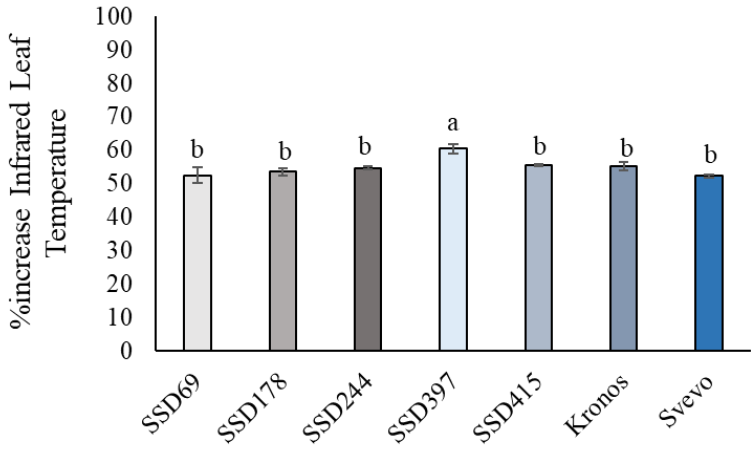

Fig 24. Percentage of increased Infrared Leaf Temperature at time T0 and that after 4hPS at 38°C for each genotype. The different alphabetical letters in superscript indicate the significant differences with the ANOVA test, *p-value* < 0.05. Error bars represent the standard error.

RWC was not effective in describing a possible tolerance to heat stress, being the leaves hydration level reduced during the heat stress (4hPS) and restored at S1W (supplementary Figure 1c).

The canopy temperature depression (CTD) was calculated as an integrative trait that reflects an overall plant water status and the level of heat stress (Kumar et al.,2017). SSD 69 and Svevo showed a significantly greater CTD values after the stress (4hPS, 6.31°C and 6.35°C), while SSD 397 showed the smaller values (4.87°C, Figure 25). At S1W the CTD values were recovered as a T0.

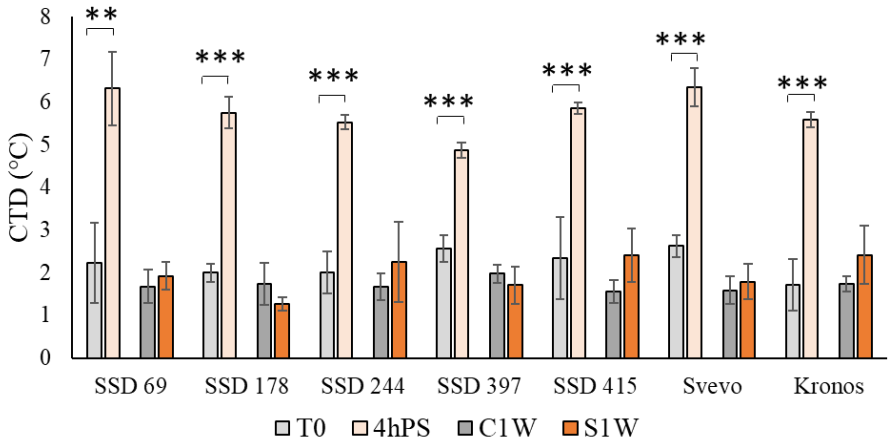

Fig 25. CTD calculated with temperatures recorded at the following points: T0/4hPS and C1W/S1W in tillering experiment. Student's t-test was applied. Error bars are reported and represent the standard error. *P <0.05, **P <0.01, ***P <0.001.

Stress indices

By using the yield data recorded (number of seeds per spike , through the Plant Abiotic Stress Index Calculator (iPASTIC) the average sum of ranks (ASR) , for nine different indexes such as: Tolerance, Mean Productivity, Geometric Mean Productivity, Harmonic Mean , Stress Susceptibility Index, Stress Tolerance Index , Yield index, Yield Stability Index and Relative Stress Index was calculated (Pour-Aboughadareh et al. 2019). The lower the value of ASR, the superior in terms of heat tolerance is the genotype. SSD69, SSD178, Svevo and Kronos showed the lowest ASR value indicating an improved tolerance to the stress (Figure 26), while SSD397 and SSD244 showed the highest value indicating low tolerance. An intermediate value was attributed to SSD415 and SSD178 which confirms the difficulty in assigning a clear phenotype to those lines.

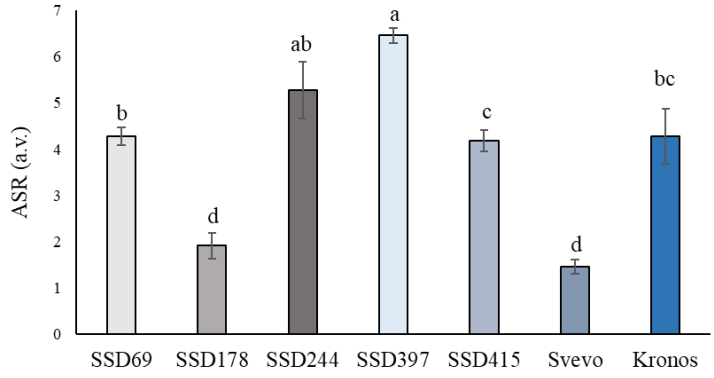

Fig 26. Average Sum Ranks, a.v = absolute value. Error bars represent the standard error. The different alphabetical letters in superscript indicate the significant differences with the ANOVA test t at a *p-value*< 0.05. Error bars represent the standard error.

4.3.2.3 Antioxidant activity and ROS accumulation

Accumulation of antioxidant enzymes that regulates the accumulation of ROS in plant cells is a key mechanism in heat stress response (Medina et al. 2021).

SSD178, SSD244, SSD397, SSD415 and Kronos showed an increase in H_2O_2 content between 4hPS and 1hPR while SSD69 and Svevo did not show an increase immediately after the stress. SSD69, SSD178, SSD397, Svevo and Kronos showed increases of 22.31%, 26.87%, 54.75%, 8.6%, 16.7% in H_2O_2 content suggesting for those genotypes a late accumulation of H_2O_2 in the putative tolerant lines (Figure 27a).

Contrasting results with respect to the literature were observed in the MDA content of SSD69, SSD244, Svevo where no increase was observed. SSD397 showed an increase of more than 100% after 4hPS and 62.48% after one week of stress. Similar results were observed for SSD415 that presents an increase of 23.56% after 4hPS and 67.43% at S1W. SSD178 showed an increase of 55.12% after 1hPR in comparison with the control, while Kronos showed a late increase of 36.33% in the stressed plants at S1W (Figure27b).

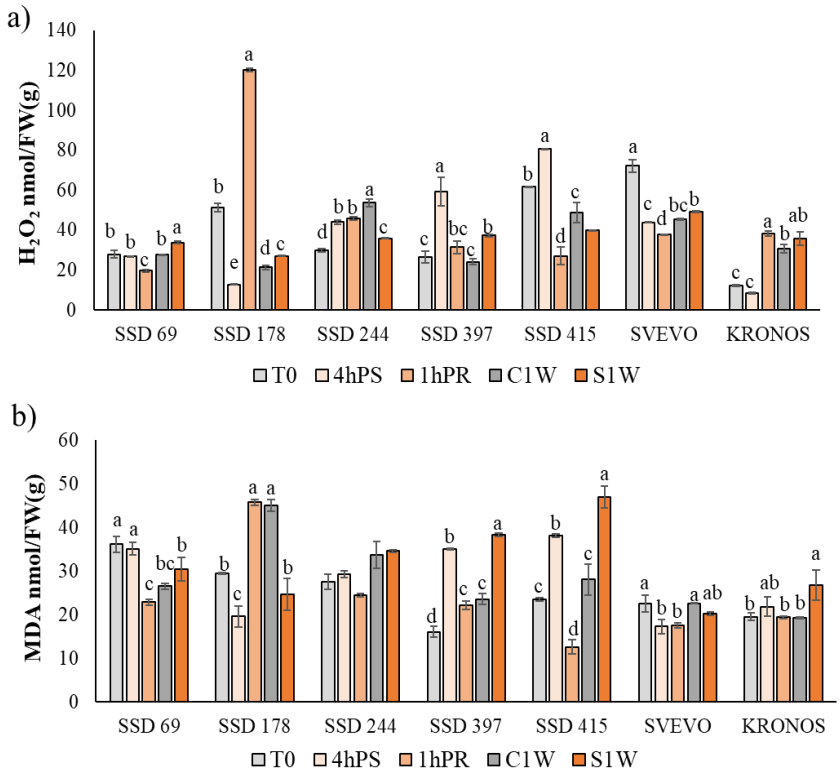

Fig 27. Plot of H_2O_2 content, a) and MDA content b) in wheat under heat stress in the tillering stage. T0, control, 4hPS, 4 hours stress at 38°C, and 1hPR, 1h recovery at 23°C, C1W, control one week post stress, S1W, treated after one week post stress. Error bars represent the standard error. The different alphabetical letters in superscript indicate the significant differences with the ANOVA test, *p-value*< *0.05*. Error bars represent the standard error.

4.3.2.4 TdHsp26-A1 and TdHsp26-B1 gene expression analysis during heat stress in tillering stage

In contrast to the seedling stage, *TdHsp26-B1* shows minimal expression in both genotypes SSD69 and SSD397 in normal growth conditions at T0 (Figure 28). Both *TdHsp26-A1* and *TdHsp26-B1* genes were significantly upregulated although at low levels in SSD69 following heat stress with a range from 1.66 at 4hPR to 1.30 at 1hPR folds for *TdHsp26-A*1 and from 1.75 folds at 4hPR to 1.03 folds at 1hPR.

SSD397 showed an overexpression of *TdHsp26* genes at 4hPS to 1hPR, but lower than SSD69, with values ranging from 1.38 to 1.19 folds for *TdHsp26-A1* and from 1.53 to 1.40 for *TdHsp26-B1*.

Moreover, for SSD397 the trend of expression for *TdHsp26-B1* did not show a significant reduction between 4hPS and 1hPR.

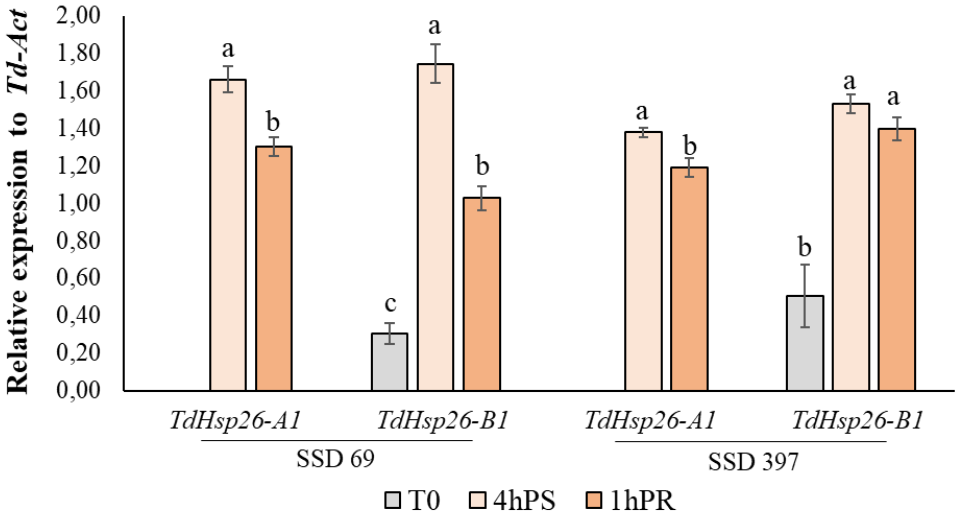

Fig 28. Semiquantitative RT-PCR of *TdHsp26*. Gene expression was normalized to the *TdAct (ID AB181991)* as reference gene. Values shown are mean ± SD. The different alphabetical letters in superscript indicate the significant differences with the ANOVA test, *p-value< 0.05*.

4.3.2.5 Yield traits

All lines produced seeds, although of smaller sizes in some genotypes. When the number of seeds of the whole plant were correlated to the kernel yield per spike (KYPS) both in controlled and in heat stressed plants, the variation in heat response appears different between lines.

SSD69 and SSD415 showed no significant (Figure 29, white dot and triangle) and small variation (dark blue dot and triangle), respectively in yield between control and treated plants, while genotype 397 is the line that showed the most divergent yield traits between control and stressed plants (Figure 29).

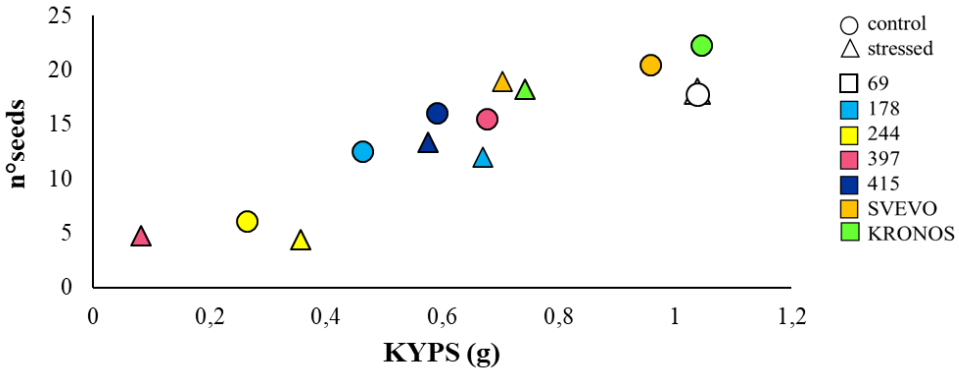

Fig 29. Plot of the correlation of the number of seeds and the kernel yield per spike (g).

4.3.3 SSD lines characterization for heat stress resilience

A principal components analysis (PCA) was performed to determine the most contributive agro-morphological traits explaining the difference encountered in heat resilience between lines. All variables and stages collected before stress and after 4h at 38°C and S1W were considered in the analysis (Figure 30). The first two principal components explained 57.7% of the total variation.

In 4hPS controls and stressed genotypes are correctly clustered in two separate groups highlighting the effect of the imposed heat treatment, but in S1W, a different clusterization was observed. While control and stressed samples of SSD69 and SSD178 clustered really close to each other supporting a possible heat tolerance for this genotype, line SSD397 are separate in the plot suggesting a higher susceptibility. Moreover, RWC, SR and CTD are highly correlated at 4hPS, while morphological traits such as canopy and leaf area are shown to be strongly correlated (Figure 30).

The cluster of morphological traits (number of culms, leaf area, plant height and number of leaves) separated by the physiological traits (SR, infrared temperature) at S1W, further support the validity of the phenotyping methods applied to characterize the wheat stress resilience in durum wheat genotypes (Figure 30).

In both PCA plots, infrared temperature and CTD are inversely correlated as expected, further validating the approach used (Figure 30).

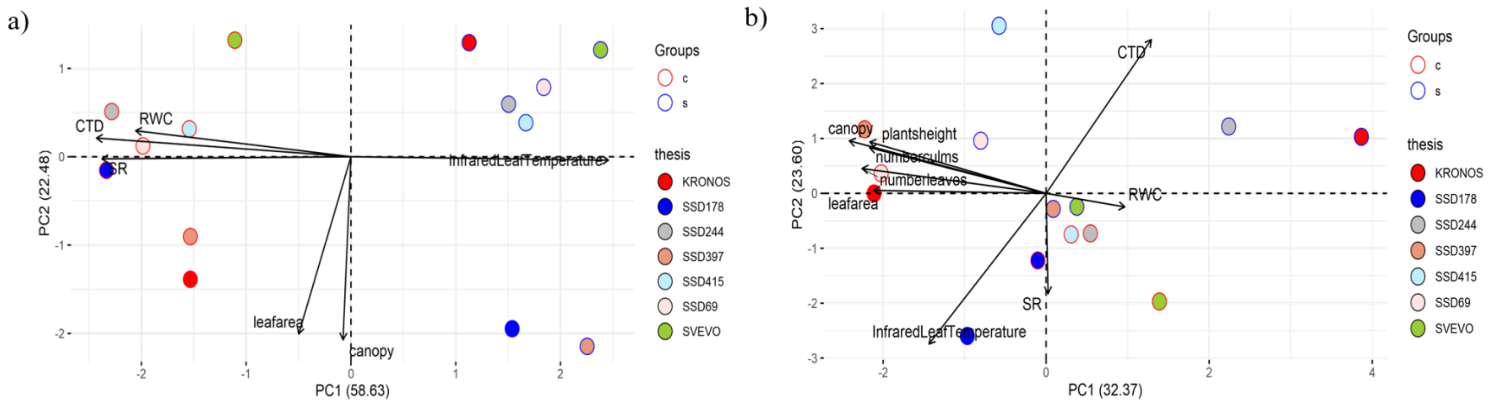

Fig 30. Principal component analysis (PCA) of the effect of heat treatment in 7 SSD genotypes. a) Biplot at 4hPS; b) Biplot S1W. RWC, Relative Water Content, CTD, Canopy Temperature Depression, Infrared Leaf Temperature, SR, Stomatal Resistance, canopy, leaf area, plant height, number culms, number leaves (individual data can be viewed in the Supplementary Figure1).

4.3.4 Discussion on the heat stress response for durum wheat lines in seedling and tillering stage

Two main objectives were the target for the heat stress experiment performed in tillering stage: i) to characterize the phenotype of the selected genotypes under heat stress and to verify, whether there were differences between seedlings and tillering; ii) to identify traits that could easily indicate whether a genotype is susceptible or tolerant to heat stress.

Heat stress in plants is known to cause a reduction in plant height (Hassan et al. 2020); here we identified three different phenotypes comparing stressed and controls: plants with decrease height (41.93%), plants higher than controls (19.35%), and plants showing no significant differences under stress (38.71%).

Plants exposed to heat stress often lead to the generation of destructive ROS, including singlet oxygen ($^1O_2$), superoxide radical (O_2^-), hydrogen peroxide (H_2O_2), and hydroxyl radical (OH^-) responsible for generating oxidative stress (Marutani et al. 2012; Suzuki et al. 2012).

Oxidative stress notably increased membrane peroxidation and decreased membrane thermo-stability in many plants including wheat (Savicka and Škute 2010) leading to the accumulation of MDA that is considered a good indicators of the damage of the cell membranes as reported in rice and maize (S. Kumar, Singh, and Nayyar 2012) and sorghum (Tan et al. 2011). In wheat (Savicka and Škute 2010), increased MDA content in all organs of wheat seedlings was observed.

The expression of *TdHsp26* seems to play a role in the heat response reducing MDA accumulation in seedlings of SSD69 indicating a low oxidative stress damage. Between the two genes, *TdHsp26-A1*, showed a strong increase in the relative expression at seedling stage while lower expression of *TdHsp26-B1* variant was observed. An hypothesis of a link between gene expression, MDA content and heat tolerance was formulated. A sharp increase of 100% in MDA was observed in SSD397 and a total lack of expression of the *TdHsp26-B1* gene. Conversely, SSD69, showed no significant variation in the MDA content a 1 week after stress (S1W) and a high expression of *TdHsp26-B1*.

In seedling, all lines showed a decrease of MDA immediately after the stress (4hPS), while a strong increase was observed at S1W supporting the hypothesis of Savicka et al. (2010). Conventional behavior was observed in the tillering stage for all lines except for SSD69 and Svevo that showed decreased values in MDA and H_2O_2 content.

This led to hypothesize a direct role of the expression in SSD durum wheat genetic resources of *TdHsp26-A1* and *-B1* haplotypes in leading a redox perturbation in late stage of development as the tillering stage that was not observed in seedling stages. This was previously reported in barley (Taratima et al. 2022), where a lower accumulation of MDA was observed and can play a critical role in triggering heat stress signaling cascades and the transcriptional effects of stressful high temperatures have been shown to be at least partially mediated by elevated H_2O_2 levels**.**

In tillering a reduced H_2O_2 accumulation and a corresponding reduction in MDA content was observed in putative heat tolerant genotype SSD69 while SSD397 showed conventional trends of H_2O_2 accumulation and MDA content after heat stress imposition. However, both genes were overexpressed in heat stress conditions.

This unconventional behavior of MDA and H_2O_2 suggests a possible mechanism of action of the variants in *TdHsp26*.

MDA and H_2O_2 traits are confirmed as good biochemical proxy of heat stress tolerance together with the canopy temperature.

All together these results suggest for SSD69 a reduced oxidative damage thus an increased tolerance to heat stress. SSD69 showed a set of phenotyping traits supporting its increased heat tolerance.

A reduced canopy temperature and increased CTD values, support that genotypes with higher CTD values and a cooler canopy temperature under drought stress use more available soil moisture to cool the canopy by transpiration that have concrete beneficial effects also on heat tolerance. On the contrary, SSD397 showed higher values of canopy temperature and lower CTD, supporting their inability to promote the activation of the transpiration process to reduce the effects of heat stress. This was also demonstrated in the PCA (Figure 30), where CTD and canopy temperature vectors are inversely correlated.

All together the results obtained in seedlings and tillering stages under short term stress allowed us to hypothesize a possible link between the expression of *TdHsp26-A1 and -B1* variants and the cascade of physiological phenomena triggered during the stress (Figure 31).

However, the results obtained were not sufficient to correlate the phenotyping effects observed with the specific SNPs. Only speculations can be done in terms of heat stress response with the geographical origin of the two genotypes (Janni et al. 2018). SSD69

originated in Morocco while SSD397 originated in Crete and showed different heat tolerance together with different HMW glutenins composition (Janni et al. 2018).

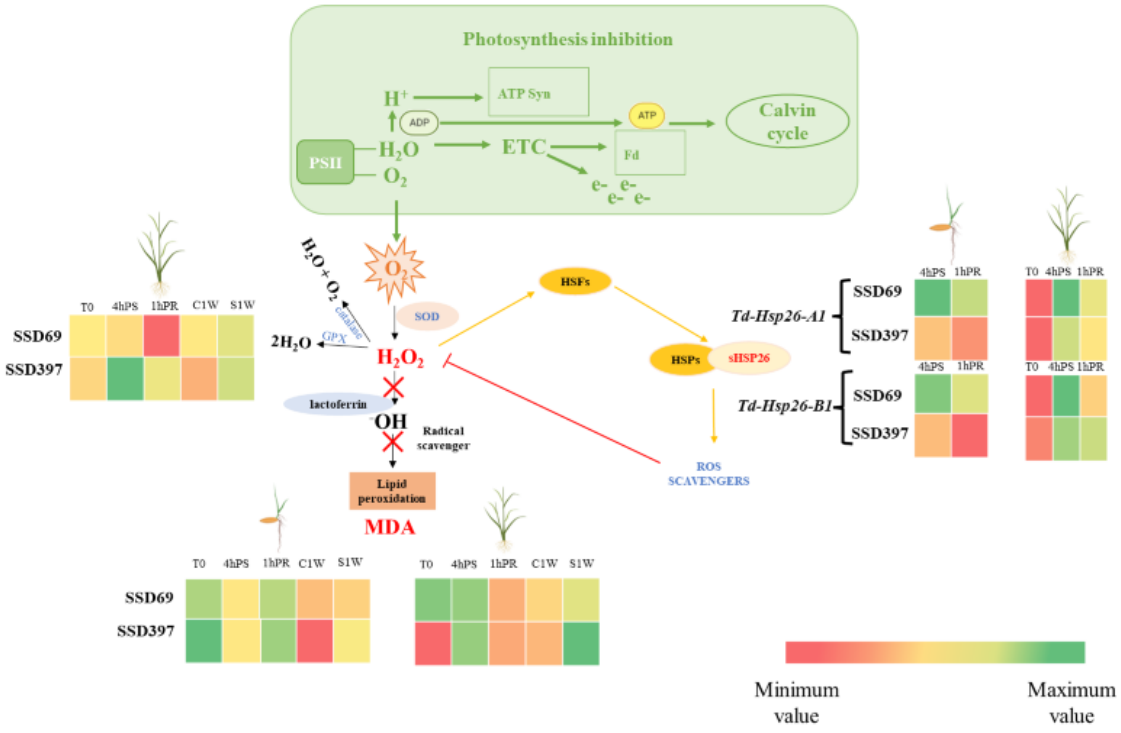

Fig 31. Hypothesize mechanism of the role of *TdHsp26* in the ROS cascade. Under heat stress, the ROS and HSP cascade is activated. H+, hydrogen molecule, adenosine diphosphate; ATP, adenosine triphosphate; H_2O, water; ETC, electron transport chain; e-, electron; Fd, ferredoxin; PSII, photosystem II; O_2, oxygen molecule; $O_2^{\bullet -}$ superoxide radical; SOD, superoxide dismutase; CAT, catalase; GPX, glutathione peroxidase; H_2O_2, hydrogen peroxide; ($^{\bullet}OH$), hydroxyl radical.

4.3.5 The heat stress response after prolonged heat stress in anthesis phase

4.3.5.1 Morphological traits

To concretely demonstrate the increased resilience of SSD69 and tolerance of SSD397 and to further demonstrate the efficacy of plant phenotyping in characterizing heat stress resilience, heat stress experiments were performed in the anthesis phase. Two cultivars were included as reference tests (Iurlaro et al. 2016).

The growth stage at which heat stress events occur has a significant impact on wheat grain yield (Djanaguiraman et al. 2020). Effects of high temperature stress during anthesis and grain filling periods on photosynthesis, lipids, and grain yield in wheat. A heat stress at 32.0◦C reduced yield per plant by 29.0% and 44.0% at anthesis and during the grain filling period, respectively. Due to the threat of food insecurity, there is a growing imperative to

identify high-yielding wheat cultivars that display resilience to the impacts of rising temperatures and maintain nutritional and end-use quality (Djanaguiraman et al. 2020).

Here, a prolonged and extremely severe heat stress was applied to mime the normal environmental events occurring in open fields in the final stages of wheat development.

Based on previous results in seedling and tillering the plant height and leaves number were scored (Figure 32). The dynamic of plant growth was significantly different between lines (Figure 33). SSD 69 and Svevo showed a comparable trend of development. At 25 DAT SSD 69 and Svevo showed a lower plant canopy, plant height, reduced number of leaves and a shorter development cycle (Figure 33b, d).

Yield traits depend mainly on tillering and flowering time both affecting the number of seeds and grain yield (Table 11).

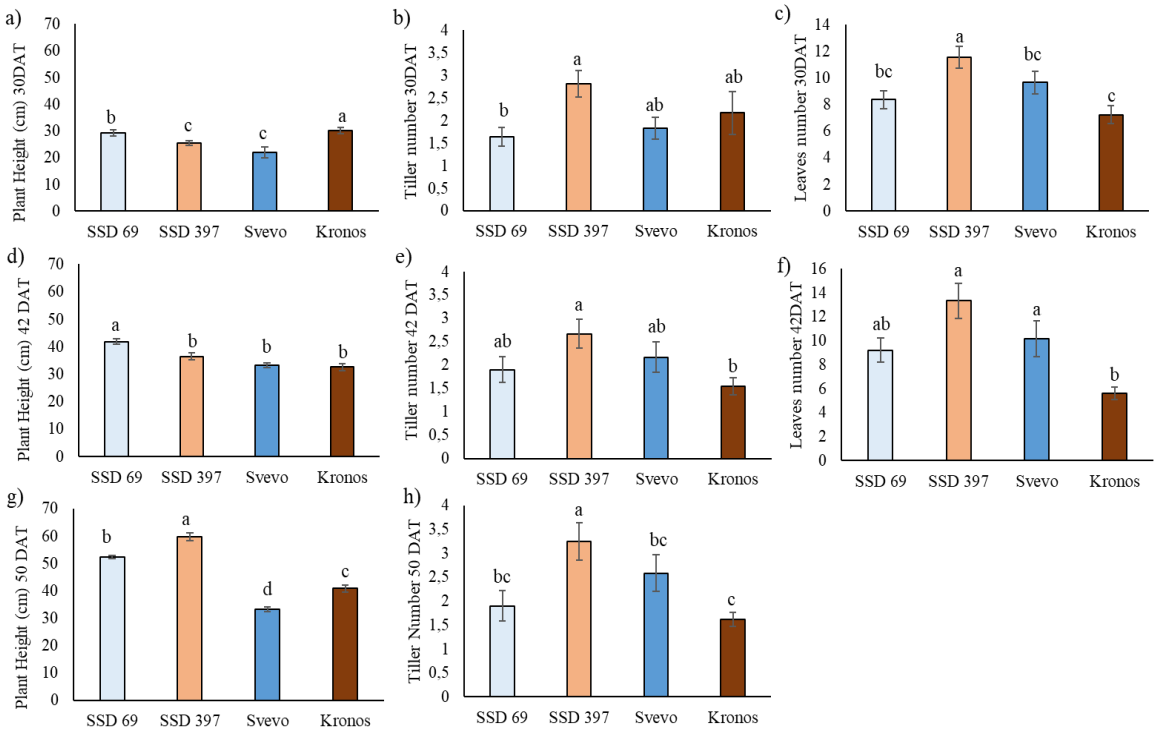

Fig 32. Plots of morphological traits scored in the anthesis phase. a), d), g) plant height on days 30, 42, 50 DAT; b), e), h) the numbers of culms on days 30, 42, 50 DAT; c), f) the numbers of leaves 30 and 42 DAT. Values shown mean ± SE. The different alphabetical letters in superscript indicate the significant differences with the ANOVA test t at *a p-value< 0.05.*

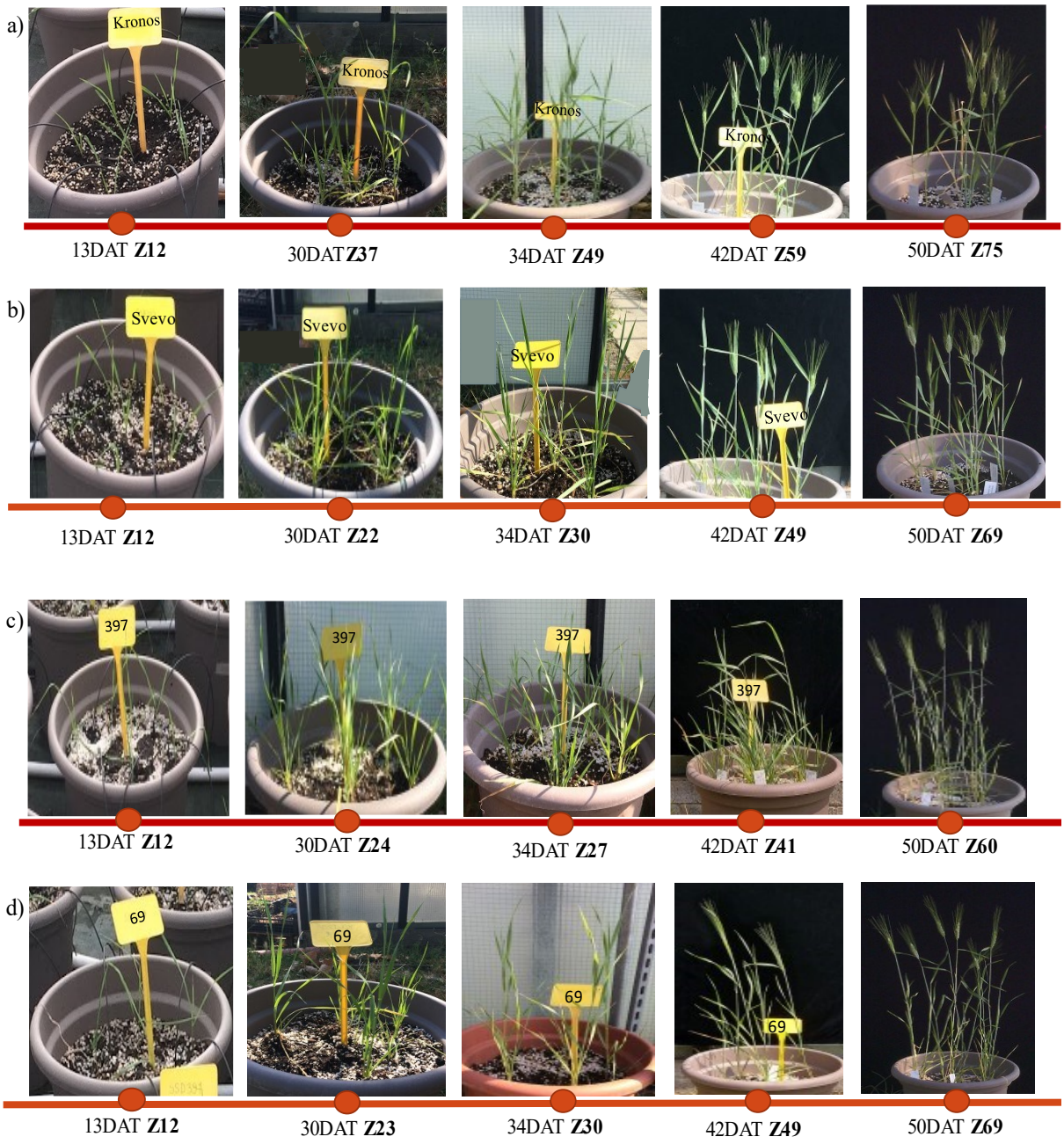

Fig 33. Growth and plant development stages expressed in Zadoks stages of SSD397, SSD69, Kronos and Svevo. DAT, Days after Transplant

Table 11 Morphological traits and temperatures recorded in the anthesis experiment.

Tillering						Anthesis					
Genotype	Zadoks stage	Date	DAT	T°C min	T°C max	Zadoks stage	Date	DAT	T°C min	T°C max	Days to flowering
Kronos	Z20	20-giu	20	21,5	51	Z60	16-lug	46	22	56	26
Svevo	Z20	20-giu	20	21,5	51	Z60	19-lug	49	19,5	54	29
SSD397	Z20	20-giu	20	21,5	51	Z60	21-lug	51	21	58	31
SSD69	Z20	22-giu	22	22,5	33	Z60	18-lug	48	20,5	51	26

Kronos showed complete ear emergence at 34 DAT followed by Svevo at 37 DAT, SSD 69 at 42 DAT and SSD 397 at 48DAT.

In terms of flowering time SSD69 and Svevo showed an earlier flowering time (48, 49 DAT). Kronos showed a reduced flowering time of about 2 days (46 DAT, Figure 33a). SSD 397 showed a delay in flowering time of about 2 days (51 DAT, Figure 33c, Table 11).

Moreover, SSD397 plants showed a denser canopy, bigger number of leaves and culms with a slower growth dynamic. For example, plant growth (in terms of height) was slow up to 42 DAT when it rapidly increased from 36.42 ± 1.23 to 59.67 ± 1.44 at 50DAT (Figure 32). Kronos had the fastest development cycle and maturation process compared to the other lines.

Kronos and Svevo showed similar length of time between ear emergence and anthesis (12 days) while SSD 397 showed the fastest days to flowering (3days), SSD69 intermediate length with 6 days (Tab. 11).

For SSD69 a staygreen phenotype under heat stress (Figure 34) was hypothesized. The staygreen phenotype is an antagonist to senescence, chlorophyll, and photosynthetic capacity of leaves were maintained or prolonged, and is considered an indicator of heat tolerance (Fokar, Blum, and Nguyen 1998) and the plant continues to produce tillers also when the first ear reaches maturity (Figure 34). Compared with the staygreen varieties, the yield and inferior grains of no-staygreen cultivar were much more influenced by high-temperature stress (Yang et al. 2014).

Fig 34. Staygreen phenotype in SSD69 (90 DAT, Z99,30 August 2022).

4.3.5.2 Physiological traits

Under heat stress, the monitoring of the regulation of the transpiration mechanisms is a possible strategy for selecting heat-tolerant varieties. The stomatal conductance (g_s) has been recorded.

Plants under high temperatures cool their canopies through transpiration, which occurs through stomata when soil water is available. Efficient reproductive development requires higher gas exchanges, which occur through open stomata, putting plants in a constant struggle for survival against harsh environments (Huggins et al. 2018).

Higher g_s is associated with better performance of tolerant genotypes under stress conditions (Saeidi and Abdoli 2015). Zhang and coworkers in their study pointed out the effects of different percentages of air humidity on winter wheat and found that their most productive genotypes had in common a strong stomatal regulatory ability in response to changing air humidity (Zhang et al. 2020).

The plot shows the temperatures recorded during the measurements, acquired in two different days, morning and afternoon plotted with the stomatal conductance (Figure 35).

The highest temperatures were recorded, as expected, during the afternoon.

SSD69 showed a reduction in stomatal conductance between the first two points, although there is not a great variation in temperature. The high conductance recorded at 42 DAT is attributable to the high humidity recorded. During those surveys, the relative humidity

was about 48.3 %, the highest ever recorded during our analysis. Several studies have shown an increased stomatal conductance with increased humidity (Zhang et al. 2020).

SSD69 and Svevo showed firstly a large variation in the g_s trend and an increase in correspondence of increasing temperature, whereas SSD397 and Kronos showed opposite trend in the stomatal conductance, supporting the occurrence of higher transpiration to mitigate the effects of increased temperature and allow to ensure good yields and quality.

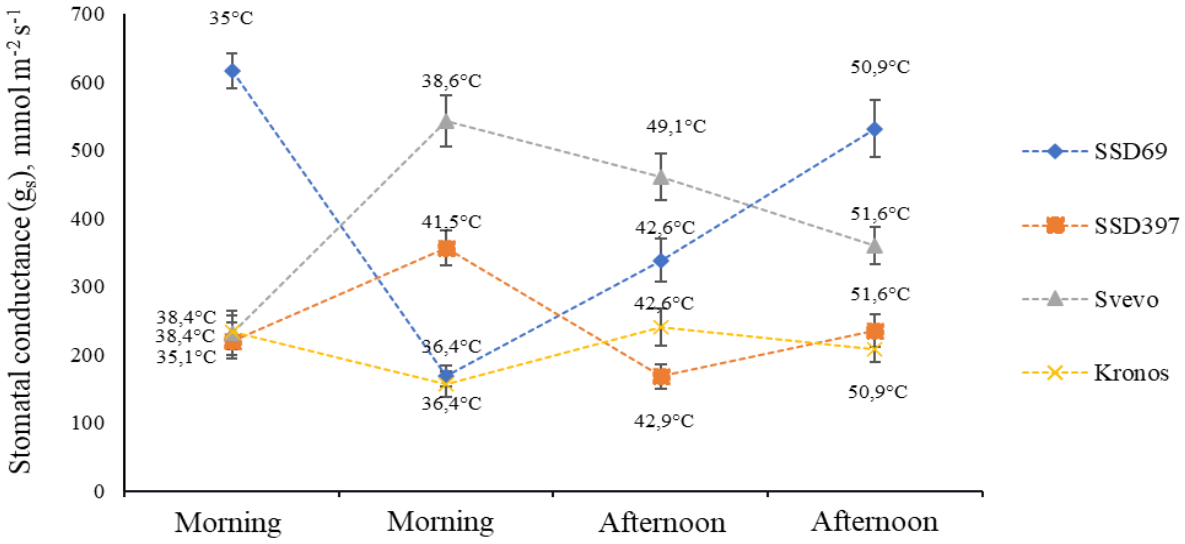

Fig 35. Stomatal conductance measured in the four genotypes under investigation. Measurements were made on two different days (50 DAT and one week after flowering specific for each SSD) morning and afternoon; conductance was correlated with temperatures recorded at the time of the survey. Values shown mean ± SE.

The analysis of the stomatal conductance in contrasting genotypes (SSD69 and SSD397) and varieties (Svevo and Kronos) shows that the analysis of a physiological trait as the variation in g_s is critical to tolerate the prolonged heat stress.

The tolerance of SSD 69 and susceptibility of SSD 397 is further supported by the analysis of key physiological processes affected by heat stress in plants.

The chlorophyll fluorescence parameter Fv/Fm reflects the maximum quantum efficiency of PSII photochemistry and has been widely used for early stress detection in plants (D. K. Sharma et al. 2015).

Here, Fv/Fm values were evaluated in morning and afternoon at 50 DAT and the temperature reached in those days indicated for each Fv/Fm point. A strong correlation with the environmental temperature was observed. SSD 397 showed a fast decrease in the slope of Fv/Fm values (25.7% decreases) right after 42°C, which rapidly further decreased with increasing temperatures, suggesting the triggering of a photoinhibition process as response (Mathur, Agrawal, and Jajoo 2014). SSD 69 showed an increase up to 38°C that remained almost constant also with temperature increase (Figure 36).

Kronos showed a similar trend of Fv/Fm of SSD397 although an earlier decrease of Fv/Fm at lower temperatures (35.8°C) with a 25.8% reduction that was stable till 50.9°C. Svevo showed a similar trend to SSD69 (Figure 36).

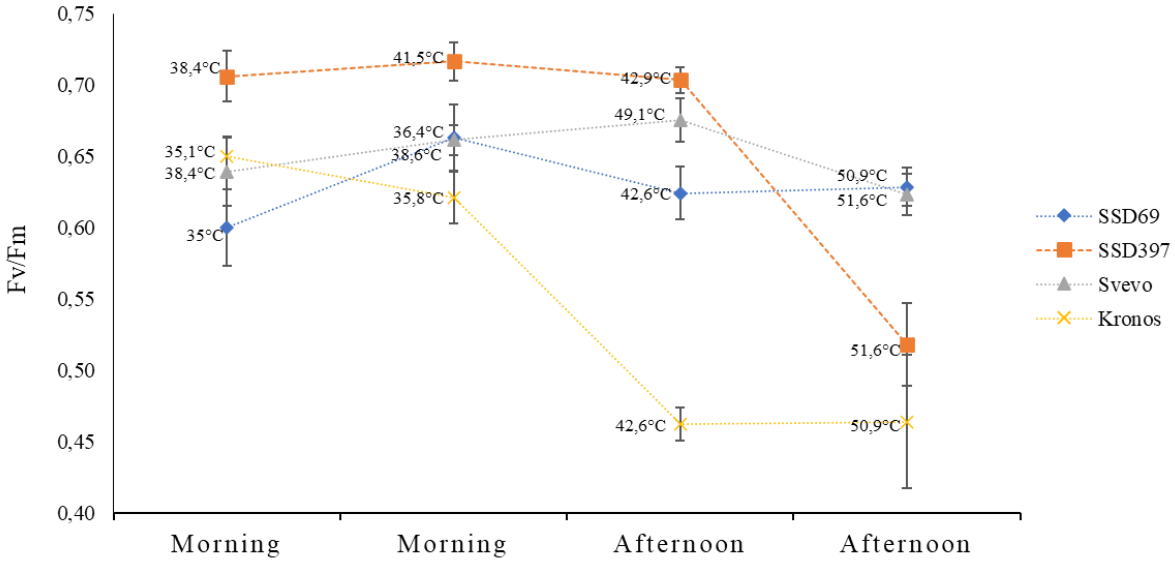

Fig 36. Fv/Fm values plotted with different temperatures recorded at 50 DAT and one week after flowering specific for each genotype. Values shown mean ± SE

The canopy temperature depression (CTD) was also investigated since reflects an overall plant water status and the level of heat stress (Kumar et al. 2017, Figure 37).

It was demonstrated to be well correlated with the transpiration status in rice, potatoes, wheat, and sugar beet (Parvaze Ahmad Sofi et al. 2018).

In anthesis phases under continuous heat stress, with temperatures slightly below 22°C as minimum in the morning and exceeding 58°C maximum in afternoon CTD is strongly reduced in SSD69 (Figure 37), leading to support previous reported data in which staygreen lines showed low CTD values and delayed senescence (Kumari et al. 2012).

However, also Kronos showed lower level of CTD although not being a staygreen suggesting that probably due to the extreme temperature conditions, CTD was not sufficiently efficient for phenotype selection.

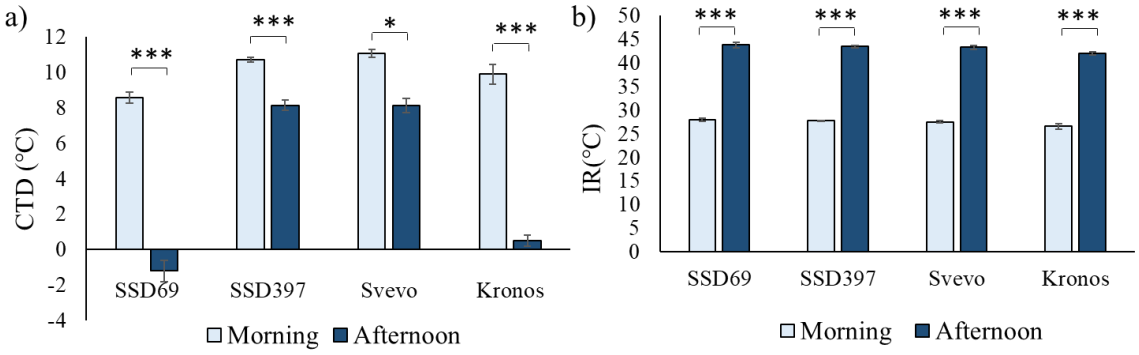

Fig 37. Plot a) CTD: Canopy Temperature Depression b) IR: Infrared Leaf Temperature. The values in SSD69, SSD397, Kronos, and Svevo. Light blue bars indicate the morning data, blue bars indicate the afternoon data. Student's t-test was applied. *P <0.05, **P <0.01, ***P <0.001

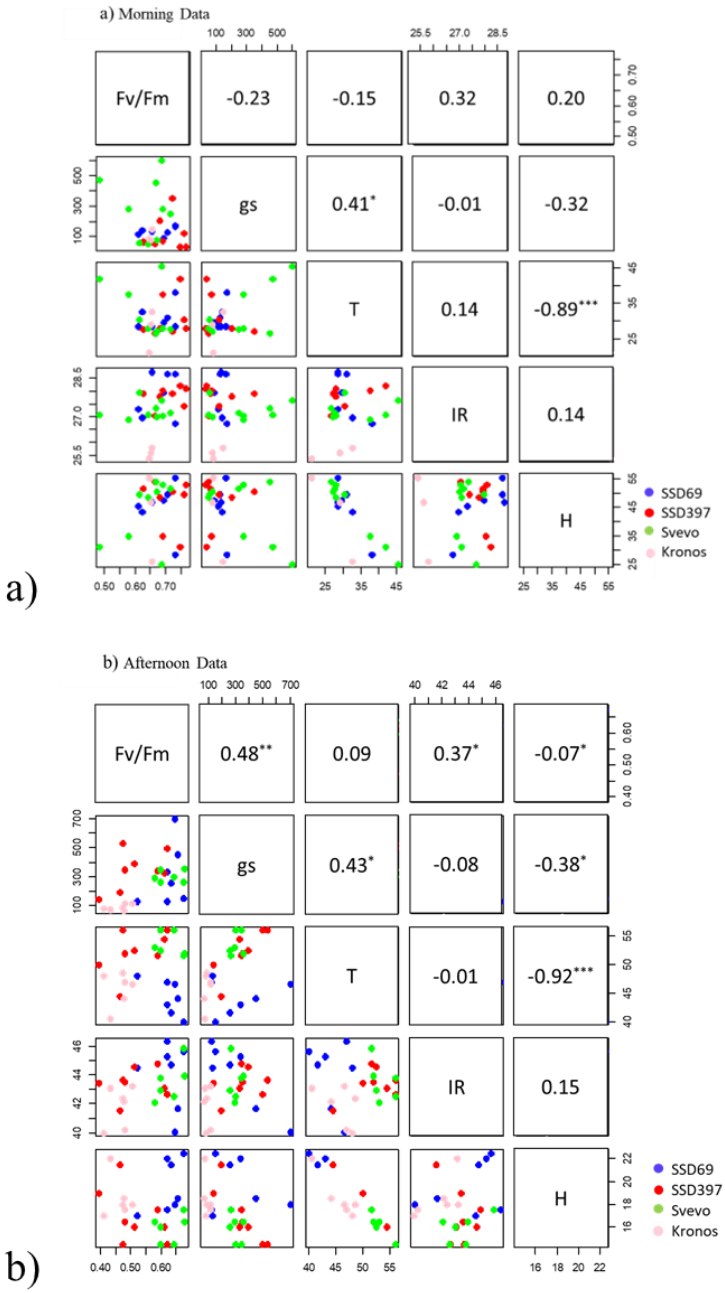

Fig 38. Correlation plot. Fv/Fm, g_s, stomatal conductance, T, temperature, IR Infrared temperature, RH relative humidity. a) morning, b) afternoon. Data were recorded at 50 DAT

When plotted together considering morning and afternoon, although an extremely severe heat stress was imposed, a good and significant correlation between temperature and

stomatal conductance in the morning and in the afternoon (0.41 and 0.43), and between IR and Fv/Fm (0.32 and 0.37) and a significant anticorrelation between temperature and relative humidity (-0.89 and -0.92) were retrieved, while only in the afternoon and a good correlation was observed between g_s and Fv/Fm (0.48, Figure 38).

Based on these results the most descriptive physiological traits seem to be those correlated with PSII function and g_s, indicating a possible role of the SNPs identified in the *TdHsp26* genes in regulating two key traits for heat resilience.

4.3.5.3 MDA content

The MDA content was analyzed in both ear and leaves at 50 DAT in the morning (10:30 am) and in the afternoon (16:30 pm, Figure 39).

In spikes, the MDA content showed no significant variation among morning and afternoon in Kronos and Svevo. SSD69 showed the already recorded reduction in MDA content while a strong increase was observed in SSD397 that, notwithstanding it showed a lower MDA content in comparison with other lines in the morning, accumulated more MDA during the day reaching the maximum in the afternoon. In the leaves, only genotype 69 showed a significant difference between the two sampling times; a different degree of MDA accumulation can be observed among the different genotypes. Kronos has the highest values of MDA with about 89.91 nmol/FW(g), while lines SSD397 and Svevo showed comparable levels of MDA. SSD69 showed the lowest MDA content of 42.30 nmol/FW(g).

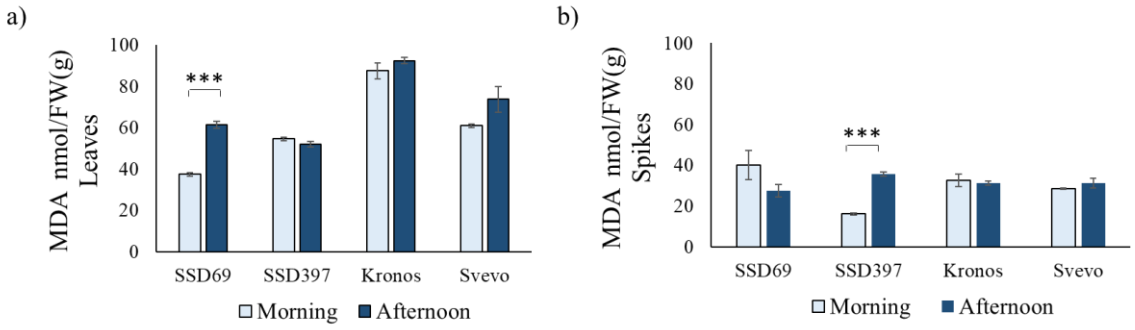

Fig 39. MDA content of leaves SSD69, SSD397, Kronos, Svevo in a) spikes and b) leaves evaluated at 53 DAT for Kronos, 55 DAT for SSD69, 57 DAT for Svevo, 59 DAT for SSD397**.** Student's t-test was applied. *P <0.05, **P <0.01, ***P <0.001.

4.3.5.4 TdHsp26-A1 and TdHsp26-B1 gene expression analysis during heat stress in anthesis stage

Two different trends in the expression of *TdHsp26-A1* and *-B1* were observed in SSD69 and SSD397 (Figure 40). SSD 69 and Svevo that showed an overexpression of the *TdHsp26-A1* gene and a down regulation of the *TdHsp26-B1* gene at 1WAF. On the contrary SSD397 showed a total absence of *TdHsp26-A1* and a higher expression of *TdHsp26-B1*.

Svevo and Kronos showed an opposite regulation of *TdHsp26* genes with Svevo showing an higher expression of *TdHsp26-A1* and lower *TdHsp26-B1* and Kronos a higher expression of *TdHsp26-B1* and a slightly lower expression of *TdHsp26-A1*.

SSD69, Svevo and Kronos express the *TdHsp26-A1* gene in the same range of 5.22, 5.23, 4.55 folds, respectively.

Regarding *TdHsp26-B1*, the 4 genotypes showed different expression levels and were all found to be significantly different from each other. The lowest expression was found in genotype 69 with -0.87 fold, the highest value was in Kronos with 5.99 fold, while SSD397 and Svevo had folds of 3.95 and 2.08 fold, respectively

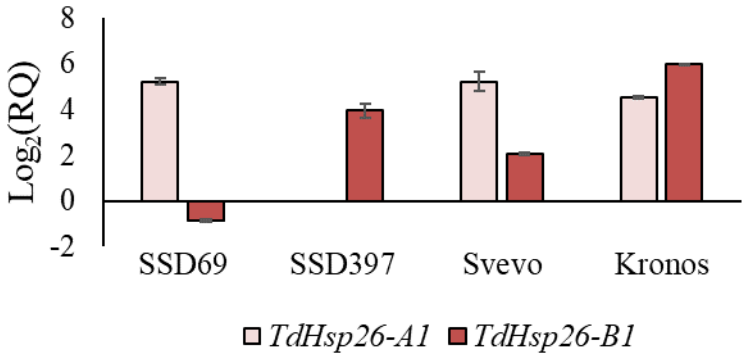

Fig 40. Expression analysis of *TdHsp26-A1* and *TdHsp26-B*1 in SSD69, SSD397, Svevo and Kronos. The induction levels are measured as the fold change (RQ) of the treated samples in respect to the controls and reported as log2(RQ) in the chart.

4.3.5.5 Yield traits

The number of spikes per plant, interacting with spikelet number and floret fertility, determines grain number and thereby final yield, thus yield traits were recorded at maturity to assess the effects of prolonged heat stress.

Overall, all yield traits were affected by the severe and prolonged stress imposed, however some differences were retrieved between genotypes reinforcing the so far observed

superior characteristics of SSD69 comparable to Svevo, while SSD397 showed to be the more susceptible genotypes with strongly reduced yield parameters.

As previously observed, SSD397 showed the bigger spikes among spikes while Svevo, Kronos and SSD69 spikes were not significantly different in spike size (Figure 41a). The number of spikelets were comparable with those produced in normal environmental growth conditions for SSD69 and SSD397 (Figure 41c). Same behavior was observed for the number of spikelets, suggesting a higher plant biomass produced during the prolonged heat stress for SSD397 (Figure 41c).

However, when the number of seeds per plant was scored although all lines suffer of the imposed prolonged stress SSD69 showed 88,34% more seeds than SSD397, comparable with the seeds produced by Svevo, 9,1% more for SSD69, while Kronos also showed a reduced number of seeds produced, indicating a higher loss of fertility for SSD397 (Figure 41b).

The grain yield was calculated confirming comparable yields for SSD69 and Svevo and almost a 50% yield reduction in comparison with SSD69 for SSD397 (Figure 41d). Kronos showed intermediate final yield.

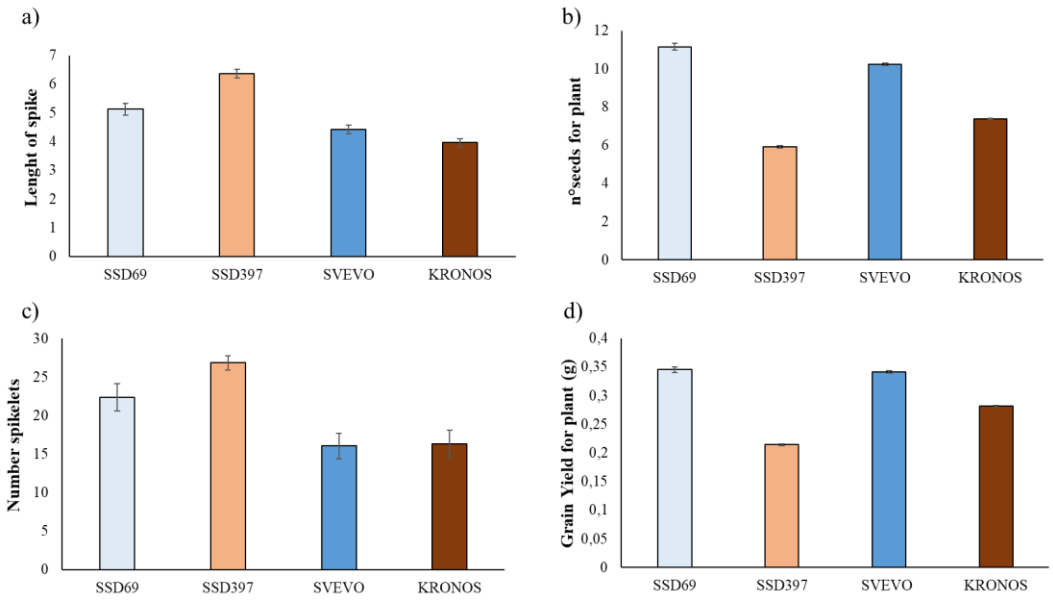

Fig.41 Yield traits recorded for all SSD lines considering the first culm produced. a) Length of spike (cm), b) number of spikelets per spike, c) number of seeds per plant, d) grain yield per plant. Standard Error are reported.

4.3.6 Discussion of the prolonged heat stress response in anthesis phase

Here, the natural environmental summer conditions, where the heat stress is often prolonged during the entire length of the durum wheat developmental stages, was exploited in pots mimicking the conditions observed in the field.

Plants were subjected for 90 days (from transplant to seed maturity) to a prolonged heat stress above 35°C were recorded for the entire length of the experiment.

The objective of this study was to firstly identify the effect of a prolonged heat stress during the entire length of the plant growth cycle from seedling (Zadoks 10) to seed maturity (Zadoks 99) on SSD genotypes on yield components. Photosynthesis is the most sensitive physiological event leading to poor growth performance in wheat (Feng et al. 2014) as also confirmed in this experiment. A major effect of heat stress is the reduction in photosynthesis resulting from decreased plant height, impaired photosynthetic machinery, reduced transpiration and reduction in wheat production (Ashraf and Harris 2013; Mathur, Agrawal, and Jajoo 2014).

Heat stress firstly damages the complex phenomena of PSII and secondly, changes the photosynthetic behavior. This is manifested when temperatures exceeding 40°C dissociate the light harvesting complex-II Chl a/b-proteins from the PSII (Iwai et al. 2010). This was constantly reached for the entire length of the experiment, mostly in the afternoon. The index Fv/Fm was appropriate in selecting most efficient genotypes in our study, in fact, SSD69 and Svevo did not show a drop in Fv/Fm values also in severe heat stress conditions, supporting that higher Fv/Fm values indicated increased tolerance to heat stress (Nagar et al. 2015; Rong Zhou et al. 2015; D. K. Sharma et al. 2017).

Previous study conducted by Sharma et al. (2015), on *T. aestivum* used Fv/Fm as a selection criteria for heat tolerance (Sharma et al. 2015).

CTD although reporting low values for SSD69 that has been described as a staygreen phenotype under heat stress as previously reported by (Kumari et al. 2012), does not seem to be highly effective in the test environmental conditions for genotype selection.

Plants under high temperatures cool their canopies through transpiration, which occurs through stomata when soil water is available. Efficient reproductive development requires higher gas exchanges, which occur through open stomata, putting plants in a constant struggle for survival against harsh environments (Huggins et al. 2018). This has been validated also in these severe conditions, in fact, g_s showed a good correlation with the temperature, higher in

the afternoon, suggesting that in presence of heat stress, an increased transpiration was operated to maintain plant functions.

Higher g_s observed in the afternoon with almost 50°C was observed in SSD69 and can be associated with better performance of tolerant genotypes under stress conditions (Saeidi and Abdoli 2015) leading to hypothesize that SSD69 and Svevo had in common a strong stomatal regulatory ability in response to increasing temperatures.

In fact, line SSD69 exhibits large variations in g_s attributable to both temperature and moisture, and we observe the same behavior in Svevo. In lines SSD397 and Kronos they did not show these traits, incentivizing the potential susceptibility of these genotypes.

Miller et al. 2009 found that heat stress increased O_2^- production in root by 68% and MDA content in leaf by 27% at the early stages, and 58% at the later stage of seedling development (Fernie et al. 2022).

In terms of yield, which are the final traits to be considered, the ability of SSD69 to overcome the severe heat stress, despite the slow and low overall plant growth, was confirmed. SSD69 and Svevo showed an increased estimated fertility that corresponds to an increased grain yield and number of seeds when compared with SSD397 that promoted high and fast plant biomass growth but at the end failed in the reproductive stage leading to low yields and reduced seed set.

The severity of grain yield depletion in wheat crops is highly dependent on the growth stage at which heat stress occurs.

Although all growth stages are susceptible, heat stress during the reproductive phase (anthesis and grain filling) can particularly hinder grain development, causing reproductive sterility and significant reduction in grain number and yield (Fernie et al. 2022).

SSD397 showed the most delayed anthesis in comparison with the other genotypes tested. This coupled with the extremely high temperatures reached (min 21°C and max 58°C) severely lowered grain yield by reducing grain number per plant as a consequence of a marked floret sterility (Kaur and Behl 2010).

As observed in almost all lines, moreover, day/night high temperatures of 31/20°C may also cause shrinking of grains resulting from changing structures of the aleurone layer and cell endosperm, as resulted in this experiment (data not shown) (Dias, Bagulho, and Lidon 2008).

SSD69 showed, in extremely severe heat stress conditions, better thermotolerance than SSD397 probably because of its increases in preventing protein degradation and PSII repair, and oxidative stress response.

Based on the real-time results, a high difference between the two genotypes have been observed. As Svevo, known as tolerant variety, SSD69 showed an higher expression of *TdHsp26-A1* with respect to *TdHsp26-B1.* SSD 397 that showed a heat susceptible phenotype under heat stress, showed no expression of *TdHsp26-A1* but good expression levels of *TdHsp26-B1*. In SSD 69 the downregulation of *TdHsp26-B1* is linked with the dynamic accumulation of MDA in SSD 69 leaf samples, leading to hypothesize a correlation between *TdHSP26-A1* and the accumulation of MDA under heat stress (Section 4.3.5), and its involvement in the membrane protection pathway.

Based on these results, in Figure 42 we summarized the formulated hypothesis of HSP26 involvement in the heat stress response. Under heat stress conditions, HSP26, participate directly and indirectly in the protection of PSII, the stomata opening to maintain high levels of transpiration and corresponding reduction in temperature, and finally it is involved in protecting the cell from ROS resulting in the reduction of MDA content.

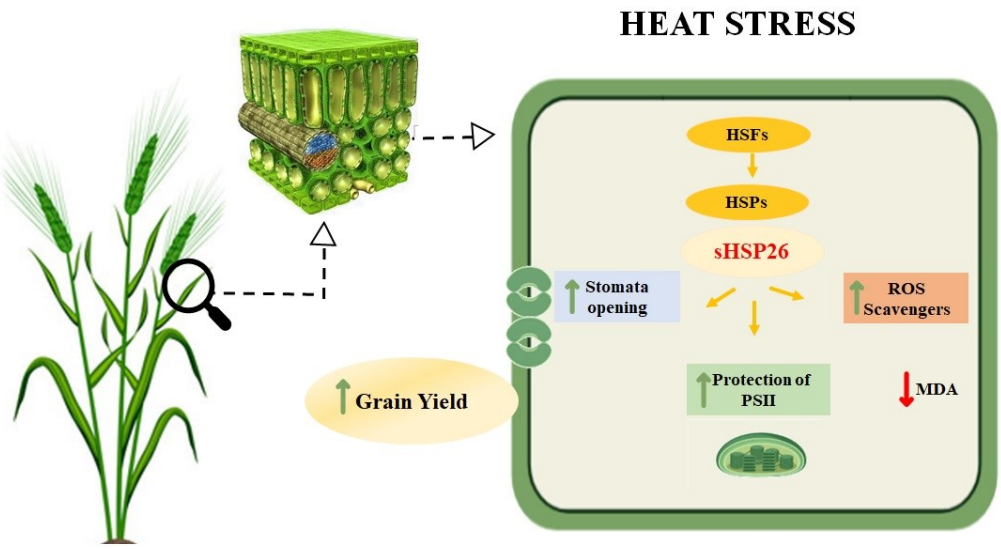

Fig 42. Proposed model of the interaction between sHSP26 and various physiological components. Red arrows mean decrease, and green arrows mean increase.

5. DISCUSSION AND CONCLUSIONS

Increasing temperatures and consequent changes in climate adversely affect plant growth and development, resulting in devastating loss of wheat productivity. Increased global mean temperatures and frequency of extreme heat days pose a significant risk to the productivity of wheat cropping systems (Sharma et al. 2022) that rely on optimal conditions between 12.0–22.0°C for favorable growth and development.

For each degree rise in temperature, wheat production is estimated to reduce by 6%. A detailed overview of morpho-physiological responses of wheat to heat stress may help formulating appropriate strategies for heat-stressed wheat yield improvement.

To address these challenges, new and innovative knowledge, resources, tools, and methods to facilitate breeding are needed (Paux et al. 2022).

The availability of high throughput genomic tools including single nucleotide polymorphism (SNP) arrays, high density molecular marker maps, and full genome sequences concretely help in accelerating the average phenotypic values of crop plants. On one hand, the use of induced mutations coupled with modern genomics tools is an effective strategy for identifying and manipulating genes for crop improvement. A successful example is High-throughput TILLING methodology, which detects mutations in mutagenized populations.

On the other hand, such powerful tools are essential to perform genome-wide association studies, to implement genomic and phenomic selection, and to characterize the richness of natural worldwide diversity (Paux et al. 2022).

In this frame, EcoTILLING identifies single nucleotide polymorphisms (SNPs) within a natural population and associates these variations with traits of breeding interest. The main advantage of this “reverse genetics” strategy is that they can be applied to any species regardless of genome size and ploidy level (Irshad et al. 2020).

However, both techniques required several rounds of backcross in wheat to stabilize the genome by reducing redundant mutation (in TILLING) and the drawbacks traits characterized in genetic material as the landraces (in EcoTILLING).

Here, the following question has been raised: how the genetic variation in the *TdHsp26* genes influenced the performance of the SSD69 line during heat stress occurring in different developmental stages?

Validation of the relationship between gene variation and key mechanisms of plant development regulating final yield has been performed.

Chlorophyll fluorescence parameter, canopy infrared temperature (IR or CTD) and plant performance under stress have been demonstrated to be effective phenotyping traits and good indicators enabling the characterization and selection of a complex environmental response as heat stress and in turn may directly or indirectly aid in crop improvement for stress tolerance in the context of global climate change.

In this work, we applied a progressive selection of durum wheat landraces, in different key development stages, revealing in final round of selection, a possible resilience to heat stress for SSD 69 and, as expected for Svevo, and susceptibility for SSD 397 and for Kronos in the tested conditions.

Heat shock proteins occur in response to high temperatures, binding to denatured proteins as protection from aggregation, before facilitating their reformation after high temperature ceases (Kumar et al. 2022).

Here in the frame of different developmental stages of different genotypes, we observed that *TdHsp26-A1* and *-B1* are genotypic and growth stage specific as hypothesized in previous studies performed in bread wheat (Kumar et al. 2018).

Especially in seedlings, we observed an alteration in the antioxidant pathway, letting hypothesize for the heat resilient genotype SSD69 a reduced production of H_2O_2 and the consequence lower production of MDA, that, in anthesis stage is not however linked with a decrease in yield.

In SSD 397 the conventional mechanism of antioxidant is maintained in all stages, with the consequence of an increased and faster biomass production, anticipating the anthesis but a lower fertility encountered.

SSD 69 put in place a set of defense mechanisms aimed at preserving final yields, under severe heat stress, in both tillering and anthesis. SSD 69 increased, in tillering experiment, the canopy temperature depression known to be an important physiological mechanism for sustaining grain yield after exposure to heat stress (Reynolds et al. 2020). In high temperature and low humidity conditions, thermotolerant cultivars expressed more efficient transpiration cooling, owing to greater stomatal conductance of the leaf. SSD69 also showed a staygreen phenotype indicating its ability to overcome heat stress and increased yield.

Concluding, in this thesis we have successfully applied a combined genotypic and phenotypic approach that leads to the identification of two contrasting durum wheat landraces, of which SSD69 showed superior heat resilience characteristics with increased yield performance also in extreme heat stress conditions.

A set of phenotyping traits have been identified as key traits for the identification of heat resilience genotypes, constituting a toolbox useful for further analysis.

6. SUPPLEMENTARY MATERIAL

Suppl. Table1 SNPs identified in the *TdHsp26-A1* and *TdHsp26-B1* sequence of the SSD genotypes, the wild type nucleotide is indicated. The position of the identified SNP on the gene elements is also reported.

GENE	POOL	SNP ID	REFERENCE POSITION	NUCLEOTIDE WILDTYPE	SSD SNP	ALLELE FREQUENCY	POSITION ON THE GENE	TYPE OF MUTATION	EFFECTS
TdHsp26-A1	LIB4	SNP1	2086	G	T	14,83	PROMOTOR		
TdHsp26-A1	LIB1	SNP2	2102	G	C	6,80	PROMOTOR		
TdHsp26-A1	LIB1	SNP5	2469	G	C	68,52	EXON1	MISSENSE	**GAG/CAG(E73Q)**
TdHsp26-A1	LIB2	SNP5	2469	G	C	29,31	EXON1	MISSENSE	**GAG/CAG(E73Q)**
TdHsp26-A1	LIB3	SNP5	2469	G	C	46,37	EXON1	MISSENSE	**GAG/CAG(E73Q**
TdHsp26-A1	LIB4	SNP5	2469	G	C	80,65	EXON1	MISSENSE	**GAG/CAG(E73Q)**
TdHsp26-A1	LIB1	SNP8	2929	G	A	68,52	EXON2	MISSENSE	**GCC/GAC(G196)**
TdHsp26-A1	LIB2	SNP8	2929	G	A	30,02	EXON2	MISSENSE	**GCC/GAC(G196)**
TdHsp26-A1	LIB3	SNP8	2929	G	A	46,32	EXON2	MISSENSE	**GCC/GAC(G196D)**
TdHsp26-A1	LIB4	SNP8	2929	G	A	80,47	EXON2	MISSENSE	**GCC/GAC(G196D)**
TdHsp26-B1	LIB1	SNP2	597	G	T	7,57	PROMOTOR		
TdHsp26-B1	LIB1	SNP3	633	A	T	11,54	PROMOTOR		
TdHsp26-B1	LIB3	SNP4	1212	G	A	21,41	PROMOTOR		
TdHsp26-B1	LIB3	SNP5	1250	G	A	14,79	PROMOTOR		
TdHsp26-B1	LIB2	SNP5	1250	G	A	5,48	PROMOTOR		
TdHsp26-B1	LIB3	SNP6	1287	A	G	96,18	PROMOTOR		
TdHsp26-B1	LIB1	SNP6	1287	A	G	98,92	PROMOTOR		
TdHsp26-B1	LIB2	SNP6	1287	A	G	94,14	PROMOTOR		
TdHsp26-B1	LIB4	SNP6	1287	A	G	99,79	PROMOTOR		
TdHsp26-B1	LIB3	SNP18	1570	C	G	4,72	PROMOTOR		
TdHsp26-B1	LIB3	SNP19	1596	G	C	4,63	PROMOTOR		
TdHsp26-B1	LIB3	SNP25	1647	A	C	5,17	PROMOTOR		
TdHsp26-B1	LIB3	SNP26	1667	A	G	5,09	5UTR'		
TdHsp26-B1	LIB4	SNP59	2180	A	G	46,37	EXON2	MISSSENSE	**ATG/GTG(M97V)**

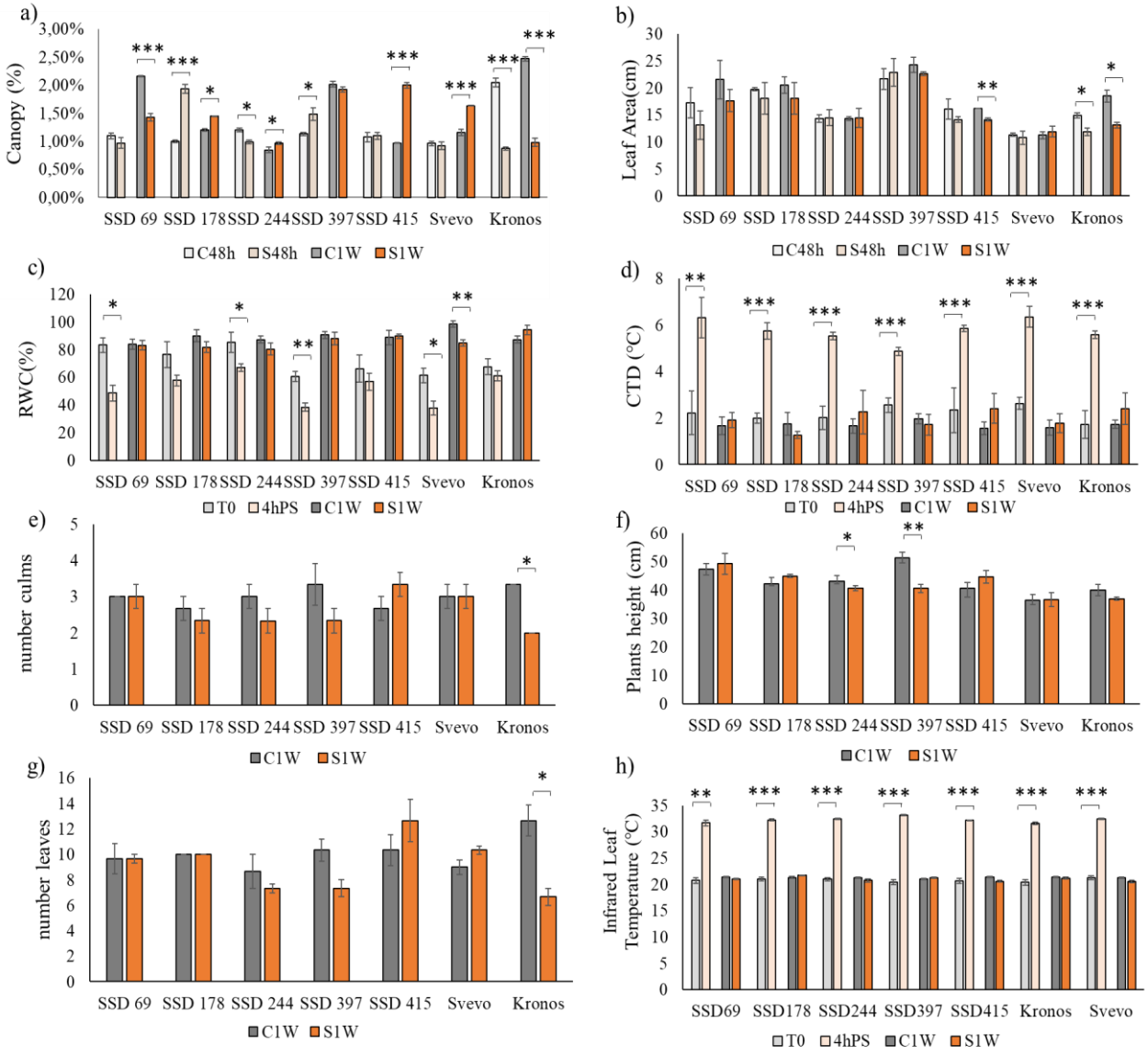

Suppl. Figure1. Morphological and physiological traits recorded in tillering stage. a) Canopy b) Leaf area, c) RWC, d) CTD, e) number of culms, f) plant heigh, g) number leaves, h) Infrared Leaf Temperature. Student's t-test was applied. Error bars are reported and represent the standard error. *P <0.05, **P <0.01, ***P <0.001.

7. ACKNOWLEDGMENTS

At the end of such an intense path, it is fitting to make some thanks.

I want to thank Professor Marmiroli, for giving me the opportunity to be able to undertake this path and for the advice he gave me in the various stages of the work.

A special, big thank you goes to my tutor Dr. Janni for the passion with which she has followed this work, dedicating much of her time to me and for showing me punctually her enormous scientific and human depth.

I would like to thank all the Professors, Researcher, Post-doc, technician and PhD Student of the Marmiroli's group.

A special thanks goes to those colleagues who became friends Dr.Sophia Luche, Dr. Valentina Gallo, Dr. Riccardo Rossi, Dr. Ilenia Iosa, Dr. Gianluigi Giannelli thanks for the laughter, support, advice and very simply for listening to me when I needed it.

I would like to thank the Stuard company for helping me with plant management during the last experiment.

I would like to thank Dr Filippo Vurro of IMEM-CNR (Parma, Italy) for helping me with the more complex statistical analyses.

I must also thank Professor Carla Ceoloni's group from University of Tuscia (Viterbo, Italy) for their great helpfulness.

Thanks, are also due to Dr Giorgio Impollonia of UNICATT (Piacenza, Italy) for his great help with thermal image analysis.

I must thank my family and friends for their support and for giving me that healthy homesickness that punctually brings me back home, which will always be my happy place.

The last thank you goes to the person who believed in this more than I did, supporting and incentivizing me to overcome every obstacle that came in front of me, thank you Fabrizio.

REFERENCES

Acharjee A., Chibon P.Y., Kloosterman B., America T., Renaut J., Maliepaard C. and Visser R.G.F. 2018. 'Genetical Genomics of Quality Related Traits in Potato Tubers Using Proteomics'. *BMC Plant Biology* 18 (1): 20. https://doi.org/10.1186/s12870-018-1229-1.

'Agricultural Production - Crops'. 2022. Eurostat Statistics Explained. 2022. https://ec.europa.eu/eurostat/statistics-explained/index.php?title=Agricultural_production_-_crops.

Ahmad S., Hakoomat A., Zartash F., Ghulam A., Irfan M., Hina A., Azam M. and Hasanuzzaman M. 2015. 'Measuring Leaf Area of Winter Cereals by Different Techniques: A Comparison'. *Pakistan Journal of Life and Social Sciences* 13(2): 117-125.

Aiqing S., Impa S., Sunoj Valiaparambil S., Kanwardeep S., Kulvinder G., Prasad P. V. V. and Krishna Jagadish S.V. 2018. 'Heat Stress during Flowering Affects Time of Day of Flowering, Seed Set, and Grain Quality in Spring Wheat'. *Crop Science* 58 (1): 380–92. https://doi.org/10.2135/cropsci2017.04.0221.

Akter N. and Islam M.R. 2017. 'Heat Stress Effects and Management in Wheat. A Review'. *Agronomy for Sustainable Development* 37 (5): 37. https://doi.org/10.1007/s13593-017-0443-9.

Al-Ghussain L. 2019. 'Global Warming: Review on Driving Forces and Mitigation'. *Environmental Progress & Sustainable Energy* 38 (1): 13–21. https://doi.org/10.1002/ep.13041.

Ali M.M. U., Roe S.M., Vaughan C.K., Meyer P., Panaretou B., Piper P.W., Prodromou C. and Pearl L.H. 2006. 'Crystal Structure of an Hsp90–Nucleotide–P23/Sba1 Closed Chaperone Complex'. *Nature* 440 (7087): 1013–17. https://doi.org/10.1038/nature04716.

Almoguera C., Prieto-Dapena P., Personat J.M., Tejedor-Cano J., Lindahl M., Diaz-Espejo A. and Jordano J. 2012. 'Protection of the Photosynthetic Apparatus from Extreme Dehydration and Oxidative Stress in Seedlings of Transgenic Tobacco'. *PLoS ONE* 7 (12): e51443. https://doi.org/10.1371/journal.pone.0051443.

Al-Whaibi M.H. 2011. 'Plant Heat-Shock Proteins: A Mini Review'. *Journal of King Saud University - Science* 23 (2): 139–50. https://doi.org/10.1016/j.jksus.2010.06.022.

Al-Yasiri Q. and Géczi G. 2021. 'Global Warming Potential: Causes and Consequences'. *Academia Letters*. Article 3202. https://doi.org/10.20935/AL3202.

Anderson T.R., Hawkins E. and Jones P.D. 2016. 'CO2, the Greenhouse Effect and Global Warming: From the Pioneering Work of Arrhenius and Callendar to Today's Earth System Models'. *Endeavour* 40 (3): 178–87. https://doi.org/10.1016/j.endeavour.2016.07.002.

Andrási N., Pettkó-Szandtner A. and Szabados L. 2021. 'Diversity of Plant Heat Shock Factors: Regulation, Interactions, and Functions'. *Journal of Experimental Botany* 72 (5): 1558–75. https://doi.org/10.1093/jxb/eraa576.

Araus J.L., Buchaillot M.L. and Kefauver S.C. 2022. 'High Throughput Field Phenotyping'. *Wheat Improvement*, 495–512. https://doi.org/10.1007/978-3-030-90673-3_27.

Araus J.L., Kefauver S.C, Zaman-Allah M., Olsen M.S. and Cairns J.E. 2018. 'Phenotyping: New Crop Breeding Frontier'. *Encyclopedia of Sustainability Science and Technology*, 1–11. https://doi.org/10.1007/978-1-4939-2493-6_1036-1.

Arofatullah N.A., Hasegawa M., Tanabata S., Ogiwara I. and Sato T. 2018. 'Heat Shock-Induced Resistance Against Pseudomonas Syringae Pv. Tomato (Okabe) Young et al. via Heat Shock Transcription Factors in Tomato'. *Agronomy* 9 (1): 2. https://doi.org/10.3390/agronomy9010002.

Asada Kozi. 2006. 'Production and Scavenging of Reactive Oxygen Species in Chloroplasts and Their Functions'. *Plant Physiology* 141 (2): 391–96. https://doi.org/10.1104/pp.106.082040.

Ashraf M. and Harris P. J. C. 2013. 'Photosynthesis under Stressful Environments: An Overview'. *Photosynthetica* 51 (2): 163–90. https://doi.org/10.1007/s11099-013-0021-6.

Avni R., Nave M., Barad O., Baruch K., Twardziok S.O., Gundlach H., Hale I., et al. 2017. 'Wild Emmer Genome Architecture and Diversity Elucidate Wheat Evolution and Domestication'. *Science* 357 (6346): 93–97. https://doi.org/10.1126/science.aan0032.

Barkley N. and Wang M. 2008. 'Application of TILLING and EcoTILLING as Reverse Genetic Approaches to Elucidate the Function of Genes in Plants and Animals'. *Current Genomics* 9 (4): 212–26. https://doi.org/10.2174/138920208784533656.

Barlow K.M., Christy B.P., O'Leary G.J., Riffkin P.A. and Nuttall J.G. 2015. 'Simulating the Impact of Extreme Heat and Frost Events on Wheat Crop Production: A Review'. *Field Crops Research* 171: 109–19. https://doi.org/10.1016/j.fcr.2014.11.010.

Deepak B., Downs C.A. and Heckathorn S.A. 2003. 'Variation in Chloroplast Small Heat-Shock Protein Function Is a Major Determinant of Variation in Thermotolerance of Photosynthetic Electron Transport among Ecotypes of Chenopodium Album'. *Functional Plant Biology* 30 (10): 1071. https://doi.org/10.1071/FP03106.

Basha E., O'Neill H. and Vierling E. 2012. 'Small Heat Shock Proteins and α-Crystallins: Dynamic Proteins with Flexible Functions'. *Trends in Biochemical Sciences* 37 (3): 106–17. https://doi.org/10.1016/j.tibs.2011.11.005.

Bigot S., Buges J., Gilly L., Jacques C., Le Boulch P., Berger M., Delcros P., et al. 2018. 'Pivotal Roles of Environmental Sensing and Signaling Mechanisms in Plant Responses to Climate Change'. *Global Change Biology* 24 (12): 5573–89. https://doi.org/10.1111/gcb.14433.

Bondino H.G., Valle E.M., and Ten Have A. 2012. 'Evolution and Functional Diversification of the Small Heat Shock Protein/α-Crystallin Family in Higher Plants'. *Planta* 235 (6): 1299–1313. https://doi.org/10.1007/s00425-011-1575-9.

Bösl B., Grimminger V. and Walter S. 2006. 'The Molecular Chaperone Hsp104—A Molecular Machine for Protein Disaggregation'. *Journal of Structural Biology* 156 (1): 139–48. https://doi.org/10.1016/j.jsb.2006.02.004.

Bourgine B. and Guihur A. 2021. 'Heat Shock Signaling in Land Plants: From Plasma Membrane Sensing to the Transcription of Small Heat Shock Proteins'. *Frontiers in Plant Science* 12 (August): 710801. https://doi.org/10.3389/fpls.2021.710801.

Branlard G., Giraldo P., He Z., Igrejas G.G., Ikeda T.M., Janni M., Labuschagne M.T., Wang D., Wentzel B. and Zhang K. 2020. 'Contribution of Genetic Resources to Grain Storage Protein Composition and Wheat Quality', 557 p. https://doi.org/10.1007/978-3-030-34163-3_4.

Buffagni V. 2019. 'Studying durum wheat genetic diversity: a molecular approach to identify new alleles for drought resilience'. Doctoral thesis, University of Parma. Department

of Chemical, Life and Environmental Sustainability Sciences. https://www.repository.unipr.it/handle/1889/3721.

Buttar Z.A., Wu S. N., Arnao M. B., Wang C., Ullah I. and Wang C. 2020. 'Melatonin Suppressed the Heat Stress-Induced Damage in Wheat Seedlings by Modulating the Antioxidant Machinery'. *Plants* 9 (7): 809. https://doi.org/10.3390/plants9070809.

Calderwood S. K., Xie X.,Wang Y., Khaleque M.A., Chou S.D., Murshid A., Prince T. and Zhang Y. 2010. 'Signal Transduction Pathways Leading to Heat Shock Transcription'. *Signal Transduction Insights* 2 (January): STI.S3994. https://doi.org/10.4137/STI.S3994.

Cao P.B. 2022. '*In silico* structural, evolutionary, and expression analysis of small heat shock protein (sHSP) encoding genes in cocoa (*Theobroma Cacao L.*)'. *The Journal of Animal and Plant Sciences* 32 (5). https://doi.org/10.36899/JAPS.2022.5.0546.

Carvalho L.C., Gonçalves E.F., Da Silva J.M. and Costa J.M. 2021. 'Potential Phenotyping Methodologies to Assess Inter- and Intravarietal Variability and to Select Grapevine Genotypes Tolerant to Abiotic Stress'. *Frontiers in Plant Science* 12 (October): 718202. https://doi.org/10.3389/fpls.2021.718202.

Caverzan A., Casassola A. and Patussi Brammer S. 2016. 'Antioxidant Responses of Wheat Plants under Stress'. *Genetics and Molecular Biology* 39 (1): 1–6. https://doi.org/10.1590/1678-4685-GMB-2015-0109.

Çelik Ö., Ayan A. and Atak Ç. 2017. 'Enzymatic and Non-Enzymatic Comparison of Two Different Industrial Tomato (Solanum Lycopersicum) Varieties against Drought Stress'. *Botanical Studies* 58 (1): 32. https://doi.org/10.1186/s40529-017-0186-6.

Chauhan H., Khurana N., Nijhavan A., Khurana J.P. and Khurana P. 2012. 'The Wheat Chloroplastic Small Heat Shock Protein (SHSP26) Is Involved in Seed Maturation and Germination and Imparts Tolerance to Heat Stress'. *Plant, Cell & Environment* 35 (11): 1912–31. https://doi.org/10.1111/j.1365-3040.2012.02525.x.

Chawade A., Alexandersson E., Bengtsson T., Andreasson E. and Levander F. 2016. 'Targeted Proteomics Approach for Precision Plant Breeding'. *Journal of Proteome Research* 15 (2): 638–46. https://doi.org/10.1021/acs.jproteome.5b01061.

Chebrolu K.K., Fritschi F.B., Ye S., Krishnan H.B., Smith J.R. and Gillman J.D. 2016. 'Impact of Heat Stress during Seed Development on Soybean Seed Metabolome'. *Metabolomics* 12 (2): 28. https://doi.org/10.1007/s11306-015-0941-1.

Chen C., Wang B., Feng P., Xing H., Fletcher A.L. and Lawes R.A. 2020. 'The Shifting Influence of Future Water and Temperature Stress on the Optimal Flowering Period for Wheat in Western Australia'. *Science of The Total Environment* 737: 139707. https://doi.org/10.1016/j.scitotenv.2020.139707.

Chen L., Huang L., Min D., Phillips A., Wang S., Madgwick P.J., Martin A. J. Parry, and Yin-Gang Hu. 2012. 'Development and Characterization of a New TILLING Population of Common Bread Wheat (Triticum Aestivum L.)'. *PLOS ONE* 7 (7): e41570. https://doi.org/10.1371/journal.pone.0041570.

Chen S.S., Jiang J., Xiao-Jiao, Han X.J., Yun-Xing Zhang Y.X. and Zhuo R.Y. 2018. 'Identification, Expression Analysis of the Hsf Family, and Characterization of Class A4 in Sedum Alfredii Hance under Cadmium Stress'. *International Journal of Molecular Sciences* 19 (4): 1216. https://doi.org/10.3390/ijms19041216.

Comastri A. 2016. 'Isolation, Characterization and Discovery of New Alleles of SHsp Genes in Durum Wheat (*Triticum Durum* Desf.)'. Doctoral thesis, University of Parma. Department of Chemical, Life and Environmental Sustainability Sciences.

Comastri A., Janni M., Simmonds J., Uauy C., Pignone D., Nguyen H.T. and Marmiroli N. 2018. 'Heat in Wheat: Exploit Reverse Genetic Techniques to Discover New Alleles Within the Triticum Durum SHsp26 Family'. *Frontiers in Plant Science* 9 (September): 1337. https://doi.org/10.3389/fpls.2018.01337.

Coppedè N., Janni M., Bettelli M., Maida C.L., Gentile F., Villani M., Ruotolo R, et al. 2017. 'An in Vivo Biosensing, Biomimetic Electrochemical Transistor with Applications in Plant Science and Precision Farming'. *Scientific Reports* 7 (1): 1–9. https://doi.org/10.1038/s41598-017-16217-4.

Crofts H. J. 1989. 'On Defining a Winter Wheat'. *Euphytica* 44 (3): 225–34. https://doi.org/10.1007/BF00037529.

Danzi D., Briglia N., Petrozza A., Summerer S., Povero G., Stivaletta A., Cellini F., Pignone D., De Paola D., and Janni M. 2019. 'Can High Throughput Phenotyping Help Food Security in the Mediterranean Area?' *Frontiers in Plant Science* 10 (January): 15. https://doi.org/10.3389/fpls.2019.00015.

Danzi D., De Paola D., Petrozza A., Summerer S., Cellini F., Pignone D. and Janni M. 2022. 'The Use of Near-Infrared Imaging (NIR) as a Fast Non-Destructive Screening Tool to Identify Drought-Tolerant Wheat Genotypes'. *Agriculture* 12 (4): 537. https://doi.org/10.3390/agriculture12040537.

Danzi D., Marino I., De Bari I., Mastrolitti S., Petretto G.L., Pignone D., Janni M., Cellini F. and Venditti T. 2021. 'Assessment of Durum Wheat (Triticum Durum Desf.) Genotypes Diversity for the Integrated Production of Bioethanol and Grains'. *Energies* 14 (22): 7735. https://doi.org/10.3390/en14227735.

De Jong L., Moreau X. and Thiéry A. 2008. 'Expression of Heat Shock Proteins as Biomarker Tool in Aquatic Invertebrates: Actual Knowledge and Ongoing Developments for the Early Detection of Environmental Changes and Ecological Risks'. Heat-Shock Proteins: New Research, 20, Nova Publishers, 375-392,

Almeida A.S., Bagulho A.S. and Lidon F.C. 2008. 'Ultrastructure and Biochemical Traits of Bread and Durum Wheat Grains under Heat Stress'. *Brazilian Journal of Plant Physiology* 20 (4): 323–33. https://doi.org/10.1590/S1677-04202008000400008.

Díaz-Villanueva J. F., Díaz-Molina R. and García-González V. 2015. 'Protein Folding and Mechanisms of Proteostasis'. *International Journal of Molecular Sciences* 16 (8): 17193–230. https://doi.org/10.3390/ijms160817193.

Djanaguiraman M., Narayanan S., Erdayani E. and Prasad P. V. V. 2020. 'Effects of High Temperature Stress during Anthesis and Grain Filling Periods on Photosynthesis, Lipids and Grain Yield in Wheat'. *BMC Plant Biology* 20 (1): 268. https://doi.org/10.1186/s12870-020-02479-0.

Dong Y., Xu L., Wang Q., Fan Z., Kong J. and Bai X. 2014. 'Effects of Exogenous Nitric Oxide on Photosynthesis, Antioxidative Ability, and Mineral Element Contents of Perennial Ryegrass under Copper Stress'. *Journal of Plant Interactions* 9 (1): 402–11. https://doi.org/10.1080/17429145.2013.845917.

Driedonks N., Xu J., Peters J.L., Park S. and Rieu I. 2015. 'Multi-Level Interactions Between Heat Shock Factors, Heat Shock Proteins, and the Redox System Regulate Acclimation to Heat'. *Frontiers in Plant Science* 6 (November). https://doi.org/10.3389/fpls.2015.00999.

EFA. 2022. 'Durum Wheat: Italian Production Falls'. 2022. https://www.efanews.eu/item/25669-durum-wheat-italian-production-falls.html.

Erenstein O., Jaleta M., Mottaleb K.A., Sonder K., Donovan J., and Braun H.J. 2022. 'Global Trends in Wheat Production, Consumption and Trade'. In *Wheat Improvement*, 47–66. Cham: Springer International Publishing. https://doi.org/10.1007/978-3-030-90673-3_4.

Ezcurra I., Wycliffe P., Nehlin L., Ellerström M. and Rask L. 2000. 'Transactivation of the Brassica Napus Napin Promoter by ABI3 Requires Interaction of the Conserved B2 and B3 Domains of ABI3 with Different Cis-Elements: B2 Mediates Activation through an ABRE, Whereas B3 Interacts with an RY/G-Box'. *The Plant Journal: For Cell and Molecular Biology* 24 (1). https://doi.org/10.1046/j.1365-313x.2000.00857.x.

'FAOSTAT'. 2022. 2022. https://www.fao.org/faostat/en/#data/QCL.

Feng B., Liu P., Li G., Dong S.T., Wang F.H., Kong L.A. and Zhang J. W. 2014. 'Effect of Heat Stress on the Photosynthetic Characteristics in Flag Leaves at the Grain-Filling Stage of Different Heat-Resistant Winter Wheat Varieties'. *Journal of Agronomy and Crop Science* 200 (2): 143–55. https://doi.org/10.1111/jac.12045.

Fernie E., Tan D.K.Y., Liu S.Y., Ullah N. and Khoddami A. 2022. 'Post-Anthesis Heat Influences Grain Yield, Physical and Nutritional Quality in Wheat: A Review'. *Agriculture* 12 (6): 886. https://doi.org/10.3390/agriculture12060886.

Ferreira M.S.L., Martre P., Mangavel C., Girousse C., Rosa N.N., Samson M.F. and Morel M.H. 2012. 'Physicochemical Control of Durum Wheat Grain Filling and Glutenin Polymer Assembly under Different Temperature Regimes'. *Journal of Cereal Science* 56 (1): 58–66. https://doi.org/10.1016/j.jcs.2011.11.001.

'Fifth Assessment Report — IPCC'. 2014. 2014. https://www.ipcc.ch/assessment-report/ar5/.

Finco A., Bentivoglio D., Chiaraluce G., Alberi M., Chiarelli E., Maino A., Mantovani F. et al. 2022. 'Combining Precision Viticulture Technologies and Economic Indices to Sustainable Water Use Management'. *Water* 14 (9): 1493. https://doi.org/10.3390/w14091493.

Fokar M., Blum A. and Nguyen H.T. 1998. 'Heat Tolerance in Spring Wheat. II. Grain Filling'. *Euphytica* 104 (1): 9–15. https://doi.org/10.1023/A:1018322502271.

Galmés J., Aranjuelo I., Medrano H. and Flexas J. 2013. 'Variation in Rubisco Content and Activity under Variable Climatic Factors'. *Photosynthesis Research* 117 (1–3): 73–90. https://doi.org/10.1007/s11120-013-9861-y.

Gupta N. K., Agarwal S., Agarwal V. P., Nathawat N. S., Gupta S., and Singh G.. 2013. 'Effect of Short-Term Heat Stress on Growth, Physiology and Antioxidative Defence System in Wheat Seedlings'. *Acta Physiologiae Plantarum* 35 (6): 1837–42. https://doi.org/10.1007/s11738-013-1221-1.

Gupta S.C., Sharma A., Mishra M., Mishra R.K. and Chowdhuri D.K. 2010. 'Heat Shock Proteins in Toxicology: How Close and How Far?' *Life Sciences* 86 (11–12): 377–84. https://doi.org/10.1016/j.lfs.2009.12.015.

Hafrén A., Hofius D., Rönnholm G., Sonnewald U. and Mäkinen K. 2010. 'HSP70 and Its Cochaperone CPIP Promote Potyvirus Infection in *Nicotiana Benthamiana* by Regulating Viral Coat Protein Functions'. *The Plant Cell* 22 (2): 523–35. https://doi.org/10.1105/tpc.109.072413.

Hahn A., Bublak D., Schleiff E. and Scharf K.D. 2011. 'Crosstalk between Hsp90 and Hsp70 Chaperones and Heat Stress Transcription Factors in Tomato'. *The Plant Cell* 23 (2): 741–55. https://doi.org/10.1105/tpc.110.076018.

Hansen James., Sato M., Hearty P., Ruedy R., Kelley M., Masson-Delmotte V., Russell G., et al. 2016. 'Ice Melt, Sea Level Rise and Superstorms: Evidence from Paleoclimate Data, Climate Modeling, and Modern Observations That 2 °C Global Warming Could

Be Dangerous'. *Atmospheric Chemistry and Physics* 16 (6): 3761–3812. https://doi.org/10.5194/acp-16-3761-2016.

Hasan Md. K., Cheng Y., Kanwar M.K., Chu X.Y., Ahammed G.J. and Qi Z.Y. 2017. 'Responses of Plant Proteins to Heavy Metal Stress—A Review'. *Frontiers in Plant Science* 8 (September): 1492. https://doi.org/10.3389/fpls.2017.01492.

Hassan M. U., Chattha M.U., Khan I., Chattha M.B., Barbanti L., Aamer M., Iqbal M.M., et al. 2020. 'Heat Stress in Cultivated Plants: Nature, Impact, Mechanisms, and Mitigation Strategies—a Review'. *Plant Biosystems - An International Journal Dealing with All Aspects of Plant Biology*, March. https://www.tandfonline.com/doi/full/10.1080/11263504.2020.1727987.

Haworth M., Belcher C.M., Killi D., Dewhirst R.A., Materassi A., Raschi A. and Centritto M. 2018. 'Impaired Photosynthesis and Increased Leaf Construction Costs May Induce Floral Stress during Episodes of Global Warming over Macroevolutionary Timescales'. *Scientific Reports* 8 (1): 6206. https://doi.org/10.1038/s41598-018-24459-z.

Hickey L.T., Hafeez A.N., Robinson H., Jackson S.A., Leal-Bertioli S.C.M., Tester M., Gao C., Godwin I.D., Hayes B.J. and Brande Wulff B.B.H. 2019. 'Breeding Crops to Feed 10 Billion'. *Nature Biotechnology* 37 (7): 744–54. https://doi.org/10.1038/s41587-019-0152-9.

Hu S., Ding Y. and Zhu C. 2020. 'Sensitivity and Responses of Chloroplasts to Heat Stress in Plants'. *Frontiers in Plant Science* 11 (April): 375. https://doi.org/10.3389/fpls.2020.00375.

Huggins T. D., Mohammed S., Sengodon P., Ibrahim A. M. H., Tilley M. and D. B. Hays. 2018. 'Changes in Leaf Epicuticular Wax Load and Its Effect on Leaf Temperature and Physiological Traits in Wheat Cultivars (*Triticum Aestivum L.*) Exposed to High Temperatures during Anthesis'. *Journal of Agronomy and Crop Science* 204 (1): 49–61. https://doi.org/10.1111/jac.12227.

Hýsková V., Bělonožníková K., Čeřovská N., and Ryšlavá H. 2021. 'HSP70 Plays an Ambiguous Role during Viral Infections in Plants'. *Biologia Plantarum* 65 (April): 68–79. https://doi.org/10.32615/bp.2021.001.

Iba K. 2002. 'A CCLIMATIVE R ESPONSE TO T EMPERATURE S TRESS IN H IGHER P LANTS: Approaches of Gene Engineering for Temperature Tolerance'. *Annual Review of Plant Biology* 53 (1): 225–45. https://doi.org/10.1146/annurev.arplant.53.100201.160729.

Impollonia G., Croci M., Blandinières H., Marcone A. and Amaducci S. 2022. 'Comparison of PROSAIL Model Inversion Methods for Estimating Leaf Chlorophyll Content and LAI Using UAV Imagery for Hemp Phenotyping'. *Remote Sensing* 14 (22): 5801. https://doi.org/10.3390/rs14225801.

'IPCC — Intergovernmental Panel on Climate Change'. 2018. 2018. https://www.ipcc.ch/.

Irshad A., Guo H., Zhang S. Liu L. 2020. 'TILLING in Cereal Crops for Allele Expansion and Mutation Detection by Using Modern Sequencing Technologies'. *Agronomy* 10 (3): 405. https://doi.org/10.3390/agronomy10030405.

Iurlaro A., De Caroli M., Sabella E., De Pascali M.R., Rampino P., De Bellis L., Perrotta C., et al. 2016. 'Drought and Heat Differentially Affect XTH Expression and XET Activity and Action in 3-Day-Old Seedlings of Durum Wheat Cultivars with Different Stress Susceptibility'. *Frontiers in Plant Science* 7 (November). https://doi.org/10.3389/fpls.2016.01686.

Iwai M., Yokono M., Inada N. and Minagawa J. 2010. 'Live-Cell Imaging of Photosystem II Antenna Dissociation during State Transitions'. *Proceedings of the National Academy of Sciences* 107 (5): 2337–42. https://doi.org/10.1073/pnas.0908808107.

Jaconis S. Y., Thompson A. J. E., Smith S.L., Trimarchi C., Cottee N.S., Bange M.P. and Conaty W.C.. 2021. 'A Standardised Approach for Determining Heat Tolerance in Cotton Using Triphenyl Tetrazolium Chloride'. *Scientific Reports* 11 (1): 5419. https://doi.org/10.1038/s41598-021-84798-2.

Janni M., Cocozza C., Brilli F., Pignattelli S., Vurro F., Coppede N., Bettelli M. Calestani D., Loreto F. and Zappettini A. 2021. 'Real-Time Monitoring of Arundo Donax Response to Saline Stress through the Application of in Vivo Sensing Technology'. *Scientific Reports* 11 (1): 1–11. https://doi.org/10.1038/s41598-021-97872-6.

Janni M., Cadonici S., Bonas U., Grasso A., Dahab A. A. D., Visioli G., Pignone D., Ceriotti A. and Marmiroli N. 2018. 'Gene-Ecology of Durum Wheat HMW Glutenin Reflects Their Diffusion from the Center of Origin'. *Scientific Reports* 8 (1): 16929. https://doi.org/10.1038/s41598-018-35251-4.

Janni M., Coppede N., Bettelli M., Briglia N., Petrozza A., Summerer S., Vurro F., et al. 2019. 'In Vivo Phenotyping for the Early Detection of Drought Stress in Tomato'. *Plant Phenomics* 2019. https://doi.org/10.34133/2019/6168209.

Janni M., Gullì M., Maestri E., Marmiroli M., Valliyodan B., Nguyen H.T. and Marmiroli N. 2020a. 'Molecular and Genetic Bases of Heat Stress Responses in Crop Plants and Breeding for Increased Resilience and Productivity'. *Journal of Experimental Botany* 71 (13): 3780. https://doi.org/10.1093/jxb/eraa034.

Jean-Baptiste K., McFaline-Figueroa J.L., Alexandre C.M., Dorrity M.W., Saunders L., Bubb K.L., Trapnell C., Fields S., Queitsch C. and Cuperus J.T. 2019. 'Dynamics of Gene Expression in Single Root Cells of *Arabidopsis Thaliana*'. *The Plant Cell* 31 (5): 993–1011. https://doi.org/10.1105/tpc.18.00785.

Jia M., Guan J., Zhai Z., Geng S., Zhang X., Mao L. and Li A. 2017. 'Wheat Functional Genomics in the Era of next Generation Sequencing: An Update'. *The Crop Journal* 6 (1): 7–14. https://doi.org/10.1016/j.cj.2017.09.003.

Kadota Y. and Shirasu K. 2012. 'The HSP90 Complex of Plants'. *Biochimica et Biophysica Acta (BBA) - Molecular Cell Research* 1823 (3): 689–97. https://doi.org/10.1016/j.bbamcr.2011.09.016.

Karademir B. and Sari-Kaplan G. 2016. 'Heat Shock Protein (HSP)'. *Encyclopedia of Signaling Molecules*, 1–10. https://doi.org/10.1007/978-1-4614-6438-9_101809-1.

Kaur V. and Behl R. 2010. '(PDF) Grain Yield in Wheat as Affected by Short Periods of High Temperature, Drought and Their Interaction during Pre- and Post-Anthesis Stages'. *ResearchGate*. https://doi.org/10.1556/CRC.38.2010.4.8.

Kazancoglu Y., Ozbiltekin-Pala M. and Ozkan-Ozen Y.D. 2021. 'Prediction and Evaluation of Greenhouse Gas Emissions for Sustainable Road Transport within Europe'. *Sustainable Cities and Society* 70: 102924. https://doi.org/10.1016/j.scs.2021.102924.

Khan A., Ahmad M., Ahmed M. and Hussain I.M. 2020. 'Rising Atmospheric Temperature Impact on Wheat and Thermotolerance Strategies'. *Plants* 10 (1): 43. https://doi.org/10.3390/plants10010043.

Kholová J., Urban M.O., Cock J., Arcos J., Arnaud E., Aytekin D., Azevedo V., et al. 2021. 'In Pursuit of a Better World: Crop Improvement and the CGIAR'. Edited by Mathew Reynolds. *Journal of Experimental Botany* 72 (14): 5158–79. https://doi.org/10.1093/jxb/erab226.

Khorobrykh S., Havurinne V., Mattila H. and Tyystjärvi E. 2020. 'Oxygen and ROS in Photosynthesis'. *Plants* 9 (1): 91. https://doi.org/10.3390/plants9010091.

Khurana N., Chauhan H. and Khurana P. 2013. 'Wheat Chloroplast Targeted SHSP26 Promoter Confers Heat and Abiotic Stress Inducible Expression in Transgenic Arabidopsis Plants'. *PLoS ONE* 8 (1): e54418. https://doi.org/10.1371/journal.pone.0054418.

Kollist H., Zandalinas S.I., Sengupta S., Nuhkat M., Kangasjärvi J. and Mittler R. 2019. 'Rapid Responses to Abiotic Stress: Priming the Landscape for the Signal Transduction Network'. *Trends in Plant Science* 24 (1): 25–37. https://doi.org/10.1016/j.tplants.2018.10.003.

Kumar G. R., Sakthivel K., Sundaram R.M., Neeraja C.N., Balachandran S.M., Rani N.S., Viraktamath B.C. and Madhav M.S. 2010. 'Allele Mining in Crops: Prospects and Potentials'. *Biotechnology Advances* 28 (4): 451–61. https://doi.org/10.1016/j.biotechadv.2010.02.007.

Kumar M.V.G., Rane J., Singh A.K., Choudhary R.L., Raina S.K., George P., Aher L.K. and Singh N.P. 2017. 'Canopy Temperature Depression (CTD) and Canopy Greenness Associated with Variation in Seed Yield of Soybean Genotypes Grown in Semi-Arid Environment'. *South African Journal of Botany* 113 (November): 230–38. https://doi.org/10.1016/j.sajb.2017.08.016.

Kumar R.R., Goswami S., Singh K., Dubey K., Rai G.K., Singh B., Singh S. et al. 2018. 'Characterization of Novel Heat-Responsive Transcription Factor (TaHSFA6e) Gene Involved in Regulation of Heat Shock Proteins (HSPs) - A Key Member of Heat Stress-Tolerance Network of Wheat'. *Journal of Biotechnology* 279 (October). https://doi.org/10.1016/j.jbiotec.2018.05.008.

Kumar S., Singh R. and Nayyar H. 2012. 'α-Tocopherol Application Modulates the Response of Wheat (Triticum Aestivum L.) Seedlings to Elevated Temperatures by Mitigation of Stress Injury and Enhancement of Antioxidants'. *Journal of Plant Growth Regulation* 32 (2). DOI:10.1007/s00344-012-9299-z

Kumar V., Roy S., Kumar Behera B. and Kumar Das B. 2022. 'Heat Shock Proteins (Hsps) in Cellular Homeostasis: A Promising Tool for Health Management in Crustacean Aquaculture'. *Life* 12 (11): 1777. https://doi.org/10.3390/life12111777.

Kumari M., Pudake R. N., Singh V. P. and Joshi A. K. 2012. 'Association of Staygreen Trait with Canopy Temperature Depression and Yield Traits under Terminal Heat Stress in Wheat (*Triticum Aestivum L.*)'. *Euphytica*, 190: 87–97

Kuzmanović, L., Gennaro A., Benedettelli S, Dodd I.C., Quarrie S.A. and Ceoloni C. 2014. 'Structural–Functional Dissection and Characterization of Yield-Contributing Traits Originating from a Group 7 Chromosome of the Wheatgrass Species *Thinopyrum Ponticum* after Transfer into Durum Wheat'. *Journal of Experimental Botany* 65 (2): 509–25. https://doi.org/10.1093/jxb/ert393.

Kweku D., Bismark O., Maxwell A., Desmond K., Danso K., Oti-Mensah E., Quachie A. and Adormaa B. 2018. 'Greenhouse Effect: Greenhouse Gases and Their Impact on Global Warming'. *Journal of Scientific Research and Reports* 17 (6): 1–9. https://doi.org/10.9734/JSRR/2017/39630.

Laloum T., Martín G. and Duque P. 2018. 'Alternative Splicing Control of Abiotic Stress Responses'. *Trends in Plant Science* 23 (2): 140–50. https://doi.org/10.1016/j.tplants.2017.09.019.

Langridge P. and Reynolds M. 2021. 'Breeding for Drought and Heat Tolerance in Wheat'. *Theoretical and Applied Genetics* 134 (6): 1753–69. https://doi.org/10.1007/s00122-021-03795-1.

Levy A.A. and Feldman M. 2022. 'Evolution and origin of bread wheat'. *The Plant Cell* 2022: 34: 2549–2. https://doi.org/10.1093/plcell/koac130

Li Y., Xiao J., Chen L., Huang X., Cheng Z., Han B., Zhang Q. and Wu C. 2018. 'Rice Functional Genomics Research: Past Decade and Future'. *Molecular Plant* 11 (3): 359–80. https://doi.org/10.1016/j.molp.2018.01.007.

Liao Y., Liu Z., Gichira A.W., Yang M., Mbichi R.W., Meng L. and Wan T. 2022. 'Deep Evaluation of the Evolutionary History of the Heat Shock Factor (HSF) Gene Family and Its Expansion Pattern in Seed Plants'. *PeerJ* 10 (August): e13603. https://doi.org/10.7717/peerj.13603.

Lin M.Y., Chai K.H., Ko S.S., Kuang L.Y., Lur H.S. and Charng Y.Y. 2014. 'A Positive Feedback Loop between HEAT SHOCK PROTEIN101 and HEAT STRESS-ASSOCIATED 32-KD PROTEIN Modulates Long-Term Acquired Thermotolerance Illustrating Diverse Heat Stress Responses in Rice Varieties'. *Plant Physiology* 164 (4): 2045–53. https://doi.org/10.1104/pp.113.229609.

Liu C., Sukumaran S., Claverie E., Sansaloni C., Dreisigacker S. and Reynolds M. 2019. 'Genetic Dissection of Heat and Drought Stress QTLs in Phenology-Controlled Synthetic-Derived Recombinant Inbred Lines in Spring Wheat'. *Molecular Breeding* 39 (3): 34. https://doi.org/10.1007/s11032-019-0938-y.

Liu H.C. and Charng Y.Y. 2013. 'Common and Distinct Functions of Arabidopsis Class A1 and A2 Heat Shock Factors in Diverse Abiotic Stress Responses and Development'. *Plant Physiology* 163 (1): 276–90. https://doi.org/10.1104/pp.113.221168.

Liu X., Zhao L., Li J., Duan L., Zhang K., Qiao X., Li W., Zheng C., Tang X. and Zhang H. 2021. 'The Chloroplastic Small Heat Shock Protein Gene *KvHSP26* Is Induced by Various Abiotic Stresses in *Kosteletzkya Virginica*'. *International Journal of Genomics* 2021 (February): 1–9. https://doi.org/10.1155/2021/6652445.

Lu Y., Li R., Wang R., Wang X., Zheng W., Sun Q., Tong S., Dai S. and Xu S. 2017. 'Comparative Proteomic Analysis of Flag Leaves Reveals New Insight into Wheat Heat Adaptation'. *Frontiers in Plant Science* 8 (June). https://doi.org/10.3389/fpls.2017.01086.

Lubben T. H., Donaldson G.K., Viitanen P.V. and Gatenby'A.A.. 1989. 'Severa1 Proteins Lmported into Chloroplasts Form Stable Complexes with the GroEL-Related Chloroplast Molecular Chaperone', 1(12):1223-30. doi: 10.1105/tpc.1.12.1223.

Lynch J., Cain M., Frame D. and Pierrehumbert R. 2021. 'Agriculture's Contribution to Climate Change and Role in Mitigation Is Distinct From Predominantly Fossil CO2-Emitting Sectors'. *Frontiers in Sustainable Food Systems* 4 (February): 518039. https://doi.org/10.3389/fsufs.2020.518039.

Maccaferri M., Harris N.S., Twardziok S.O., Pasam R.K., Gundlach H., Spannagl M., Ormanbekova D., et al. 2019. 'Durum Wheat Genome Highlights Past Domestication Signatures and Future Improvement Targets'. *Nature Genetics* 51 (5): 885–95. https://doi.org/10.1038/s41588-019-0381-3.

Madec S., Baret F., De Solan B., Thomas S., Dutartre D., Jezequel S., Hemmerlé M., Gallian Colombeau G. and Comar A. 2017. 'High-Throughput Phenotyping of Plant Height: Comparing Unmanned Aerial Vehicles and Ground LiDAR Estimates'. *Frontiers in Plant Science* 8 (November). https://doi.org/10.3389/fpls.2017.02002.

Maestri E., Klueva N., Perrotta C., Gulli M., Nguyen H.T. and Marmiroli N. 2002. 'Molecular Genetics of Heat Tolerance and Heat Shock Proteins in Cereals'. *Plant Molecular Biology* 48 (5): 667–81. https://doi.org/10.1023/A:1014826730024.

Marutani Y., Yamauchi Y., Kimura Y., Mizutani M. and Sugimoto Y. 2012. 'Damage to Photosystem II Due to Heat Stress without Light-Driven Electron Flow: Involvement of Enhanced Introduction of Reducing Power into Thylakoid Membranes'. *Planta* 236 (2): 753–61. https://doi.org/10.1007/s00425-012-1647-5.

Mathur S., Agrawal D. and Jajoo A. 2014. 'Photosynthesis: Response to High Temperature Stress'. *Journal of Photochemistry and Photobiology B: Biology* 137 (August): 116–26. https://doi.org/10.1016/j.jphotobiol.2014.01.010.

Mattiolo E., Licciardello F., Lombardo G.M., Muratore G., and Anastasi U. 2017. 'Volatile Profiling of Durum Wheat Kernels by HS–SPME/GC–MS'. *European Food Research and Technology* 243 (1): 147–55. https://doi.org/10.1007/s00217-016-2731-z.

Medina E., Kim S.H., Yun M. and Choi W.G. 2021. 'Recapitulation of the Function and Role of ROS Generated in Response to Heat Stress in Plants'. *Plants* 10 (2): 371. https://doi.org/10.3390/plants10020371.

Meng G., Xiao M., Xiao M., De-Xu L., Zhen-Hui G. and Ming-Hui L. 2016. 'The Plant Heat Stress Transcription Factors (HSFs): Structure, Regulation, and Function in Response to Abiotic Stresses'. *Frontiers in Plant Science* 7: 3. https://doi.org/10.3389/fpls.2016.001143.

Miller G., Schlauch K., Tam R., Cortes D.T, Torres M.A., Shulaev V., Dangl J.L and Mittler.R. 2009. 'The Plant NADPH Oxidase RBOHD Mediates Rapid Systemic Signaling in Response to Diverse Stimuli'. *Science Signaling* 2 (84). https://doi.org/10.1126/scisignal.2000448.

Miller G. and Mittler R. 2006. 'Could Heat Shock Transcription Factors Function as Hydrogen Peroxide Sensors in Plants?' *Annals of Botany* 98 (2): 279–88. https://doi.org/10.1093/aob/mcl107.

Mittler R., Finka A. and Goloubinoff P. 2012. 'How Do Plants Feel the Heat?' *Trends in Biochemical Sciences* 37 (3): 118–25. https://doi.org/10.1016/j.tibs.2011.11.007.

Morgil H., Gercek Y.C., Tulum I., Morgil H., Gercek Y.C. and Tulum I. 2020. Single Nucleotide Polymorphisms (SNPs) in Plant Genetics and Breeding. The Recent Topics in Genetic Polymorphisms. *IntechOpen.* https://doi.org/10.5772/intechopen.91886.

Mu Q., Zhang W., Zhang Y., Yan H., Liu K., Matsui T., Tian X. and Yang P. 2017. 'ITRAQ-Based Quantitative Proteomics Analysis on Rice Anther Responding to High Temperature'. *International Journal of Molecular Sciences* 18 (9): 1811. https://doi.org/10.3390/ijms18091811.

Nagar S., Singh V. P., Arora A., Dhakar R. and Ramakrishnan S. 2015. 'Assessment of Terminal Heat Tolerance Ability of Wheat Genotypes Based on Physiological Traits Using Multivariate Analysis'. *Acta Physiologiae Plantarum* 37 (12): 257. https://doi.org/10.1007/s11738-015-2017-2.

Nelson C.J., Alexova R., Jacoby R.P. and Millar A.H. 2014. 'Proteins with High Turnover Rate in Barley Leaves Estimated by Proteome Analysis Combined with in Planta Isotope Labeling'. *Plant Physiology* 166 (1): 91–108. https://doi.org/10.1104/pp.114.243014.

Neta-Sharir I., Isaacson T., Lurie S. and Weiss D. 2005. 'Dual Role for Tomato Heat Shock Protein 21: Protecting Photosystem II from Oxidative Stress and Promoting Color

Changes during Fruit Maturation'. *The Plant Cell* 17 (6): 1829–38. https://doi.org/10.1105/tpc.105.031914.
Ng P. C. and Henikoff S. 2003. 'SIFT: Predicting Amino Acid Changes That Affect Protein Function'. *Nucleic Acids Research* 31 (13): 3812. https://doi.org/10.1093/nar/gkg509.
Liliane T.N. and Charles M.S. 2020. 'Factors Affecting Yield of Crops'. In *Agronomy - Climate Change and Food Security*, edited by Amanullah. *IntechOpen*. https://doi.org/10.5772/intechopen.90672.
Nuttall J.G., O'Leary G.J., Panozzo J.F., Walker C.K., Barlow K.M. and Fitzgerald G.J. 2015. 'Models of Grain Quality in Wheat—A Review'. *Field Crops Research* 202: 136–45. https://doi.org/10.1016/j.fcr.2015.12.011.
Ogunbode C. A., Doran R. and Gisela Böhm. 2020. 'Exposure to the IPCC Special Report on 1.5 °C Global Warming Is Linked to Perceived Threat and Increased Concern about Climate Change'. *Climatic Change* 158 (3–4): 361–75. https://doi.org/10.1007/s10584-019-02609-0.
Ohama N., Sato H., Shinozaki K. and Yamaguchi-Shinozaki K. 2017. 'Transcriptional Regulatory Network of Plant Heat Stress Response'. *Trends in Plant Science* 22 (1): 53–65. https://doi.org/10.1016/j.tplants.2016.08.015.
Pandino G., Mattiolo E., Lombardo S., Lombardo G.M., and Mauromicale G. 2020. 'Organic Cropping System Affects Grain Chemical Composition, Rheological and Agronomic Performance of Durum Wheat'. *Agriculture* 10 (2): 46. https://doi.org/10.3390/agriculture10020046.
ark C.J., and Seo Y.Su. 2015. 'Heat Shock Proteins: A Review of the Molecular Chaperones for Plant Immunity'. *The Plant Pathology Journal* 31 (4): 323–33. https://doi.org/10.5423/PPJ.RW.08.2015.0150.
Patrignani A. and Ochsner T. E. 2015. 'Canopeo: A Powerful New Tool for Measuring Fractional Green Canopy Cover'. *Agronomy Journal* 107 (6): 2312–20. https://doi.org/10.2134/agronj15.0150.
Paupière M. J., Van Haperen P., Rieu I., Visser R.G.F., Tikunov Y.M. and Bovy A.G. 2017. 'Screening for Pollen Tolerance to High Temperatures in Tomato'. *Euphytica* 213 (6): 1–8. https://doi.org/10.1007/s10681-017-1927-z.
Paux E., Lafarge S., Balfourier F., Derory J., Charmet G., Alaux M., Perchet G., et al. 2022. 'Breeding for Economically and Environmentally Sustainable Wheat Varieties: An Integrated Approach from Genomics to Selection'. *Biology* 11 (1): 149. https://doi.org/10.3390/biology11010149.
Pearl L. H. and Prodromou C. 2006. 'Structure and Mechanism of the Hsp90 Molecular Chaperone Machinery'. *Annual Review of Biochemistry* 75 (1): 271–94. https://doi.org/10.1146/annurev.biochem.75.103004.142738.
Perdomo J. A., Capó-Bauçà S., Carmo-Silva E. and Galmés J. 2017. 'Rubisco and Rubisco Activase Play an Important Role in the Biochemical Limitations of Photosynthesis in Rice, Wheat, and Maize under High Temperature and Water Deficit'. *Frontiers in Plant Science* 8 (April). https://doi.org/10.3389/fpls.2017.00490.
Pérez-Salamó I., Papdi C., Rigó G., Zsigmond L., Vilela B., Lumbreras V., Nagy I., et al. 2014. 'The Heat Shock Factor A4A Confers Salt Tolerance and Is Regulated by Oxidative Stress and the Mitogen-Activated Protein Kinases MPK3 and MPK6'. *Plant Physiology* 165 (1): 319–34. https://doi.org/10.1104/pp.114.237891.
Pignone D., De Paola D., Rapanà N. and Janni M. 2015. 'Single Seed Descent: A Tool to Exploit Durum Wheat (Triticum Durum Desf.) Genetic Resources'. *Genetic*

Resources and Crop Evolution 62 (7): 1029–35. https://doi.org/10.1007/s10722-014-0206-2.

Pospíšil P. 2016. 'Production of Reactive Oxygen Species by Photosystem II as a Response to Light and Temperature Stress'. *Frontiers in Plant Science* 7 (December). https://doi.org/10.3389/fpls.2016.01950.

Pospíšil P. and Prasad A. 2014. 'Formation of Singlet Oxygen and Protection against Its Oxidative Damage in Photosystem II under Abiotic Stress'. *Journal of Photochemistry and Photobiology B: Biology* 137 (August): 39–48. https://doi.org/10.1016/j.jphotobiol.2014.04.025.

Pour-Aboughadareh A., Yousefian M., Moradkhani H., Vahed M.M., Poczai P. and Siddique K.H.M. 2019. '*I* PASTIC: An Online Toolkit to Estimate Plant Abiotic Stress Indices: *I* PASTIC to Estimate Plant Abiotic Stress Indices'. *Applications in Plant Sciences* 7 (7): e11278. https://doi.org/10.1002/aps3.11278.

Prasad P. V. V. and Djanaguiraman M. 2014. 'Response of Floret Fertility and Individual Grain Weight of Wheat to High Temperature Stress: Sensitive Stages and Thresholds for Temperature and Duration'. *Functional Plant Biology* 41 (12): 1261. https://doi.org/10.1071/FP14061.

Prodromou C. 2016. 'Mechanisms of Hsp90 Regulation'. *Biochemical Journal* 473 (16): 2439–52. https://doi.org/10.1042/BCJ20160005.

Ramkumar G., Madhav M. S., Rama Devi S. J. S., Prasad M. S. and Ravindra Babu V. 2015. 'Nucleotide Variation and Identification of Novel Blast Resistance Alleles of Pib by Allele Mining Strategy'. *Physiology and Molecular Biology of Plants* 21 (2): 301. https://doi.org/10.1007/s12298-015-0284-4.

Rampino P., Mita G., Fasano P., Borrelli G.M., Aprile A., Dalessandro G., De Bellis L. and Perrotta C. 2012. 'Novel Durum Wheat Genes Up-Regulated in Response to a Combination of Heat and Drought Stress'. *Plant Physiology and Biochemistry* 56 (July): 72–78. https://doi.org/10.1016/j.plaphy.2012.04.006.

Reynolds M., Chapman S., Crespo-Herrera L., Molero G., Mondal S., Pequeno D.N.L., Pinto F., et al 2020. 'Breeder Friendly Phenotyping - ScienceDirect'. 2020. *Plant Science.* 295:110396. DOI: 10.1016/j.plantsci.2019.110396.

Ribeiro M., Nunes F.M., Rodriguez-Quijano M., Carrillo J.M., Branlard G. and Igrejas G. 2018. 'Next-Generation Therapies for Celiac Disease: The Gluten-Targeted Approaches'. *Trends in Food Science & Technology* 75: 56–71. https://doi.org/10.1016/j.tifs.2018.02.021.

Rich-Griffin C., Stechemesser A., Finch J., Lucas E., Ott S. and Schäfer P. 2020. 'Single-Cell Transcriptomics: A High-Resolution Avenue for Plant Functional Genomics'. *Trends in Plant Science* 25 (2). https://doi.org/10.1016/j.tplants.2019.10.008.

Roche D. 2015. 'Stomatal Conductance Is Essential for Higher Yield Potential of C3 Crops'. *Critical Reviews in Plant Sciences*, July. https://www.tandfonline.com/doi/abs/10.1080/07352689.2015.1023677.

Rogers H. J., Bate N., Combe J., Sullivan J., Sweetman J., Swan C., Lonsdale D. M. and Twell D. 2001. 'Functional Analysis of Cis-Regulatory Elements within the Promoter of the Tobacco Late Pollen Gene G10'. *Plant Molecular Biology* 45 (5): 577–85. https://doi.org/10.1023/A:1010695226241.

Rutsdottir G., Härmark J., Weide Y., Hebert H., Rasmussen M.I., Wernersson S., Respondek M. et al. 2017. 'Structural Model of Dodecameric Heat-Shock Protein Hsp21: Flexible N-Terminal Arms Interact with Client Proteins While C-Terminal Tails Maintain the

Dodecamer and Chaperone Activity'. *Journal of Biological Chemistry* 292 (19): 8103–21. https://doi.org/10.1074/jbc.M116.766816.

Saeidi M. and Abdoli M. 2015. 'Effect of Drought Stress during Grain Filling on Yield and Its Components, Gas Exchange Variables, and Some Physiological Traits of Wheat Cultivars'. *Journal of Agricultural Science and Technology* 17 (4): 885–98.

Saidi Y., Finka A. and Goloubinoff P. 2011. 'Heat Perception and Signalling in Plants: A Tortuous Path to Thermotolerance'. *New Phytologist* 190 (3): 556–65. https://doi.org/10.1111/j.1469-8137.2010.03571.x.

Sanchez-Bragado R., Newcomb M., Chairi F., Condorelli G.E., Ward R.W., White J.W., Maccaferri M., Tuberosa R., Araus R.L. and Serret Molins M.D. 2020. 'Carbon Isotope Composition and the NDVI as Phenotyping Approaches for Drought Adaptation in Durum Wheat: Beyond Trait Selection'. *Agronomy* 10 (11): 1679. https://doi.org/10.3390/agronomy10111679.

Sato Y., Murakami T., Funatsuki H., Matsuba S., Saruyama H. and Tanida M. 2001. 'Heat Shock-Mediated APX Gene Expression and Protection against Chilling Injury in Rice Seedlings'. *Journal of Experimental Botany* 52(354):145-51.

Savicka M. and Škute N. 2010. 'Eff Ects of High Temperature on Malondialdehyde Content, Superoxide Production and Growth Changes in Wheat Seedlings (*Triticum Aestivum L.*)'. *Ekologija* 56(1). https://doi.org/10.2478/v10055-010-0004-x.

Scharf K. D. 2012. 'The Plant Heat Stress Transcription Factor (Hsf) Family: Structure, Function and Evolution'. *Biochimica et Biophysica Acta*, 16. DOI: 10.1016/j.bbagrm.2011.10.002

Sedaghatmehr M., Mueller-Roeber B. and Balazadeh S. 2016. 'The Plastid Metalloprotease FtsH6 and Small Heat Shock Protein HSP21 Jointly Regulate Thermomemory in Arabidopsis'. *Nature Communications* 7 (1): 12439. https://doi.org/10.1038/ncomms12439.

Sekaran U., Lai L., Ussiri D.A.N., Kumar S. and Clay S. 2021. 'Role of Integrated Crop-Livestock Systems in Improving Agriculture Production and Addressing Food Security – A Review'. *Journal of Agriculture and Food Research* 5 (September): 100190. https://doi.org/10.1016/j.jafr.2021.100190.

Senthilkumar M., Amaresan N. and Sankaranarayanan A. 2021. 'Estimation of Malondialdehyde (MDA) by Thiobarbituric Acid (TBA) Assay'. *Plant-Microbe Interactions*, 103–5. https://doi.org/10.1007/978-1-0716-1080-0_25.

Sestili F., Botticella E., Bedo Z., Phillips A. and Lafiandra D. 2010. 'Production of Novel Allelic Variation for Genes Involved in Starch Biosynthesis through Mutagenesis'. *Molecular Breeding* 25 (1): 145–54. https://doi.org/10.1007/s11032-009-9314-7.

Setia R.C. and Setia N. 2018. 'The Omics Technologies and Crop Improvement'. 2018. *Crop Improvement: Strategies and Applications.* New Dehli: International Publishing House Pvt. Ltd, 1–18.

Shanker A. K., Bhanu D. and Maheswari M. 2020. 'Epigenetics and Transgenerational Memory in Plants under Heat Stress'. *Plant Physiology Reports* 25 (4): 583–93. https://doi.org/10.1007/s40502-020-00557-x.

Shanmugavel P., Rajaprakasam S., Chockalingam V., Ramasamy G., Thiyagarajan K., and Marimuthu R. 2021. 'Breeding Mechanisms for High Temperature Tolerance in Crop Plants'. In *Plant Breeding - Current and Future Views*. IntechOpen. https://doi.org/10.5772/intechopen.94693.

Sharma D. K., Andersen S.B., Ottosen C.O. and Rosenqvist E. 2015. 'Wheat Cultivars Selected for High F_v/F_m under Heat Stress Maintain High Photosynthesis, Total Chlorophyll, Stomatal Conductance, Transpiration and Dry Matter'. *Physiologia Plantarum* 153 (2): 284–98. https://doi.org/10.1111/ppl.12245.

Sharma D. K., Torp A.M., Rosenqvist E., Ottosen C.O. and Andersen S.B. 2017. 'QTLs and Potential Candidate Genes for Heat Stress Tolerance Identified from the Mapping Populations Specifically Segregating for Fv/Fm in Wheat'. *Frontiers in Plant Science* 8 (September): 1668. https://doi.org/10.3389/fpls.2017.01668.

Sharma R. K., Kumar S., Vatta K., Bheemanahalli R., Dhillon J. and Reddy K.N. 2022. 'Impact of Recent Climate Change on Corn, Rice, and Wheat in Southeastern USA'. *Scientific Reports* 12 (1): 1–14. https://doi.org/10.1038/s41598-022-21454-3.

Shaw A. K., Bhardwaj P.K., Ghosh S., Roy S., Saha S., Sherpa A.R., Saha S.K. and Hossain Z. 2016. 'β-Aminobutyric Acid Mediated Drought Stress Alleviation in Maize (*Zea Mays L.)*'. *Environmental Science and Pollution Research* 23 (3): 2437–53. https://doi.org/10.1007/s11356-015-5445-z.

Shirdelmoghanloo H., Lohraseb I., Rabie H.S., Brien C., Parent B. and Collins N.C. 2016. 'Heat Susceptibility of Grain Filling in Wheat (*Triticum Aestivum L.*) Linked with Rapid Chlorophyll Loss during a 3-Day Heat Treatment'. *Acta Physiologiae Plantarum* 38 (8): 208. https://doi.org/10.1007/s11738-016-2208-5.

Smart R.E. and G. E. Bingham. 1974. 'Rapid Estimates of Relative Water Content'. *Plant Physiology* 53 (2): 258–60. https://doi.org/10.1104/pp.53.2.258.

Soda N. 2015. 'Omics Study for Abiotic Stress Responses in Plants'. *Advances in Plants & Agriculture Research* 2 (1). https://doi.org/10.15406/apar.2015.02.00037.

Soreng R. J., Peterson P.L., Romaschenko K., Davidse G., Zuloaga F.O., Judziewicz E.J., Filgueiras T.S., Davis J.I. and Morrone O. 2015. 'A Worldwide Phylogenetic Classification of the Poaceae (Gramineae): Phylogenetic Classification of the Grasses'. *Journal of Systematics and Evolution* 53 (2): 117–37. https://doi.org/10.1111/jse.12150.

Srivastava S., Pathak A.D., Gupta P.S., Shrivastava A.K. and Srivastava A.K. 2012. 'Hydrogen Peroxide-Scavenging Enzymes Impart Tolerance to High Temperature Induced Oxidative Stress in Sugarcane'. *Journal of Environmental Biology* 33 (3): 657–61.

Srivastava S. and Dubey R. S. 2011. 'Manganese-Excess Induces Oxidative Stress, Lowers the Pool of Antioxidants and Elevates Activities of Key Antioxidative Enzymes in Rice Seedlings'. *Plant Growth Regulation* 64 (1): 1–16. https://doi.org/10.1007/s10725-010-9526-1.

Storozhenko S., De Pauw P., Van Montagu M., Inzé D. and Kushnir S. 1998. 'The Heat-Shock Element Is a Functional Component of the Arabidopsis *APX1* Gene Promoter'. *Plant Physiology* 118 (3): 1005–14. https://doi.org/10.1104/pp.118.3.1005.

Sun W., Van Montagu M. and Verbruggen N. 2002. 'Small Heat Shock Proteins and Stress Tolerance in Plants'. *Biochimica et Biophysica Acta (BBA) - Gene Structure and Expression* 1577 (1): 1–9. https://doi.org/10.1016/S0167-4781(02)00417-7.

Sung D.Y., Kaplan F. and Guy C.L. 2001. 'Plant Hsp70 Molecular Chaperones: Protein Structure, Gene Family, Expression and Function'. *Physiologia Plantarum* 113 (4): 443–51. https://doi.org/10.1034/j.1399-3054.2001.1130402.x.

Suzuki N., Koussevitzky S., Mittler R. and Miller G. 2012. 'ROS and Redox Signalling in the Response of Plants to Abiotic Stress'. *Plant, Cell & Environment* 35 (2): 259–70. https://doi.org/10.1111/j.1365-3040.2011.02336.x.

Taratima W., Chuanchumkan C., Maneerattanarungroj P., Trunjaruen A., Theerakulpisut P. and Dongsansuk A. 2022. 'Effect of Heat Stress on Some Physiological and Anatomical Characteristics of Rice (Oryza sativa L.) cv. KDML105 Callus and Seedling'. *Biology* 11, 1587. https:// doi.org/10.3390/biology11111587.

Tadesse W. 2019. 'Genetic Gains in Wheat Breeding and Its Role in Feeding the World'. *Crop Breeding, Genetics and Genomics*. https://doi.org/10.20900/cbgg20190005.

Tan W., Meng Qw., Brestic M., Olsovska K. and Yang X. 2011. 'Photosynthesis Is Improved by Exogenous Calcium in Heat-Stressed Tobacco Plants'. *Journal of Plant Physiology* 168 (17). https://doi.org/10.1016/j.jplph.2011.06.009.

Tardieu F. 2017. 'Plant Phenomics, From Sensors to Knowledge'. *Current Biology* 27 (15): R770–83. https://doi.org/10.1016/j.cub.2017.05.055.

'The Greenhouse Effect and Our Planet | National Geographic Society'. 2022. https://education.nationalgeographic.org/resource/greenhouse-effect-our-planet.

The International Wheat Genome Sequencing Consortium (IWGSC), Mayer K.F.X, Jane Rogers, Doležel J., Pozniak C., Eversole K., Feuillet C., et al. 2014. 'A Chromosome-Based Draft Sequence of the Hexaploid Bread Wheat (*Triticum Aestivum*) Genome'. *Science* 345 (6194): 1251788. https://doi.org/10.1126/science.1251788.

Ul Haq S.,Khan A., Ali M., Khattan A.M., and Gai W.X. 2019. 'Heat Shock Proteins: Dynamic Biomolecules to Counter Plant Biotic and Abiotic Stresses'. *International Journal of Molecular Sciences* 20 (21): 5321. https://doi.org/10.3390/ijms20215321.

Ullah S., Bramley H., Mahmood T. and Trethowan R. 2020. 'The Impact of Emmer Genetic Diversity on Grain Protein Content and Test Weight of Hexaploid Wheat under High Temperature Stress'. *Journal of Cereal Science* 95: 103052. https://doi.org/10.1016/j.jcs.2020.103052.

UNAFPA. 2022. 'Statistics'. UNAFPA. 2022. https://www.pasta-unafpa.org/newt/unafpa/default.aspx?IDCONTENT=102.

Untergasser A., Cutcutache I., Koressaar T., Ye J., Faircloth B.C., Remm M. and Rozen S.G. 2012. 'Primer3—New Capabilities and Interfaces'. *Nucleic Acids Research* 40 (15): e115–e115. https://doi.org/10.1093/nar/gks596.

US EPA, OAR. 2015. 'Climate Change Indicators: Greenhouse Gases'. Reports and Assessments. 16 December 2015. https://www.epa.gov/climate-indicators/greenhouse-gases.

Velikova V., Fares S. and Loreto F. 2008. 'Isoprene and Nitric Oxide Reduce Damages in Leaves Exposed to Oxidative Stress'. *Plant, Cell & Environment* 31 (12): 1882–94. https://doi.org/10.1111/j.1365-3040.2008.01893.x.

Villain P., Mache R. and Zhou D.X. 1996. 'The Mechanism of GT Element-Mediated Cell Type-Specific Transcriptional Control'. *The Journal of Biological Chemistry* 271 (51). https://doi.org/10.1074/jbc.271.51.32593.

Vurro F., Janni M., Coppedè N., Gentile F., Manfredi R., Bettelli M. and Zappettini A. 2019. 'Development of an In Vivo Sensor to Monitor the Effects of Vapour Pressure Deficit (VPD) Changes to Improve Water Productivity in Agriculture'. *Sensors* 19 (21): 4667. https://doi.org/10.3390/s19214667.

Wahid A., Gelani S., Ashraf M. and Foolad M. 2007. 'Heat Tolerance in Plants: An Overview'. *Environmental and Experimental Botany* 61 (3): 199–223. https://doi.org/10.1016/j.envexpbot.2007.05.011.

Wang C., Hu S., Gardner C. and Lübberstedt T. 2017. 'Emerging Avenues for Utilization of Exotic Germplasm'. *Trends in Plant Science* 22 (7): 624–37. https://doi.org/10.1016/j.tplants.2017.04.002.

Wang F., Harindintwali J.D., Yuan Z., Wang M., Wang F., Li S., Yin Z., et al. 2021. 'Technologies and Perspectives for Achieving Carbon Neutrality'. *The Innovation* 2 (4): 100180. https://doi.org/10.1016/j.xinn.2021.100180.

Wang Q.L., Chen J.H., He N.Y. and Guo F.Q. 2018. 'Metabolic Reprogramming in Chloroplasts under Heat Stress in Plants'. *International Journal of Molecular Sciences* 19 (3): 849. https://doi.org/10.3390/ijms19030849.

Wang W., Vinocur B., Shoseyov O. and Altman A. 2004. 'Role of Plant Heat-Shock Proteins and Molecular Chaperones in the Abiotic Stress Response'. *Trends in Plant Science* 9 (5): 244–52. https://doi.org/10.1016/j.tplants.2004.03.006.

Waters E. R. 2013. 'The Evolution, Function, Structure, and Expression of the Plant SHSPs'. *Journal of Experimental Botany* 64 (2): 391–403. https://doi.org/10.1093/jxb/ers355.

Watt M., Fiorani F., Usadel B., Rascher U., Muller O. and Schurr U. 2020. 'Phenotyping: New Windows into the Plant for Breeders'. *Annual Review of Plant Biology* 71 (1): 689–712. https://doi.org/10.1146/annurev-arplant-042916-041124.

Wen J., Jiang F., Liu M., Zhou R., Sun M., Shi X., Zhu Z. and Wu Z. 2021. 'Identification and Expression Analysis of Cathepsin B-like Protease 2 Genes in Tomato at Abiotic Stresses Especially at High Temperature'. https://pubag.nal.usda.gov/catalog/7171009.

'Wheat Production by Country 2022'. 2022. https://worldpopulationreview.com/country-rankings/wheat-production-by-country.

Xu Z.S., Li Z.Y., Chen Y., Chen M., Li L.C.and Ma Y.Z. 2012. 'Heat Shock Protein 90 in Plants: Molecular Mechanisms and Roles in Stress Responses'. *International Journal of Molecular Sciences* 13 (12): 15706–23. https://doi.org/10.3390/ijms131215706.

Xue G.P., Sadat S., Drenth J. and McIntyre C.L. 2014. 'The Heat Shock Factor Family from *Triticum Aestivum* in Response to Heat and Other Major Abiotic Stresses and Their Role in Regulation of Heat Shock Protein Genes'. *Journal of Experimental Botany* 65 (2): 539–57. https://doi.org/10.1093/jxb/ert399.

Yang D., Luo Y., Ni Y. and Yion Y. 2014. 'Effects of Exogenous ABA Application on Post-Anthesis Dry Matter Redistribution and Grain Starch Accumulation of Winter Wheat with Different Staygreen Characteristics'. *The Crop Journal* 2(2014):144–153. https://doi.org/10.1016/j.cj.2014.02.004.

Zadoks J. C., Chang T. T. and Konzak C. F. 1974. 'A Decimal Code for the Growth Stages of Cereals'. *Weed Research* 14 (6): 415–21. https://doi.org/10.1111/j.1365-3180.1974.tb01084.x.

Zandalinas S.I., Fritschi F.B. and Mittler R. 2021. 'Global Warming, Climate Change, and Environmental Pollution: Recipe for a Multifactorial Stress Combination Disaster'. *Trends in Plant Science* 26 (6): 588–99. https://doi.org/10.1016/j.tplants.2021.02.011.

Zhang X., Wang Y., Huang G., Feng F., Liu X., Guo R., Gu F., et al. 2020. 'Atmospheric Humidity and Genotype Are Key Determinants of the Diurnal Stomatal Conductance Pattern'. *Journal of Agronomy and Crop Science* 206 (2): 161–68. https://doi.org/10.1111/jac.12375.

Zhao C., Liu B., Piao S., Wang X., Lobell D.B., Huang Y., Huang M., et al. 2017. 'Temperature Increase Reduces Global Yields of Major Crops in Four Independent Estimates'. *Proceedings of the National Academy of Sciences* 114 (35): 9326–31. https://doi.org/10.1073/pnas.1701762114.

Zhao F., Zhang D., Zhao Y., Wang W., Yang H., Tai F., Li C. and Hu X. 2016. 'The Difference of Physiological and Proteomic Changes in Maize Leaves Adaptation to Drought, Heat, and Combined Both Stresses'. *Frontiers in Plant Science* 7 (October). https://doi.org/10.3389/fpls.2016.01471.

Zhao J., Lu Z., Wang L. and Jin B. 2020. 'Plant Responses to Heat Stress: Physiology, Transcription, Noncoding RNAs, and Epigenetics'. *International Journal of Molecular Sciences* 22 (1): 117. https://doi.org/10.3390/ijms22010117.

Zhou R., Li B., Liu H. and Sun D. 2009. 'Progress in the Participation of Ca2+–Calmodulin in Heat Shock Signal Transduction'. *Progress in Natural Science* 19 (10): 1201–8. https://doi.org/10.1016/j.pnsc.2008.12.011.

Rong Z., Jiang F., Niu L., Song X., Yu L., Yang Y. and Wu Z. 2022. 'Increase Crop Resilience to Heat Stress Using Omic Strategies'. *Frontiers in Plant Science* 13 (May). https://doi.org/10.3389/fpls.2022.891861.

Zhou R., Yu X., Kjær K.H., Rosenqvist E., Ottosen C.O. and Wu Z. 2015. 'Screening and Validation of Tomato Genotypes under Heat Stress Using Fv/Fm to Reveal the Physiological Mechanism of Heat Tolerance'. *Environmental and Experimental Botany* 118 (October): 1–11. https://doi.org/10.1016/j.envexpbot.2015.05.006.

Zimin A. V., Puiu D., Hall R., Kingan S., Clavijo B.J. and Salzberg S.L. 2017. 'The First Near-Complete Assembly of the Hexaploid Bread Wheat Genome, *Triticum Aestivum'*. *GigaScience* 6 (11). https://doi.org/10.1093/gigascience/gix097.

Zingale S., Guarnaccia P., Matarazzo A., Lagioia G. and Ingrao C. 2022. 'A Systematic Literature Review of Life Cycle Assessments in the Durum Wheat Sector'. *Science of The Total Environment* 844: 157230. https://doi.org/10.1016/j.scitotenv.2022.157230.

Zou J., Guo Y., Guettouche T., David F Smith, and Richard Voellmy. 1998. 'Repression of Heat Shock Transcription Factor HSF1 Activation by HSP90 (HSP90 Complex) That Forms a Stress-Sensitive Complex with HSF1'. *Cell* 94 (4): 471–80. https://doi.org/10.1016/S0092-8674(00)81588-3.